P-07-74

Oskarshamn site investigation

Fracture mineralogy

Results from drill cores KLX03, KLX04, KLX06, KLX07A, KLX08 and KLX10A

Henrik Drake
Department of Geology, Earth Sciences Centre
Göteborg University

Eva-Lena Tullborg, Terralogica AB

September 2007

Svensk Kärnbränslehantering AB
Swedish Nuclear Fuel
and Waste Management Co
Box 5864
SE-102 40 Stockholm Sweden
Tel 08-459 84 00
+46 8 459 84 00
Fax 08-661 57 19
+46 8 661 57 19

ISSN 1651-4416
SKB P-07-74

Oskarshamn site investigation

Fracture mineralogy

Results from drill cores KLX03, KLX04, KLX06, KLX07A, KLX08 and KLX10A

Henrik Drake
Department of Geology, Earth Sciences Centre
Göteborg University

Eva-Lena Tullborg, Terralogica AB

September 2007

Keywords: Fracture minerals, Laxemar, Relative dating, Calcite, Pyrite, Gypsum, Barite, Stable isotopes, Hematite, Clay minerals, SEM-EDS, ICP-MS, AP PS 400-05-053 and AP PS 400-05-074.

Abstract

The drill cores KLX03, KLX04, KLX06, KLX07A, KLX08 and KLX10A from the Laxemar subarea have been sampled for detailed studies of fracture mineralogy. The results from this study have been compared to the detailed fracture mineralogy studies of drill cores KSH01A+B and KSH03A+B from Simpevarp /Drake and Tullborg 2004, 2006a/, KLX02 from Laxemar, KAS 04 and KA1755A from Äspö /Drake and Tullborg 2005/, and KKR01, KKR02, KKR03 from Götemar /Drake and Tullborg 2006b/.

In order to investigate the features of the fracture fillings and their relative relations 18 thin sections and 40 fracture surface samples have been analysed using petrographic microscope and scanning electron microscope (SEM-EDS). Calcite has been analysed for $\delta^{18}O$ and $\delta^{13}C$ (49 samples) and $^{87}Sr/^{86}Sr$ (19 samples). Fluorite (6 samples) and gypsum (7 samples) have been analysed for $^{87}Sr/^{86}Sr$. Pyrite (17 samples), gypsum (9 samples) and barite (4 samples) have been analysed for $\delta^{34}S$. The isotope studies give suggestions about formation conditions of fracture fillings from different generations and are used in the discussion of relative ages of different generations. Calcite (14 samples) and gypsum (5 samples) have been analysed for trace elements. $^{87}Sr/^{86}Sr$-analyses of whole rock samples from Ävrö granite, quartz monzodiorite, fine-grained dioritoid and the Götemar granite were carried out for evaluation of the $^{87}Sr/^{86}Sr$-ratios in fracture filling calcite with different wall rock compositions.

The relative sequence of fracture filling events in the Laxemar subarea is very similar to what has earlier been reported from Simpevarp and Äspö /Drake and Tullborg 2004, 2005, 2006a/. Re-activation at different events is a common phenomenon. Mylonites, where present, are often re-activated by cataclasite and later formed brittle fractures. The formation temperatures of the different generations of fracture fillings are successively lower with time, indicated by early formed epidote followed by minerals of lower formation temperature like prehnite and even later zeolites (laumontite and later harmotome). The earliest deformation in the area (mylonites, cataclasites and fractures filled with epidote, prehnite and early formed laumontite) are Pre-Cambrian (older than 1,400 Ma). The fracture mineralization with calcite, fluorite, pyrite, gypsum, barite, apophyllite and harmotome is Phaneorozoic (mainly Palaeozoic). Gypsum and apophyllite are more common in the Laxemar subarea than in the Simpevarp subarea, where in contrast cataclasites are more common. The fracture frequency in the Simpevarp subarea is also higher than in the Laxemar subarea. In borehole KLX06 below the deformation zone ZSMEW002 (The Mederhult Zone), greisen-like alteration and coarse-grained quartz, muscovite, fluorite and pyrite have been observed. Gypsum-filled fractures and greisen-related fractures have the most preferred directions (sub-vertical NNW-trending and sub-horizontal, respectively), while fractures occupied by minerals of other generations show more scattered directions due to re-activation of older fractures, mylonites and cataclasites.

Stable isotopes, Sr-isotopes and trace element analyses confirm that calcite and pyrite have been formed at different events with gradually lower temperatures (and increasing biogenic influence), while all analysed gypsum and probably also barite have been formed during a shorter time interval (or less likely at several events with similar conditions).

Sammanfattning

Sprickmineralogiska undersökningar har utförts för de djupa kärnborrhålen KLX03, KLX04, KLX06, KLX07A, KLX08 och KLX10A, Laxemar, inom ramen för SKB:s (Svensk Kärnbränslehantering AB) platsundersökningar. Resultaten från denna studie har jämförts med detaljerade sprickmineralundersökningar från borrhål KSH01A+B och KSH03A+B, Simpevarp /Drake och Tullborg 2004, 2006a/, KLX02, Laxemar, KAS 04 och KA1755A, Äspö /Drake och Tullborg 2005/ och KKR01, KKR02 och KKR03, Götemar /Drake och Tullborg 2006b/.

Totalt har arton tunnslip från läkta sprickor och sprickytor från 40 öppna sprickor undersökts för att utröna karaktärsdrag och relativa relationer mellan olika sprickfyllningar. Proverna har huvudsakligen undersökts med svepelektronmikroskop (SEM-EDS) och petrografiskt mikroskop. Kalcit har analyserats med avseende på $\delta^{18}O$, $\delta^{13}C$ (49 prover) och $^{87}Sr/^{86}Sr$ (19 prover). Fluorit (6 prover) och gips (7 prover) har analyserats med avseende på $^{87}Sr/^{86}Sr$. Pyrit (17 prover), gips (9 prover) och baryt (4 prover) har analyserats med avseende på $\delta^{34}S$. Isotopanalyserna ger information om bildningsförhållanden för sprickfyllningarna och bidrar till den relativa dateringen av olika sprickfyllningsgenerationer. Spårämnesanalyser har genomförts på kalcit (14 prover) och gips (5 prover). $^{87}Sr/^{86}Sr$-förhållandet i Ävrögranit, Kvartsmonzodiorit, ”Finkornig dioritoid” och Götemargranit har analyserats för att underlätta utvärderingen av $^{87}Sr/^{86}Sr$-ration i kalcit i sprickor med olika sidobergssammansättning.

Den relativa sprickfyllnadssekvensen för Laxemarområdet är väldigt lik den som tidigare rapporterats från Simpevarp och Äspö /Drake och Tullborg 2004, 2005, 2006a/. Sprickorna har vanligen varit öppna under flera tillfällen. De få myloniter som finns i borrhålen är ofta reaktiverade varvid kataklasit bildats och senare också spröda sprickor. De olika generationernas bildningstemperaturer är successivt lägre med tiden, indikerat av tidigt bildad epidot, som följs av mineral med lägre bildningstemperatur som prehnit och ännu senare zeoliter (laumontit och harmotom). Den tidigaste deformationen i området (mylonit, kataklasit och sprickor läkta av epidot, prehnit och tidigt bildad laumontit) är med största säkerhet prekambrisk. Generationen av sprickor läkta av t ex kalcit, fluorit, pyrit, gips, baryt, apofyllit och harmotom är troligen palaeozoisk. Gips och apofyllit är vanligare i Laxemarområdet än i Simpevarpsområdet, där kataklasiter är vanligare och sprickfrekvensen är högre än i Laxemarområdet. Greisenliknande omvandling och grovkorniga sprickfyllningar med kvarts, muskovit, fluorit och pyrit har påträffats under deformationszonen ZSMEW002 i KLX06. Gipsfyllda sprickor och greisenrelaterade sprickor har de mest utpräglade sprickriktningarna (subvertikala NNW-strykande respektive subhorisontella) medan riktningar på sprickor fyllda med andra mineral varierar i hög grad beroende på reaktivering av äldre sprickor, myloniter och kataklasiter.

Analyser av stabila isotoper, Sr-isotoper och spårämnen visar att kalcit och pyrit har bildats vid flera tillfällen med gradvis lägre temperatur (och ökande biogena inslag). All analyserad gips och troligen också all baryt, har däremot troligen bildats vid ett och samma tillfälle, eller mindre troligt, vid flera tillfällen under liknande förhållanden.

Contents

1 Introduction

The Swedish Nuclear Fuel and Waste Management Company (SKB) is currently carrying out site investigations in the Simpevarp/Laxemar area in the Oskarshamn region, in order to find a place suitable for a long-time storage of spent nuclear fuel. The drill cores KLX03, KLX04, KLX06, KLX07A, KLX08 and KLX10A from Laxemar subarea (Figure 1-1) have been sampled for detailed studies of fracture minerals. As fracture fillings occur in different, often small, amounts scattered across the drill cores it is difficult to know how representative the samples are. The sampling was mainly focused on samples that give information about relative order of fracture filling generations and not on the relative amounts of different fracture fillings. The results from this study have been compared to the detailed fracture filling studies of drill cores KSH01A+B and KSH03A+B from Simpevarp /Drake and Tullborg 2004, 2006a/, KLX02 from Laxemar, KAS 04 and KA1755A from Äspö /Drake and Tullborg 2005/, and KKR01, KKR02, KKR03 from Götemar /Drake and Tullborg 2006b/.

In order to investigate the features of the fracture fillings and their relative relations 18 thin sections and 40 fracture surface samples have been analysed using petrographic microscope and scanning electron microscope (SEM-EDS). Calcite has been analysed for $\delta^{18}O$, $\delta^{13}C$ (49 samples) and $^{87}Sr/^{86}Sr$ (19 samples). Fluorite (6 samples) and gypsum (7 samples) have been analysed for $^{87}Sr/^{86}Sr$. Pyrite (17 samples), gypsum (9 samples) and barite (4 samples) have been analysed for $\delta^{34}S$. The isotope studies give suggestions about formation conditions of fracture fillings from different generations and are used in the discussion of relative ages of different generations. Calcite (14 samples) and gypsum (5 samples) have been analysed for

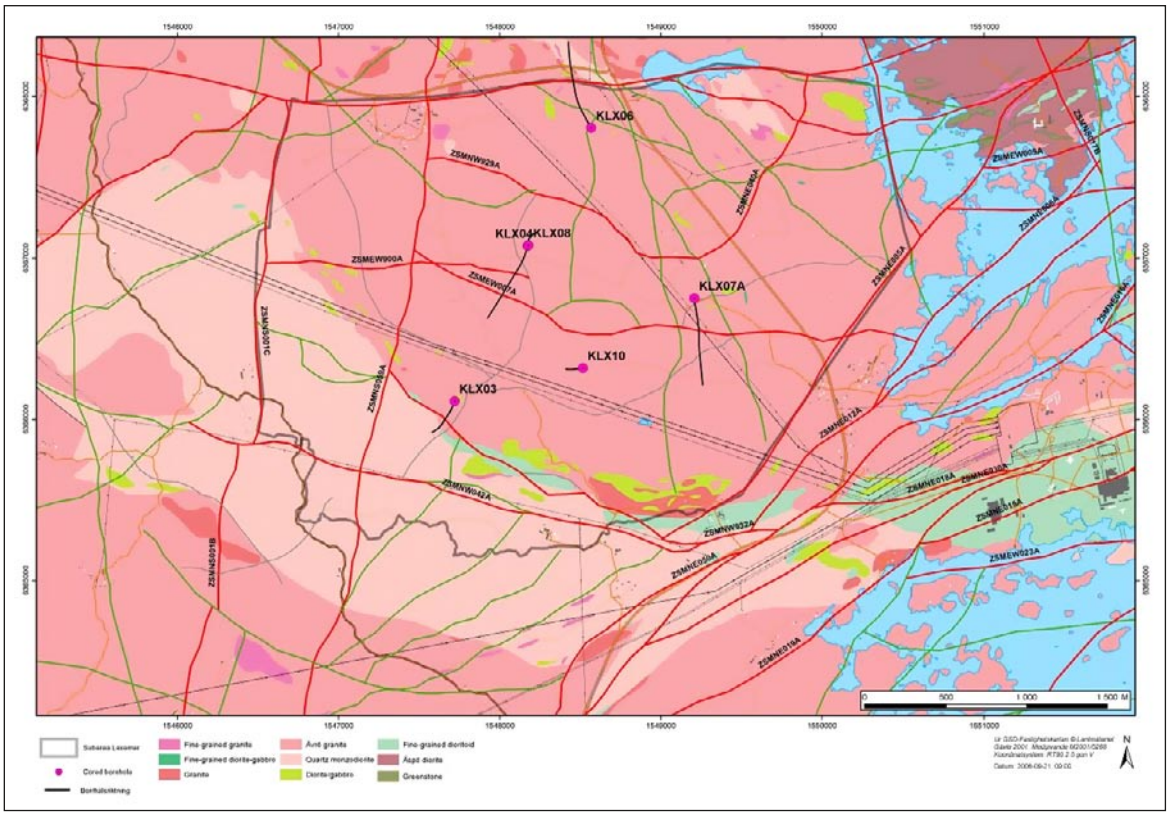

Figure 1-1. *Geological map showing the surface-location and projection of the boreholes KLX03, KLX04, KLX06, KLX07A, KLX08 and KLX10A in the Laxemar subarea.*

trace element composition. $^{87}Sr/^{86}Sr$-analyses of whole rock samples from the Ävrö granite, the quartz monzodiorite, the fine-grained dioritoid and the Götemar granite were performed to give input to the evaluation of the $^{87}Sr/^{86}Sr$-ratios in fracture filling calcite with different wall rock compositions.

Additional analyses ($^{87}Sr/^{86}Sr$, $\delta^{13}C$, $\delta^{18}O$ and ICP-MS analyses of calcite and $\delta^{34}S$ analyses of pyrite and gypsum) that were finished after the reports by e.g. /Drake and Tullborg 2004, 2005, 2006ab/ were published, are found in Appendix 13 along with some analyses from borehole KAS17 (Äspö) and one sample from a road cutting.

The work was carried out in accordance with activity plans SKB PS 400-05-053 (KLX03, KLX04 and KLX06) and SKB PS 400-05-074 (KLX07, KLX08, KLX10). In Table 1-1 controlling documents for performing this activity are listed. Both activity plans and method descriptions are SKB's internal controlling documents.

Table 1-1. Controlling documents for the performance of the activity.

Activity plan	**Number**	**Version**
Sprickmineralogiska undersökningar i KLX03, KLX04 och KLX06	AP PS 400-05-053	1.0
Sprickmineralogiska undersökningar i KLX07 (A+B), KLX08 och KLX10	AP PS 400-05-074	1.0
Method descriptions	**Number**	**Version**
Sprickmineralogi	SKB MD 144.000	1.0

2 Objective and scope

The aim of this study is to obtain a detailed description, including mineralogy, geochemistry, relative dating and isotopic composition, of fracture fillings from boreholes KLX03, KLX04, KLX06, KLX07A, KLX08 and KLX10A.

This study is a part of a PhD project at the Department of Geology, Earth Sciences Centre, Göteborg University.

3 Geological background

The bedrock in the Simpevarp/Laxemar area north of Oskarshamn is dominated by Småland granitoids and dioritoids of the Transscandinavian Igneous Belt (TIB) e.g. /Gaal and Gorbatschev 1987, Kornfält and Wikman 1987, Kornfält et al. 1997, Wahlgren et al. 2004/. The Småland granitoids in the Simpevarp/Laxemar/Äspö area belong to the TIB 1 /Larson and Berglund 1992, Åhäll and Larson 2000/ and have been dated with U-Pb-dating to 1,804+/–4 Ma (zircon) /Kornfält et al. 1997/ and 1,802+/–4 Ma (zircon), 1,793+/–4 (titanite) and 1,800+/–4 Ma (titanite and zircon) /Wahlgren et al. 2004/. Other intrusions are e.g. Götemar /Kresten and Chyssler 1976, Åberg et al. 1984/ and Uthammar. These coarse-grained granites were emplaced at 1,452 +11/–9 Ma (Götemar) and 1,441 +5/–3 Ma (Uthammar) /Åhäll 2001/. Dating and determination of a paleomagnetic pole of the "Äspö diorite" from Äspö HRL, show that the rock has not been heated above 550–600°C since its crystallization /Maddock et al. 1993/.

The bedrock surface in the Laxemar subarea (cf Figure 1-1) is dominated by the Ävrö granite (80%) /Persson Nilsson et al. 2004/. The Ävrö granite is a collective name for a suite of more or less porphyritic rocks that vary in composition from quartz monzodiorite to granite, including quartz dioritic and quartz monzonitic varieties. The Ävrö granite is reddish grey to greyish red, medium-grained with megacrysts of microcline that are usually 1–2 cm in size. The Ävrö granite has been observed to mix and mingle with the equigranular quartz monzodiorite and gradual contact relationships indicate that the two rock types formed more or less synchronously /Persson Nilsson et al. 2004, Wahlgren et al. 2004/.

The rocks in the Laxemar subarea are generally well preserved. A week foliation is occasionally observed in the Ävrö granite and this foliation affects the matrix whereas the megacrysts of microcline show no or weak preferred orientation. Several local shear zones (mylonitic, ductile shear zones and brittle-ductile shear zones) have been mapped /Persson Nilsson et al. 2004/. The width of these zones varies between a decimetre to several tens of metres. A characteristic phenomenon that affects all rock types in the Laxemar subarea is inhomogeneous red staining /Persson Nilsson et al. 2004/. Geological surface mapping of the adjacent Simpevarp subarea reveals that similar red-staining is present also in this subarea, although more common than in the Laxemar subarea /Wahlgren et al. 2004/. The red-staining in the Simpevarp/Laxemar area has been studied in detail from drill cores KSH01A+B and KSH03A+B, Simpevarp /Drake and Tullborg 2006c/, and KLX04, Laxemar /Drake and Tullborg 2006d/.

Earlier studies of the fracture minerals within the Simpevarp/Laxemar site investigations have been carried out by e.g. /Drake and Tullborg 2004, 2005, 2006a/. Other studies of fracture minerals in the region have been carried out by e.g. /Tullborg 1988, 1997, Alm and Sundblad 2002, Drake and Tullborg 2006b/.

4 The drill cores

The boreholes KLX03, KLX04, KLX06, KLX07A, KLX08 and KLX10A are all 845–1,000-meter deep cored boreholes, drilled within the site investigation program in the Laxemar subarea. The boreholes are telescopic implying that the upper part, 0–100 m, is percussion drilled and has a larger diameter than the core drilled part. To cover up for the missing core of the uppermost 100 m another core drilled borehole is occasionally drilled adjacent to the other borehole (e.g. KLX07B and KLX10B). However, no samples from 0–100 m are included in this study. The inclination, orientation and length of the drill cores are found in Table 4-1. The diameter of the boreholes is 76 mm and the core diameter is about 50 mm.

The drill cores are normally dominated by Ävrö granite but larger sections of quartz monzodiorite are also found. Occasionally, fine-grained dioritoid, diorite to gabbro, granite, pegmatite and fine-grained granite are found.

Pronounced deformation zones are found in e.g. KLX04 (ZSMEW007A; 314–391 m and ZSMNW929A; 861–968 m), KLX06 (ZSMEW002A; "Mederhult zone": 300–430 m), KLX03 (ZSMNW932A; 505 m) and KLX10A according to the geological model /Wahlgren et al. 2006/.

Table 4-1. Length, orientation and inclination of the cored boreholes used in this report. The cored boreholes start at ~ 100 m below the bedrock surface.

Borehole	Core (m)	Borehole orientation
Laxemar subarea		
KLX03	100–1,000	199/–75°
KLX04	100–1,000	0/–85°
KLX06	100–995	329/–65°
KLX07A	100–845	174/–65°
KLX08	100–990	199/–60°
KLX10A	100–1,000	251/–85°

5 Equipment

5.1 Description of equipment

The following equipment was used in the fracture mineralogy investigations.

- Scanning electron microscope (Zeiss DSM 940) with EDS (Oxford Instruments Link).
- Scanning electron microscope (Hitachi S-3400N) with EDS (Oxford Instruments).
- Microscopes (Leica DMRXP and Leica DMLP).
- Stereo microscope (Leica MZ12).
- Microscope camera (JVC TK-1280E).
- Digital camera (Konica Revio KD-420Z).
- Rock saw.
- Rock Labs swing mill.
- Knife.
- Magnifying lens – 10x.
- Scanner (Epson 3200) and Polaroid filters.
- Computer software, e.g. Corel Draw 11, Microsoft Word, Microsoft Excel, WellCad, BIPS, Link ISIS.
- Stable carbon and oxygen isotope analysis equipment.
- Agilent ICP-MS, model 7500a.

All of the equipment mentioned above is the property of the Earth Sciences Centre, Göteborg University, SKB or the authors.

External laboratory equipment was used for:

- $^{87}Sr/^{86}Sr$-isotope analyses.
- Sulphur isotope analyses.

See chapter 6 (Execution) for more details.

6 Execution

6.1 Sample collection

Samples suitable for fracture mineral investigations were collected from the drill cores. The length of the samples ranges from 4 to 100 centimetres, but are normally 10–15 centimetres. All analysed samples are listed in Table 6-1. $^{87}Sr/^{86}Sr$ analyses on rock types were performed on powdered rock samples of unaltered rock with representative composition from earlier studies in the area. The sample from Simpevarp is fine-grained dioritoid, sample KSH01:536-2G /Drake and Tullborg 2006c/. The samples from Laxemar are Ävrö granite sample KLX04:108G /Drake and Tullborg 2006d/ and quartz monzodiorite, sample PSM004484A /Wahlgren et al. 2005/. The sample from the Götemar granite is KKR03: 643.82–643.90 m /Drake and Tullborg 2006b/.

6.2 Sample preparation and analyses

6.2.1 Thin sections and surface samples

The samples were photographed and sawed and 18 thin sections were prepared by Ali Firoozan, Earth Sciences Centre, Göteborg University and by Kjell Helge, Minoprep AB, respectively. The thickness of the thin sections is about 30 μm. The thin sections were scanned with Epson 3200 scanner, using Polaroid filters, in order to optimize SEM-EDS investigations. The prepared samples were initially examined with petrographic microscope. Selected parts of the samples were photographed in the microscope. 40 samples from the fracture surfaces of open fractures were also prepared and scanned with an Epson 3200 scanner without Polaroid filters.

SEM-EDS microanalyses of thin sections were carried out on two different SEM-EDS units at the Earth Sciences Centre, Göteborg University, Sweden. Polished thin-sections were coated with carbon for electron conductivity. The instruments were calibrated at least twice every hour using a cobalt standard linked to simple oxide and mineral standards, to confirm that the instrument drift was acceptable. Fe^{2+} and Fe^{3+} are not distinguished and the H_2O content is not calculated.

One of the two SEM-units, used for thin sections, is an Oxford Instruments energy dispersive system mounted on a Zeiss DSM 940 SEM. The acceleration voltage was 25 kV, the working distance 24 mm and the specimen current was about 0.7nA. ZAF corrections were performed by an on-line LINK ISIS computer system. Detection limit is 0.1 oxide % (0.3% for Na_2O).

The other unit, used for thin sections and surface samples, is an Oxford Instruments energy dispersive system mounted on a Hitachi S-3400N SEM. The acceleration voltage was 20 kV, the working distance 10 mm and the specimen current was about 1nA. X-ray spectrometric corrections were made by an on-line computer system. Detection limit is 0.1 oxide %.

Representative SEM-EDS analyses were obtained from the thin section but this was not possible for the surface samples due to the rough morphology of these samples.

Table 6-1. Sample types and analyses used for each sample.

Sample (m)	Thin section	Surface sample	$\Delta^{18}O/\ \delta^{13}C$ calcite	$^{87}Sr/^{86}Sr$ calcite	ICP-MS calcite	$^{87}Sr/^{86}Sr$ fluorite	$^{87}Sr/^{86}Sr$ gypsum	ICP-MS gypsum	$\delta^{34}S$ gypsum	$\delta^{34}S$ pyrite	$\delta^{34}S$ barite
KLX03											
195.95–196.15		x	x								
266.62–266.71		x									
416.46–416.58			x								
457.60–457.75		x	xx							x	x
533.10–533.25							x		x		
535.58–535.70									x		
572.10–572.30									x		
590.79–590.96							x		x		
591.33–591.33										x	
627.26–627.31										x	
662.33–662.65		x	xx	x	x					x	x
722.72–722.96	xx		x		xx						
733.49–733.53			x	x	xx					x	
742.23–742.36			x	x						x	
897.76–897.89											
970.04–970.07		x									
KLX04											
114.12–114.33			x								
188.19–188.39						x					
274.65–274.92											
322.04–322.25	x		x								
346.46–346.58			x								
349.66–349.79	x										
669.31–669.55		x	xx	x	x					x	x
673.78–674.05			xx	x						x	
677.39–677.70		x	x	x	x					x	
878.18–878.24			x								
925.60–925.68		x	x	x	x	x					
970.48–970.52			x								

Sample (m)	Thin section	Surface sample	$\Delta^{18}O$/ $\delta^{13}C$ calcite	$^{87}Sr/^{86}Sr$ calcite	ICP-MS calcite	$^{87}Sr/^{86}Sr$ fluorite	$^{87}Sr/^{86}Sr$ gypsum	ICP-MS gypsum	$\delta^{34}S$ gypsum	$\delta^{34}S$ pyrite	$\delta^{34}S$ barite
KLX06											
321.01–321.16	x		x								
333.53–333.67											
381.42–381.58											
384.23–384.28	x										
387.95–388.07	x										
392.23–392.57			x								
394.83–394.96			x	x							
446.67–446.80											
472.84–472.92											
499.03–499.13											
535.10–535.26		x								x	
535.40–535.50											
557.81–557.91											
565.22–565.38						x					
566.25–566.35										x	
572.40–572.46											
576.09–576.21		x									
590.66–590.72										x	
593.40–593.55			x	x		x					
595.08–595.18	xx					x					
607.06–607.14											
622.57–622.73	x										
789.41–789.48		x									
814.86–814.95		x	x	x	x	x					
831.32–831.38		x									

Sample (m)	Thin section	Surface sample	$\Delta^{18}O$/ $\delta^{13}C$ calcite	$^{87}Sr/^{86}Sr$ calcite	ICP-MS calcite	$^{87}Sr/^{86}Sr$ fluorite	$^{87}Sr/^{86}Sr$ gypsum	ICP-MS gypsum	$\delta^{34}S$ gypsum	$\delta^{34}S$ pyrite	$\delta^{34}S$ barite
KLX07A											
106.25–106.41	x		x		x						
184.83–184.92		x									
193.63–193.87		x									x
227.24–227.38			x								
320.32–320.49		x									
321.47–321.58		xx									
346.73–346.82		x	x								
356.93–356.96		x	x	x						xx	
364.17–364.41		x	x		x					x	
373.70–373.97		x	x							x	
423.21–423.39			x							x	
557.83–557.94		x									
668.98–669.22		x	x	x							
696.68–696.83		x	x	x							
KLX08											
108.24–108.33		x	x	x	x						
218.29–218.39		x	x		x						
366.43–366.58			x	x							
478.87–479.13	x		x		x						
676.92–677.13	x										
679.83–680.01		x									
772.49–772.69	x		x	x							
792.43–792.72											
795.15–795.36		x					x	x	x		
820.93–821.16		x							x		
821.70–821.92											
822.41–822.61	x	x							x	xx	

Sample (m)	Thin section	Surface sample	$\Delta^{18}O$/ $\delta^{13}C$ calcite	$^{87}Sr/^{86}Sr$ calcite	ICP-MS calcite	$^{87}Sr/^{86}Sr$ fluorite	$^{87}Sr/^{86}Sr$ gypsum	ICP-MS gypsum	$\delta^{34}S$ gypsum	$\delta^{34}S$ pyrite	$\delta^{34}S$ barite
868.65–868.83	x						x	x	x		
916.16–916.36	x	x									
919.75–919.90							x	x	x		
933.15–933.30	x										
KLX010A											
108.27–108.38		x	x								
112.66–112.72			x								
200.72–201.02		x	x								
228.14–228.80		x	xxx	xx	xx						
406.29–406.49			x								
519.40–519.62											
610.85–611.19		xx									
789.80–790.10			x								
790.50–790.63											
895.00–895.20			x								
919.44–919.62			x	x	x						
969.13–969.28		x					x	x			
970.50–970.65		x					x	xx			
971.70–972.00		x									

6.2.2 Carbon and oxygen isotope analyses

The stable carbon and oxygen isotope analyses carried out at the Earth Sciences Centre, Göteborg University, on calcite samples were made accordingly: Samples, usually between 150 and 250 µg each, were roasted in vacuum for 30 minutes at 400°C to remove possible organic material and moisture. Thereafter, the samples were analysed using a VG Prism Series II mass spectrometer with a VG Isocarb preparation system on line. In the preparation system each sample was reacted with 100% phosphoric acid at 90°C for 10 minutes, whereupon the released CO_2 gas was analysed in the mass spectrometer. All isotope results are reported as δ per mil relative to the Vienna Pee Dee Belemnite (VPDB) standard. The analyses are calibrated to the PDB scale via NBS-19.

6.2.3 Strontium isotope analyses

Göran Åberg at Institute for Energy Technology, Norway, carried out the Sr-isotope analyses on calcite, fluorite and gypsum and the preparation according to the following procedure. About 30 to 40 mg of the carbonate samples were transferred to 2 ml centrifuge tubes, added 200 µl 0.2 M HCl, and shaken. The samples were let to react for 10 minutes while shaken in order to release the CO_2 gas. If not completely dissolved 20 µl 2 M HCl is added once or twice until most of the calcite has been decomposed.

The fluorite and gypsum samples were finely ground in an agate mortar and transferred to a Savillex Teflon beaker with lid. A few ml of supra-pure HNO_3 was added and the lid was screwed loosely on and the beaker was put on a hotplate at low temperature for 48 hours. During this time the beaker was shaken several times in order to leach the fluorite and gypsum as good as possible.

All the samples were centrifuged for about 4 minutes and the liquids transferred to new clean centrifuge tubes by use of a pipette. New pipette tips are used for each sample. The centrifuge tubes are put on a hotplate and evaporated to dryness. To avoid disturbances in measuring the isotopic composition, strontium had to be separated from other elements present in the sample. After evaporation to dryness the samples were dissolved in 200 µl ultrapure 3M HNO_3, centrifuged and loaded onto ion-exchange columns packed with a Sr-Spec crown-ether resin from EIChrom, which retained Sr and allowed most other elements to pass. After rinsing out the remaining unwanted elements from the columns, strontium was collected with ultra-pure water (Millipore). The collected Sr-fractions were then evaporated to dryness and loaded on pre-gassed Re filaments on a turret holding 12 samples and 1 NIST/NBS 987 Sr standard. The isotopic composition of Sr was determined by thermal ionization mass spectrometry (TIMS) on a Finnigan MAT 261 with a precision of about 20 ppm and a Sr blank of 50–100 pg. The $^{87}Sr/^{86}Sr$ ratio of the carbonate analyses are monitored by analysing one NIST/NBS SRM 987 Sr standard, for each turret of 12 samples, and the standard has a recommended $^{87}Sr/^{86}Sr$ value of 0.710248. The presented results are not corrected to the NBS 987 recommended value but are given together with the specific measured NBS 987 value for the relevant turret.

Rock samples were analysed on their $^{87}Sr/^{86}Sr$ ratio by Göran Åberg at the Institute for Energy Technology, Norway, according to the following procedure: Between 50 and 100 mg sample was transferred to a 5 ml Savillex Teflon beaker with lid, added 3 ml conc. HF and 0.5 ml concentrated HNO_3. The lid was screwed on loosely and the beaker was put on a hotplate at c. 90°C overnight. After that the samples were dissolved, the clear solution was evaporated to dryness. 3 ml of 6 M HCl was added to each sample and the lid was screwed loosely on. The beaker was put back on the hotplate at 90°C until next day. The clear solution was evaporated to dryness and then dissolved in 200 µl ultrapure 3 M HNO_3, centrifuged and loaded onto ion-exchange columns packed with a Sr-Spec crown-ether resin from EIChrom, which retained Sr and allowed most other elements to pass. After rinsing out the remaining unwanted elements from the columns, Sr was collected with ultrapure water (Millipore). The collected Sr-fractions were then evaporated to dryness and loaded onto pre-gassed Re filaments on a turret holding

12 samples and a NIST/NBS 987 Sr standard. The isotopic composition was determined by thermal ionization mass spectrometry (TIMS) on a Finnigan MAT 261 with a precision of c. 20 ppm and a Sr blank of 50–100 pg.

6.2.4 Sulphur isotope analyses

Samples of pyrite, gypsum and barite were analysed for their stable-isotope composition, expressed as $\delta^{34}S$ ‰ CDT. The crystals were scraped of the fracture surfaces with a knife. Bigger crystals were handpicked from the surface with a pair of tweezers. Some pyrite crystals from sealed fractures were scraped off from the fractures with a knife or the sample was ground in a Rock labs swing mill and the crystals were hand-picked under the stereo microscope. The analyses were carried out at the Scottish Universities Environmental Research Centre (SUERC), Glasgow by Professor Tony Fallick. Sulphur dioxide was liberated from sulphides following the method of /Robinson and Kusakabe 1975/, whereby samples were combusted at 1,070°C for 25 minutes in the presence of excess Cu_2O. A high temperature furnace containing pure copper ensured that any sulphur trioxide in the combustion products was reduced to SO_2. Sulphur dioxide was separated from excess oxygen and the other combustion products by standard vacuum line techniques, and the purified gas analysed for $^{34}S/^{32}S$ ratio on a dual-inlet Micromass SIRA2 multiple-collector mass spectrometer. Reproducibility of calibrated standards is ± 0.2‰ at one sigma and data are reported in the delta notation relative to V-CDT.

6.2.5 ICP-MS analyses of calcite and gypsum

The ICP-MS analyses on calcites and gypsum leachates were carried out following the here given procedure: 12 mg calcite sample (weight registered ± 0,01mg) was placed in a 50 ml tube, where 47 ml 5% HNO_3 was added containing 15 ppb of indium and rhenium respectively, to be used as internal standards. The sample was leached for 1 hour with stirring every 15 minutes (20 hours for the gypsum samples, with stirring every hour). Thereafter, 20 ml of the solution was used for analyses carried out on an Agilent ICP-MS, model 7500a. Certified multi element standards from Merck (nr VI) and Agilent (nr 1) were used.

7 Results and discussion

In this section, results from thin section analyses, surface sample analyses, stable isotopes, Sr-isotopes, and trace element analyses are presented and discussed. Relative ages of different fracture filling generations are shown in a schematic sequence of fracture filling events (Table 7-1). Earlier studies in the area e.g. /Tullborg 1988, 1997, Drake and Tullborg 2004, 2005, 2006a/ show that the general fracture mineralogical features and occurrences are similar throughout the Simpevarp-Laxemar-Äspö area, although some differences exist. The major difference is that the Simpevarp subarea is characterized by a higher degree of brittle deformation, resulting in breccias and cataclasites and generally higher fracture frequencies compared to the Laxemar subarea. Gypsum and apophyllite are more common in the Laxemar subarea than in the Simpevarp subarea.

Thin section descriptions with images, stable isotope results, Sr-isotope results, trace element results, SEM-EDS analyses are found in the Appendix.

7.1 Fracture filling sequence

The fracture filling sequence presented below (Table 7-1) is slightly modified from /Drake and Tullborg 2006a/ and is representative for the results from the present study. The sequence comprises a relative chronological sequence of the characteristic minerals in each fracture filling generation from the Simpevarp, Laxemar and Äspö areas, with results from drill cores KSH01

Table 7-1. Schematic fracture filling-sequence from Simpevarp/Laxemar/Äspö. The most abundant minerals in each generation are in bold letters. Minerals in brackets are only found occasionally.

1. **Quartz- and epidote-rich mylonite,** occasionally including muscovite, titanite, Fe-Mg-chlorite, albite, (apatite), (calcite), (K-feldspar)
2. **Cataclasite**
   a. Early green coloured **epidote**-rich, with **quartz, Fe-Mg-chlorite,** (titanite, K-feldspar, albite)
   b. Late red-brown colour; **K-feldspar, chlorite, quartz, hematite,** albite, (and illite)
3. Euhedral **quartz, epidote, Fe-Mg chlorite, calcite[1],** pyrite, fluorite, muscovite, (K-feldspar)
4. **Prehnite,** (fluorite)
5.
   a. **Calcite[2],** (fluorite, hematite)
   b. **Dark red/brown filling – Adularia, Mg-chlorite** (also as ML-clay with Illite), **hematite** (quartz, apatite); sometimes cataclastic.
   c. **Calcite[3], adularia, laumontite, Mg-chlorite, quartz, illite** (also in ML-clay with chlorite), **hematite,** (albite and apatite)
6. **Calcite[4], adularia, Fe-chlorite, hematite, fluorite, quartz, pyrite, barite, gypsum, corrensite** (and other types of mixed-layer clay), harmotome, REE-carbonate, galena, apophyllite, illite, chalcopyrite, sphalerite, U-silicate, Cu(Zn,Ni,Sn,Fe)-rich minerals, apatite, (Ti-oxide, laumontite, sylvite, Fe-oxyhydroxide, Mg-chlorite, albite, wolframite, gold and argentite)
7. **Calcite[5],** pyrite, Fe-oxyhydroxide (near surface)

[1] Commonly coarse-grained euhedral with abundant twinning lamellae.

[2] Euhedral to subhedral crystals with abundant twinning lamellae, filling prehnite coated fractures.

[3] Commonly as subhedral crystals with abundant twinning lamellae, in narrow fractures.

[4] Commonly as fine-grained subhedral crystals with a small number of twinning lamellae, in undulating and very narrow fractures. Commonly scalenohedral crystal shapes on fracture surfaces (possibly Palaeozoic).

[5] Crystals in open fractures and voids.

and KSH03 /Drake and Tullborg 2004, 2006a/, KLX02, KAS04, KA1755A /Drake and Tullborg 2005/, KKR01, KKR02, KKR03 /Drake and Tullborg 2006b/ and the present study. Only a few of the minerals in each generation are commonly observed in a single sample. The relative abundance of the minerals from each generation varies widely between different samples. Calcite and chlorite are present in most of the generations. These minerals have precipitated at several events under different conditions. Stable isotope analyses of calcite provide information about these conditions and from what type of fluid the calcite precipitated, which gives input to the discussion about the relative age of the fracture filling generations. SEM-EDS analyses of chlorite reveal differences in chemistry between chlorite of different generations.

The characteristics of each fracture filling generation are described below.

7.1.1 Generation 1 and 2

No mylonites (generation 1) were sampled in this study. A couple of samples include cataclasite (generation 2). These cataclasites are from drill cores KLX04 (from the deformation zones ZSMEW007A and ZSMNW929A), KLX06 (from the deformation zone ZSMEW002A) and KLX08 and are commonly red-brown in colour and made up of wall rock fragments and K-feldspar, Mg-rich chlorite, quartz, hematite and occasionally epidote. Some cataclasites are dark green in colour and contain more chlorite and epidote than the red variety. The green coloured cataclasite is thought to be formed prior to the red-colour variety. Mylonite and cataclasite are not as common in the Laxemar subarea as in the Simpevarp subarea /Drake and Tullborg 2004, 2006a/.

7.1.2 Generation 3

This fracture filling generation (Figure 7-2) is quite common in the Laxemar subarea and often consists of thick quartz fillings, Fe-Mg-chlorite, calcite, epidote, pyrite, fluorite, muscovite and occasionally K-feldspar.

The Fe-Mg-chlorite is chemically similar to Fe-Mg-rich chlorite of generation 3 from Simpevarp, Laxemar and Äspö /Drake and Tullborg 2004, 2005, 2006a/.

Figure 7-1. *Photograph of drill core sample KLX04 349.66–349.79 m that shows red-brown coloured cataclasite cut by later formed fractures. The green-coloured cataclasite type is found in the left part of the sample.*

Figure 7-2. *Photograph of a fracture filling made up of calcite (white), quartz (grey) and Fe-Mg-chlorite (dark green). Sample KLX03: 733.49–733.53 m.*

7.1.3 Generation 4

Prehnite is also very common in the studied drill cores, although not as common as in the Simpevarp subarea /Drake and Tullborg 2004/. Fluorite is occasionally found along with prehnite. The wall rock adjacent to prehnite filled fractures is commonly red-stained (Figure 7-3) /cf Drake and Tullborg 2006c, 2006d/. The orientations of the prehnite filled fractures vary widely but fractures with low dips (mostly sub-horizontal) are the most common, especially in KLX08.

7.1.4 Generation 5

Fracture filling generation 5 (Table 7-1) is the most difficult to distinguish in the present study. Stable isotopes and Sr isotopes of calcite (Chapters 7.3 and 7.4) indicate that the fillings are formed at several events. Most of the fillings rich in calcite, adularia, laumontite, illite, and hematite (Figure 7-4) post-date dark red/brown fillings (sometimes cataclastic), which are rich in adularia, Mg-chlorite (also as ML-clay with illite) and hematite.

The calcite normally shows moderately to high amount of twinning-lamellae. Laumontite and adularia often coat the fractures that are later filled by calcite. However, these three minerals are generally thought to be coeval. The paragenesis of calcite, adularia, Mg-rich chlorite, laumontite and illite has been documented earlier from Simpevarp, Laxemar and Äspö /Drake and Tullborg 2004, 2005, 2006a/ but is thought to be most common in the

Figure 7-3(a-b). *a) Photograph of a fracture filled with prehnite. The wall rock is hydrothermally altered and red-stained. Sample KLX08: 366.43–366.58 m. b) Photograph of prehnite (generation 4) in a fracture cutting through earlier formed chlorite, calcite and quartz (generation 3). Sample KLX03: 722.72–722.96 m.*

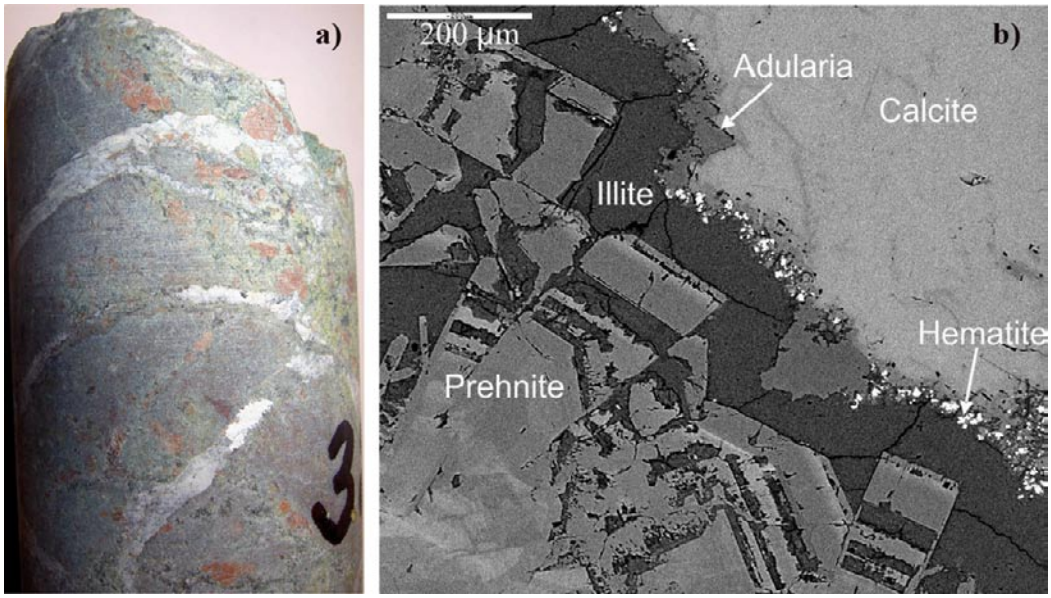

Figure 7-4(a-b). *a) Photograph of the drill core. Dark areas are chlorite- and K-feldspar rich (+hematite), green areas are prehnite-rich. Both of these fillings are cut by fractures filled with white-grey calcite, adularia, illite, laumontite and hematite. b) Back-scattered SEM-image of the contact between prehnite and later formed illite, adularia, hematite and calcite. Note the dissolution of prehnite. Sample KLX04: 322.04–322.25 m.*

Simpevarp subarea. The Mg-rich chlorite is similar in composition to the chlorite found in earlier formed hematite-rich fillings and hematite-cataclasite in the Laxemar subarea and from KSH01, KSH03, KAS04 and KA1755A. Laumontite is also found in a section in the lower part of zone ZSMEW002A in KLX06 (c. 380–410 m borehole length) where it has replaced epidote in mylonites and plagioclase in the altered wall rock (Figure 7-5b).

Figure 7-5(a-b). *a) Photograph of quartz, calcite (whitish grey, lower part of the filling), and laumontite (orange). Sample KLX07A: 106,25–106,41 m. b) Photograph of parts of the laumontite-rich zone in KLX06 (392–394 m).*

7.1.5 Generation 6

Thin fractures that cut through calcite, laumontite, adularia etc of generation 5 are commonly filled with calcite of generation 6 (Table 7-1). This calcite is often found together with fluorite (Figure 7-9), adularia, Fe-chlorite, pyrite, hematite, fluorite, corrensite (Figure 7-9) and barite (Figure 7-6). REE-carbonate, illite (often in mixed-layer clay), harmotome (Ba-zeolite; the latter not found below 300 m vertical depth, Figure 7-7), apophyllite (Figure 7-8) chalcopyrite, U-silicate, galena, sphalerite, laumontite, Cu(Zn,Ni,Sn,Fe)-rich minerals and apatite are occasionally found in paragenesis with calcite as well.

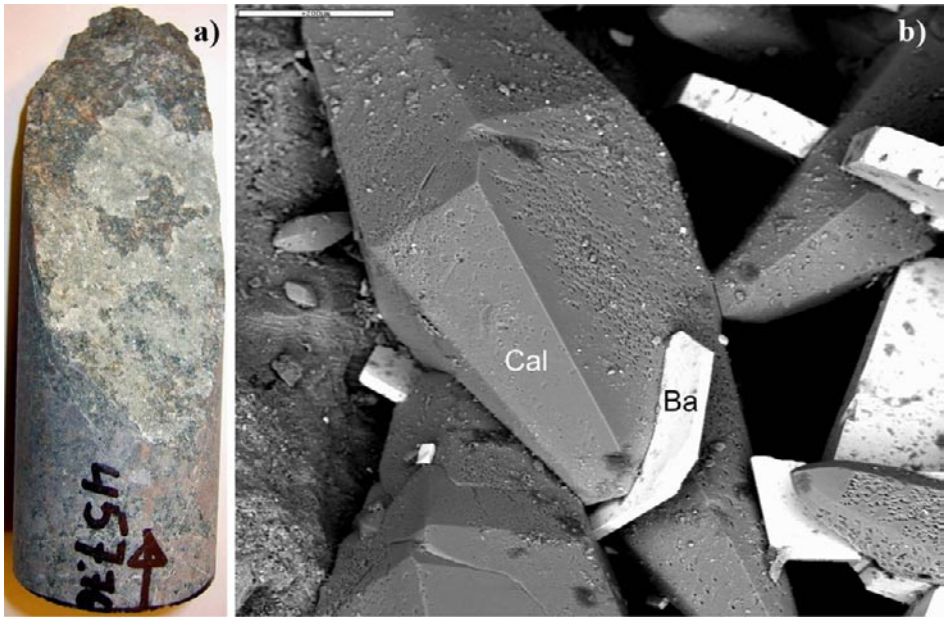

Figure 7-6(a-b). *a) Photograph of an open fracture, mainly coated with calcite, barite and pyrite. b) Back-scattered SEM-image of scalenohedral calcite (Cal) and barite (Ba) from the fracture surface in figure a. Scale marker is 200 µm. Sample KLX03: 457.60–457.75 m.*

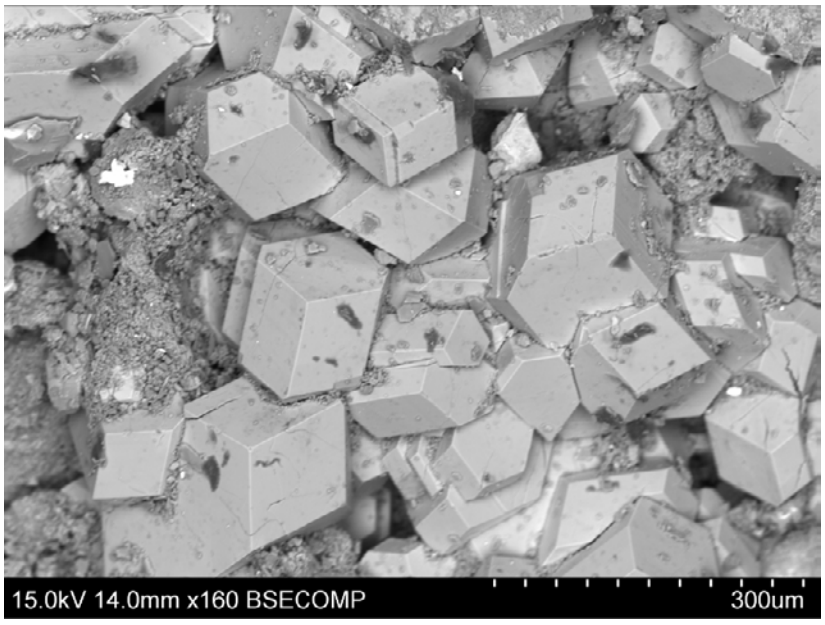

Figure 7-7. *Back-scattered SEM-image of harmotome (Ba-zeolite). Sample KLX03: 266.62–266.71 m.*

Figure 7-8(a-b). *a) Photograph of an open fracture, mainly coated with apophyllite. b) Back-scattered SEM-image of apophyllite from the fracture surface in figure a. Scale marker is 200 µm. Sample KLX03: 970.04–970.07 m.*

Figure 7-9(a-b). *a) Photograph of an open fracture, mainly coated with fluorite, corrensite and hematite. b) Back-scattered SEM-image of fluorite (cubic) and corrensite (spherulitic aggregates) from the fracture surface in figure a. Sample KLX06: 831.32–831.38 m.*

The calcite has a low amount of twin-lamellae and is commonly found as c-axis elongated crystals with scalenohedral morphology in open fractures (Figure 7-6). Sometimes the calcite crystals have overgrowths (Figure 7-10). These overgrowths commonly have a higher amount of Mn than the original crystal. Equant and needle shaped (Figure 7-11) crystals are also present but may have been formed later than generation 6. Generation 6 minerals have been found throughout the area (Simpevarp, Laxemar, Äspö and Götemar) /Drake and Tullborg 2004, 2005, 2006ab/. The calcite-fluorite filling may belong to the same generation as similar fracture fillings described from the Götemar granite, where fractures cut across fractures filled with Palaeozoic sandstone /Alm and Sundblad 2002, Drake and Tullborg 2006a/. Calcite-fluorite fillings in the Götemar granite, dated to 405 ± 27 Ma /Sundblad et al. 2004/ show similar stable isotope results and mineral paragenesis as fillings of generation 6 /Drake and Tullborg 2006ab and this study/. Fluid inclusions in these fillings from Laxemar and Götemar also show similar homogenisation temperatures and salinities /Alm and Sundblad 2002, Milodowski et al. 2005/.

The chemistry of Fe-rich chlorite of generation 6 resembles Fe-rich chlorite found in other parts of the area including the Götemar granite /Drake and Tullborg 2006ab/.

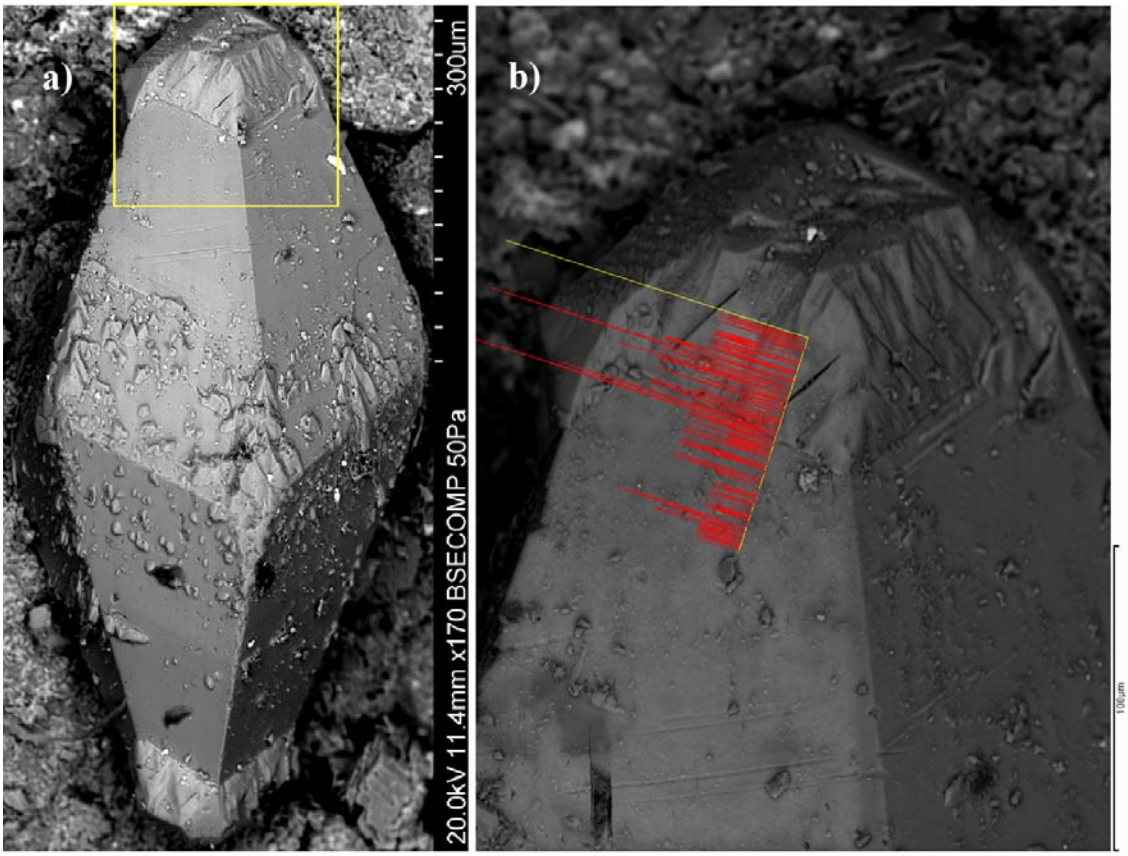

Figure 7-10(a-b). *a) Back-scattered SEM-image of scalenohedral calcite with overgrowths (brighter). b) Close-up of the area within the box in figure a, with a line-scan of the MnO-content shown (higher MnO-content in the overgrowth). Sample KLX07A: 373.70–373.97 m.*

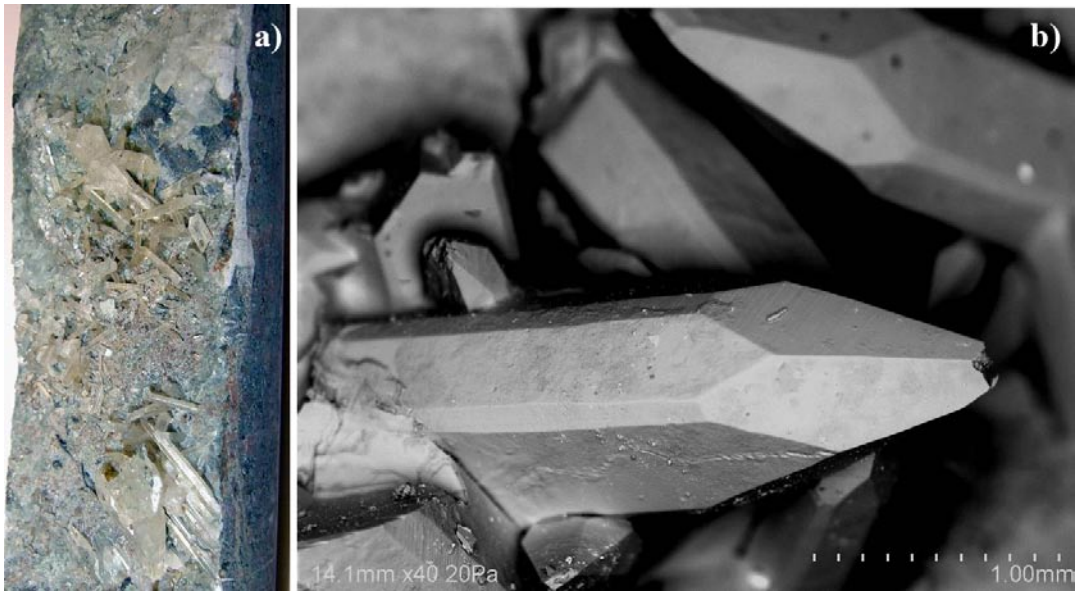

Figure 7-11(a-b). *a) Photograph of the fracture surfaces of an open fracture coated with needle shaped calcite. b) Back-scattered SEM-image of needle shaped calcite crystals from the fracture surface in figure a. Sample KLX10A: 228.14–228.80 m.*

Gypsum (Figure 7-12) is found along with apophyllite and some calcite at certain depths (below ~ 500 m) in drill cores KLX03, KLX08 and KLX10A. Gypsum is also found along with fluorite and calcite at below 500 m in KLX06. It is commonly found in fractures with relatively fresh wall rock and not in older re-activated fractures. The gypsum filled fractures (Figure 7-13) also have much more preferred orientations (sub-vertical: WNW-ESE) compared to the fractures filled with other minerals (except for muscovite-quartz-fluorite fractures in KLX06 see chapter 7-2). Apophyllite and gypsum are much more common in the Laxemar drill cores than in the Simpevarp drill cores /Drake and Tullborg 2004, 2006a/.

7.1.6 Generation 7

Calcite that is considered to be formed later than generation 6 is occasionally found on fracture surfaces (Figure 7-14). These calcite crystals are rounder than those of generation 6.

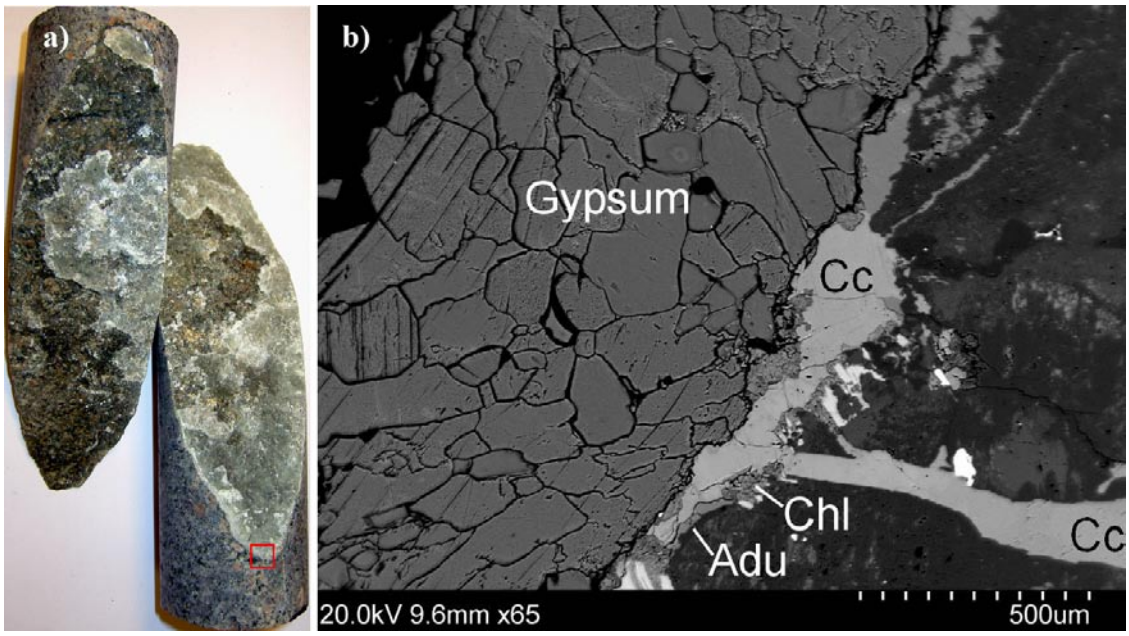

Figure 7-12(a-b). *a) Photograph of the surfaces of an open fracture coated with calcite and gypsum. b) Back-scattered SEM-image of the contact between the wall rock, calcite (Cc), adularia (Adu) chlorite (Chl) and gypsum (the red square in "a"). Sample KLX08: 868.65–868.83 m.*

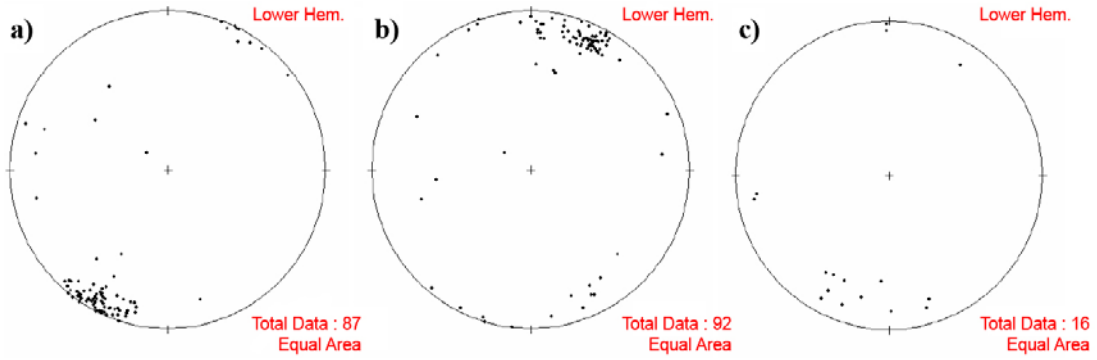

Figure 7-13(a-c). *Stereographic plots showing poles to fracture surfaces (open and sealed) with gypsum (excluding a small number of fractures with altered wall rock). a) KLX03, b) KLX08, c) KLX10. Values from /Ehrenborg and Dahlin 2005a, 2006ab/.*

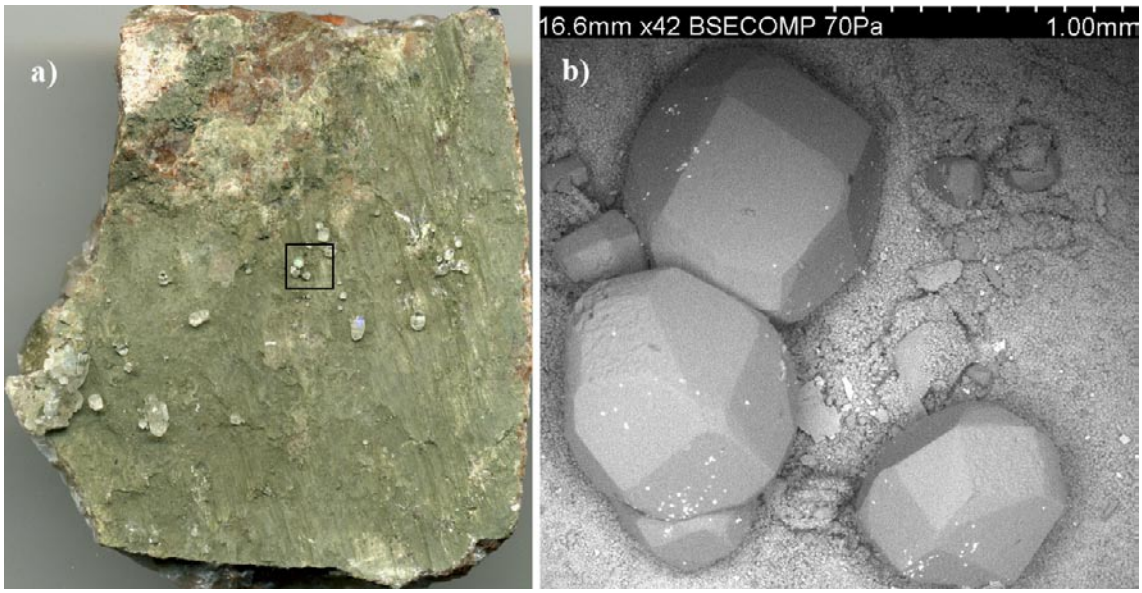

Figure 7-14(a-b). *a) Photograph of calcite crystals on a fracture surface dominated by mixed-layer clay and chlorite. Width of photograph is about 3 cm. b) Back-scattered SEM-image of calcite crystals within the box in figure a. Sample KLX07A: 696.68–696.83 m.*

7.2 Muscovite-quartz-fluorite-pyrite fillings in KLX06

Below the zone ZSMEW002A in KLX06 (and in three fractures below 900 m in KLX10A) there are fractures which have mineralogy and wall rock alteration features (Figure 7-15 and 7-16) different from what is normally found in the Laxemar subarea. These fractures are filled with coarse-grained quartz, muscovite, fluorite, pyrite and some calcite along with smaller amounts of topaz and Fe-Mg-chlorite and trace amounts of Ti-oxide (Nb/Ta-rich), chalcopyrite, sphalerite, sylvite, albite, halite, gold, barite, Fe-oxide, Mn-Fe-oxide, zircon, and sulphides (rich in Cu, As, Sn, Sb and Fe). They are mostly sub-horizontal (Figure 7-17). The wall rock shows high degree of sericitization and the contact between the wall rock and the fracture fillings is often very diffuse. These features indicate greisen-alteration cf /Shcherba 1970/, probably related to the intrusion and/or post-magmatic circulation associated to the nearby Götemar granite. Greisen-alteration features have earlier been observed in outcrops close to the Götemar granite contact with TIB /Kresten and Chyssler 1976/.

Figure 7-15. *Photograph "greisen-like" alteration and coarse-grained pyrite and muscovite. Sample KLX06: 535.10–535.26 m.*

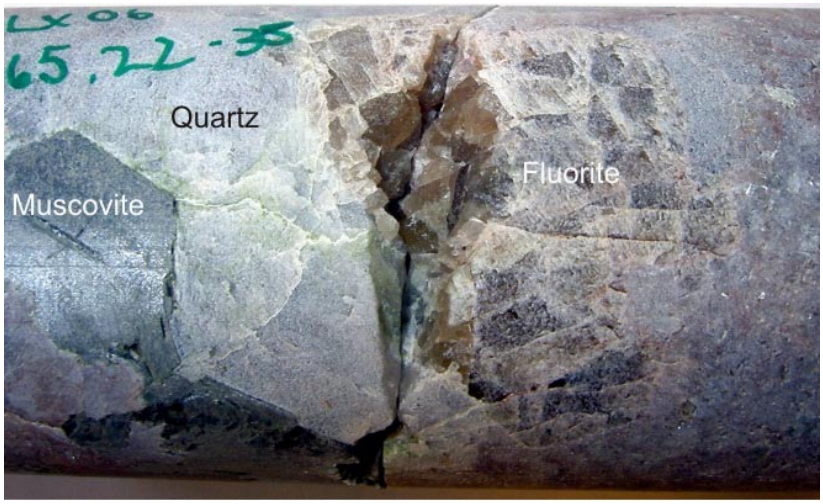

Figure 7-16. *Photograph of coarse-grained muscovite, quartz and fluorite in sample KLX06: 565.22–565.38 m.*

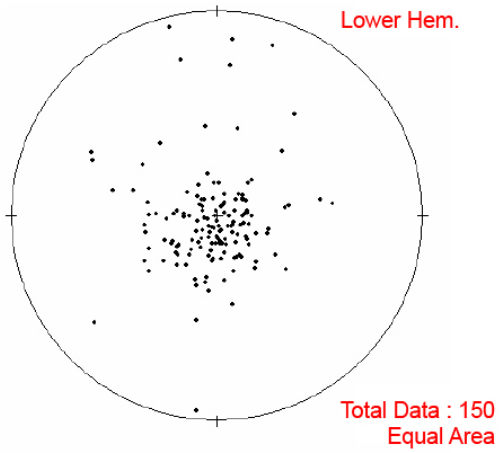

Figure 7-17. *Stereographic plot showing poles to planes of sealed fractures with muscovite. Values from KLX06 /Ehrenborg and Dahlin 2005/.*

7.3 $\delta^{13}C$ and $\delta^{18}O$ in calcite

The stable isotope results ($\delta^{13}C$ and $\delta^{18}O$) are presented in the Appendix 9. The analysed calcite samples are from different generations, based on cross-cutting relations and paragenesis.

$\delta^{13}C$- and $\delta^{18}O$-results show that the calcite samples are similar in isotopic composition to calcite of earlier studies in the area e.g. /Wallin and Peterman 1999, Bath et al. 2000, Tullborg 2000, Drake and Tullborg 2004, Tullborg 2004, Drake and Tullborg 2006a/. They also show that the calcite precipitated at several events with different, mostly hydrothermal conditions (low $\delta^{18}O$, relatively high $\delta^{13}C$, Figures 7-18 and 7-19, generation 3–5) and at moderate temperatures (low $\delta^{13}C$, higher $\delta^{18}O$, generation 5 and later). Calcite in generation 6 mostly have $\delta^{13}C$-values between –20 and –10‰ and $\delta^{18}O$-values between –15 and –9‰ (but also with somewhat higher $\delta^{18}O$ and lower $\delta^{13}C$, see calcite in "young sealed fractures" in Figure 7-19) which is in accordance with calcite, precipitated from "warm brine", in similar paragenesis from Simpevarp, Laxemar, Äspö and Götemar e.g. /Bath et al. 2000, Drake and Tullborg 2004, Tullborg 2004, Drake and Tullborg 2006ab/, interpreted by /Drake and Tullborg 2006b/ to be ~ 400–430 Ma

(based on datings of fluorite by /Sundblad et al. 2004/). Three samples have extremely low $\delta^{13}C$ values (–68 to –55‰) suggesting biogenic activity in the groundwater aquifers causing disequilibria in situ. It should be noted that the fractionation between HCO_3^- and $CaCO_3$ is only a few per mille and the $\delta^{13}C$ value in the calcite therefore largely reflects the $\delta^{13}C$ value in the bicarbonate at the time of calcite formation. In situ activity of microbes indicates temperatures mainly below 100°C and a low temperature origin for these calcites is thus suggested. Assuming formation temperatures as low as the ambient 7–15°C, the calcites may have formed from water similar to the present meteoric or brackish Baltic Sea water at the site (based on fractionation factors by /O'Neil et al. 1969/). Some samples have high $\delta^{18}O$ and low $\delta^{13}C$, which indicate that they might be formed from meteoric to brackish waters.

A plot of the different morphological types of calcite from the present study is shown in Figure 7-19. Needle shaped crystals have quite high $\delta^{18}O$ and $\delta^{13}C$, and equant shaped crystals have somewhat lower $\delta^{13}C$ than the needle shaped crystals. However, scalenohedral crystals have $\delta^{18}O$- and $\delta^{13}C$-values that vary, from "warm brine" type signature to meteoric-brackish to extremely low $\delta^{13}C$. It should be noted that many of the scalenohedral crystals have younger overgrowths (see sample descriptions in appendix), which make interpretation of these samples difficult.

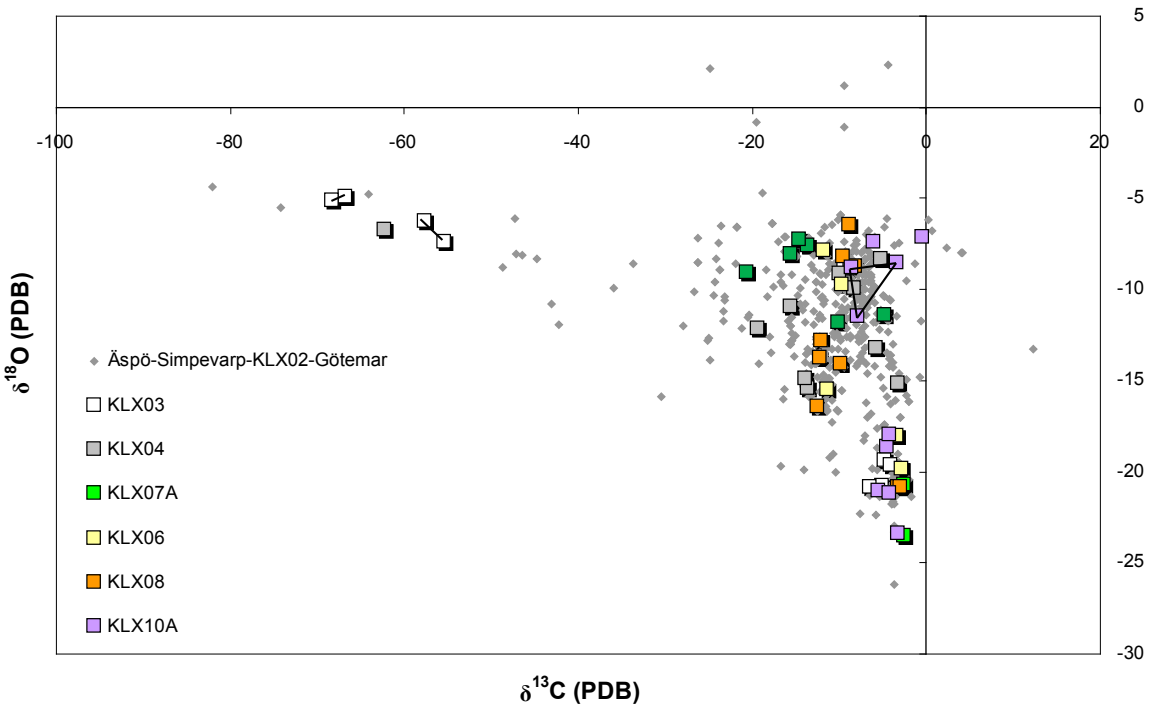

Figure 7-18. *Plot of $\delta^{13}C$ and $\delta^{18}O$ values for fracture calcites from Laxemar plotted together with earlier analysed samples from KSH01 and KSH03, Simpevarp /Drake and Tullborg 2004, 2006a/, KKR02, KKR03, Götemar /Drake and Tullborg 2006b/, and samples from earlier investigations of the Laxemar and Äspö areas /Milodowski et al. 2005 and references therein/. Re-analysed samples are connected by a line.*

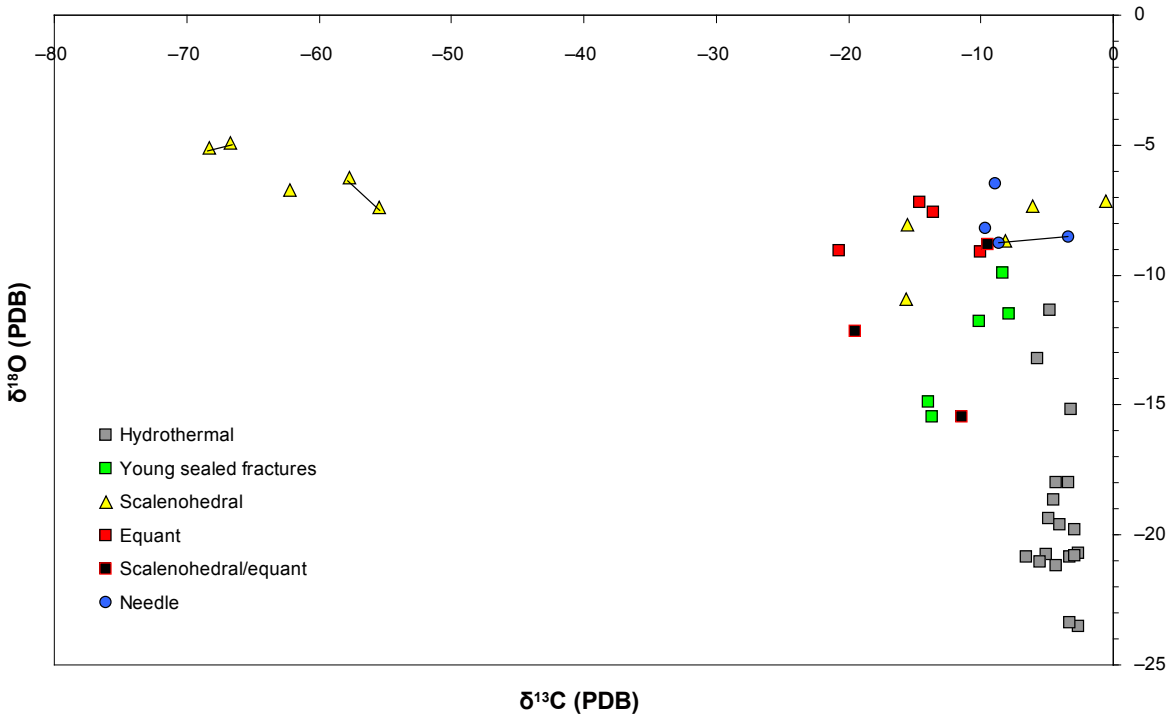

Figure 7-19. *Plot of $\delta^{13}C$ and $\delta^{18}O$ values for different kinds of fracture calcites from Laxemar. Re-analysed samples are connected by a line.*

7.4 $^{87}Sr/^{86}Sr$ in calcite, fluorite and gypsum

The $^{87}Sr/^{86}Sr$ results are presented in the Appendix 9. The analysed calcite and fluorite samples are from different generations, based on cross-cutting relations and paragenesis. The gypsum samples are considered to be of a single generation.

The Sr isotope values in the analysed calcites range from about 0.7071 to 0.7164. A plot of Sr-isotope ratio versus $\delta^{18}O$ values for fracture calcites from the present study along with calcite from KSH01 and KSH03 /Drake and Tullborg 2004, 2006a/, KKR02, KKR03 /Drake and Tullborg 2006b/, and KAS17 (see Appendix 13) is shown in Figure 7-20.

There is positive correlation between $^{87}Sr/^{86}Sr$ ratios and $\delta^{18}O$ values which is in agreement with earlier observations by /Wallin and Peterman, 1999, Bath et al. 2000, Drake and Tullborg, 2004, 2006ab/, showing the lowest $^{87}Sr/^{86}Sr$ isotope ratios and the lowest $\delta^{18}O$ values for the hydrothermal calcites. Especially for Generation 5 the $^{87}Sr/^{86}Sr$-ratios vary and the wide range (from 0.707 to 0.712) supports the suspicion that this "generation" in fact consists of several generations. This also suggest that laumontite may have formed at very different occasions; The major part is formed early in the fracture filling sequence whereas minor amounts are formed late in the sequence.

Calcite from generation 6 shows higher $^{87}Sr/^{86}Sr$-ratios (0.7132–0.7165) than calcite from earlier generations, which is in agreement with similar calcite samples from KSH01 and KSH03, Simpevarp /Drake and Tullborg 2004, 2006a/, although the ratios are generally somewhat higher in the Laxemar samples. However, compared with generation 6 fracture calcites from the Götemar granite the corresponding Sr isotope ratios from Laxemar are generally lower. Since the generation 6 calcite fillings from Simpevarp, Laxemar and Götemar are thought to be coeval /Drake and Tullborg 2006ab/ the differences in $^{87}Sr/^{86}Sr$-ratios are attributed to the local environment during formation. $^{87}Sr/^{86}Sr$-ratios of host rock samples (Appendix 12) show large differences in $^{87}Sr/^{86}Sr$-ratios in different rocks types of the area; Ävrögranite, 0.716009, quartz monzodiorite, 0.713540, fine-grained dioritoid 0.715110 and Götemar granite 0.976111. One possibility is that the local variation of in Sr isotope ratios in generation 6 calcites reflects the

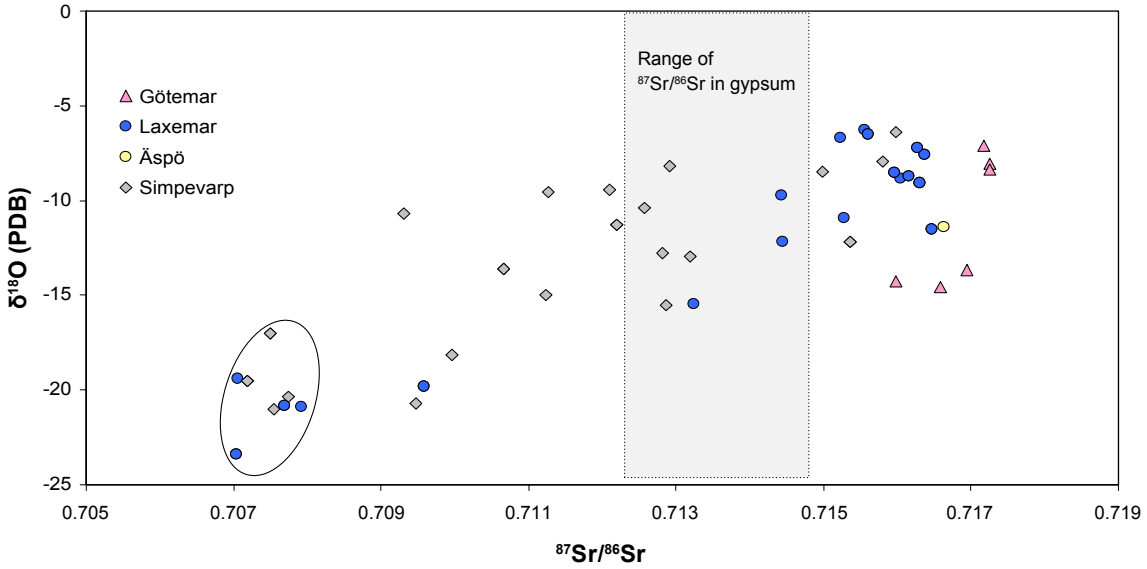

Figure 7-20. *$^{87}Sr/^{86}Sr$-ratios plotted versus $\delta^{18}O$ values for fracture calcites in Laxemar along with calcite from KSH01 and KSH03 /Drake and Tullborg 2004, 2006a/, KKR02, KKR03 /Drake and Tullborg 2006b/, and KAS17 (from the additional data in Appendix 13). Range of the $^{87}Sr/^{86}Sr$-ratio in gypsum is also shown (Gypsum was not analysed for $\delta^{18}O$).*

wall rock chemistry, with generally lower $^{87}Sr/^{86}Sr$-ratios in Simpevarp rocks (mostly quartz monzodiorite, fine-grained dioritoid and quartz monzodioritic Ävrö granite) than in Laxemar (mostly granitic Ävrö granite), which in turn has lower $^{87}Sr/^{86}Sr$-ratios than the Götemar granite (see $^{87}Sr/^{86}Sr$-ratios for the rock types in the appendix).

$^{87}Sr/^{86}Sr$-ratios in gypsum range from 0.7123 to 0.7148 which is similar to the calcites of generation 6 with low $^{87}Sr/^{86}Sr$-ratios. This suggests that gypsum is formed early in generation 6 which is supported by thin section observations.

The fluorite samples analysed for $^{87}Sr/^{86}Sr$-ratios are from four old samples (generation 3 and from the "greisen alteration" fractures in KLX06) and two younger samples (generation 6). The sample from generation 3 (related to epidote) has an $^{87}Sr/^{86}Sr$-ratio of 0.707967 which is very similar to calcite from generation 3. Two of the fluorite samples from the "greisen alteration" fractures have similar $^{87}Sr/^{86}Sr$-ratios as generation 3, although somewhat lower (0.70593 and 0.70676), while one sample has a considerably higher ratio (0.746809). The two generation 6-fluorites have values that are both lower (0.711632) and higher (0.720744) than the calcite from the same samples, which are 0.713247 and 0.716041, respectively.

7.5 $\delta^{34}S$ in pyrite, gypsum and barite

The $\delta^{34}S$ results are presented in the Appendix 9. The analysed pyrite samples are from different generations, based on cross-cutting relations and paragenesis. The gypsum and barite samples are thought to be from a single generation. Figure 7-21 shows the $\delta^{34}S$ results from the present study along with gypsum and pyrite $\delta^{34}S$ results from Simpevarp and Götemar fracture fillings. The old hydrothermal pyrite from generation 3 and from the "greisen-alteration" fractures in KLX06 show $\delta^{34}S$-values of –3 to +3‰ that are characteristic for pyrite formed from quite high temperature hydrothermal fluids or is igneous cf /Ohmoto and Rye 1979, Field and Fifarek 1985/, in accordance with samples from generation 3 from Simpevarp.

The younger pyrite samples have higher $\delta^{34}S$ values (+5 to +55‰, except for one sample which has –42‰). Large fractionation from microbial reduction in situ, in a "closed" system, with a limited sulphate source, is a more possible process for the samples with high $\delta^{34}S$. Microbial

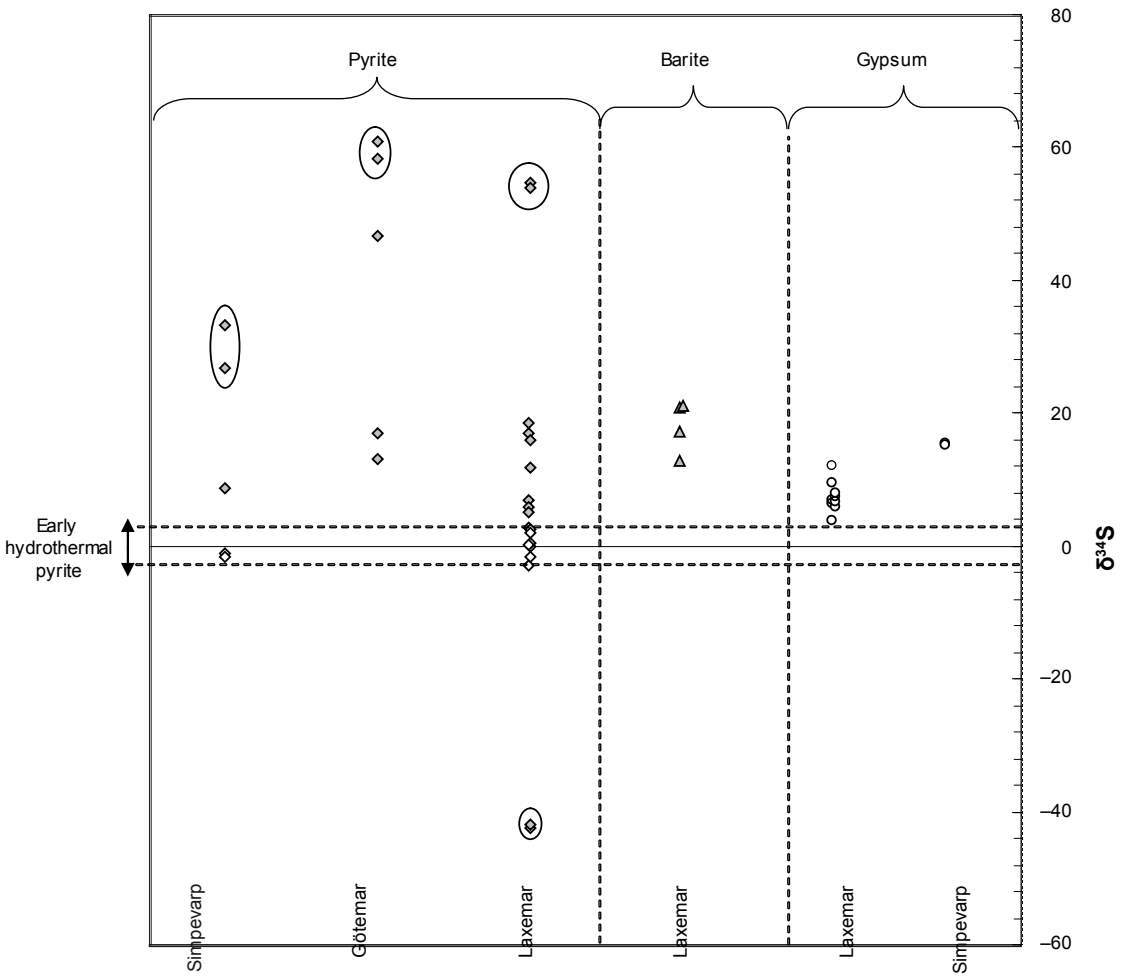

Figure 7-21. *Plot of δ^{34}S-ratios in pyrite, barite and gypsum along with pyrite and gypsum from Simpevarp and Götemar (from Appendix 13 and /Drake and Tullborg 2006b/). Re-analysed samples are indicated by rings.*

sulphate reduction can take place at temperatures up to 100–120°C /Jorgensen et al. 1992, Machel et al. 1995/. These temperatures overlap with those determined from fluid inclusion studies /Alm and Sundblad 2002/ of similar fracture fillings in the Götemar granite. The highest δ^{34}S values in the studied pyrites might be a late stage product in a microbial reduction process, as a fluid undergoing a Rayleigh distillation process of in situ sulphate reduction would incorporate extremely enriched H_2S in the last fraction of deposited pyrite /McKibben and Eldridge 1994/. Large local variations within the system (e.g. within the same fracture, in different fractures and at different depths) or between coeval systems may explain the large differences between the pyrite samples. The δ^{34}S values of the young pyrite (generation 6 and possibly later) overlap with results form the Götemar granite and Simpevarp /Drake and Tullborg 2006b/. The extremely negative δ^{34}S value of one sample is typical for microbial reduction of sulphate e.g. /Ohmoto and Rye 1979/. Microbial influence in the fracture system is also indicated by low δ^{13}C values in calcite of the same generation and/or of the same samples.

Barite samples from the same generation as the young pyrite, have δ^{34}S-values of +12.8, +17.3, +20.8 and +21.0‰. As expected, δ^{34}S values in barite are higher than in the related pyrite in two of the samples. However, one sample has lower δ^{34}S value in barite than in the related pyrite. One sample has no co-precipitated pyrite.

Gypsum $\delta^{34}S$-values are +5.9 to +6.6‰ in KLX03 and +3.7 to +12.1‰ in KLX08, which is slightly lower than values from two samples from KSH03 which are +15.1 and +15.5‰ (see Appendix 13). The generally lower $\delta^{34}S$ values in gypsum compared with barite in combination with the slightly lower $^{87}Sr/^{86}Sr$-ratios of gypsum compared to $^{87}Sr/^{86}Sr$-ratios in barite-related calcite indicate that gypsum and barite are not strictly coeval. Based on the small number of analyses it is proposed that gypsum is probably formed somewhat earlier than barite.

7.6 Trace elements in calcite and gypsum

The trace element results are presented in Appendices 10 and 11. The analysed calcite samples are from different generations, based on cross-cutting relations and paragenesis. The gypsum samples are thought to be from a single generation.

The early formed calcite (generation 3–5) has low REE-values (Figure 7-22), although HREE- enrichment is found in two samples, in accordance with samples from Simpevarp of the same generation /Drake and Tullborg 2004/.

The calcite samples from generation 6 have higher REE-values than older calcite generations (except for KLX04: 925 m). Most of the samples are high in LREE and have a small Eu depletion. The REE-content differs between the samples but the chondrite normalised REE-patterns are very similar (Figure 7-23). The needle shaped crystals show similar patterns as other calcites from generation 6.

Sr concentrations are generally higher in the old hydrothermal calcite samples compared to the samples from generation 6, in accordance with earlier studies from Simpevarp /Drake and Tullborg 2004/. A plot of Sr concentrations vs. $^{87}Sr/^{86}Sr$-ratios in calcite is found in Figure 7-24. This plot shows a negative correlation between $^{87}Sr/^{86}Sr$-ratios and Sr concentrations.

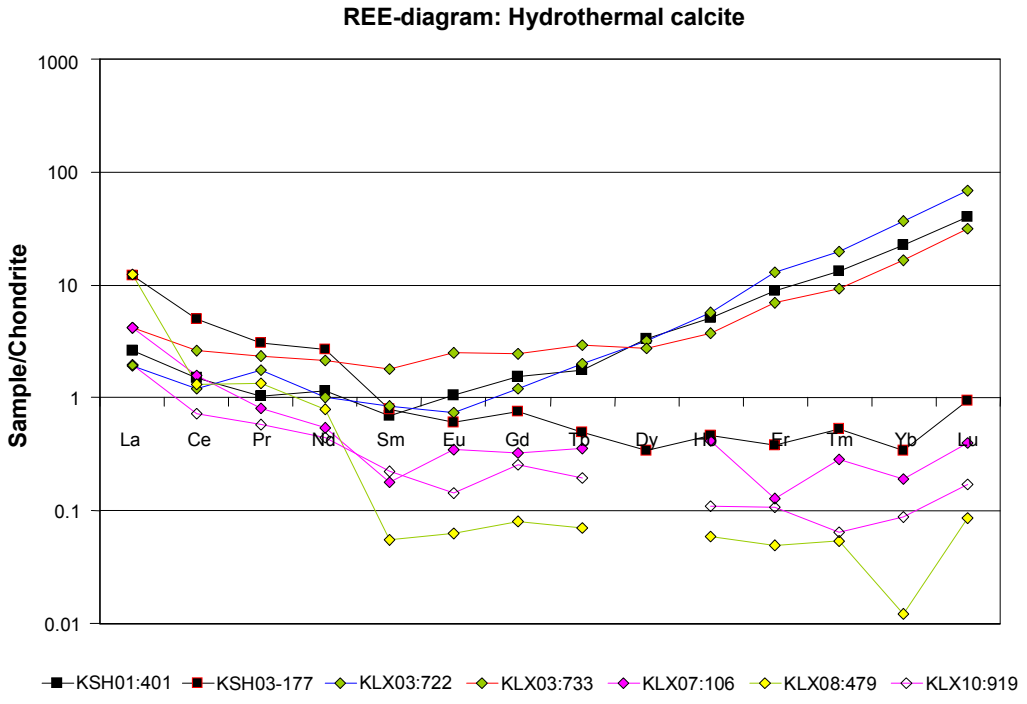

Figure 7-22. *Old hydrothermal calcite (generation 3–5) from Laxemar along with two "KSH"-samples from Simpevarp (from the additional data in Appendix 13 and /Drake and Tullborg 2004/). Chondrite values from /Evansen et al. 1978/.*

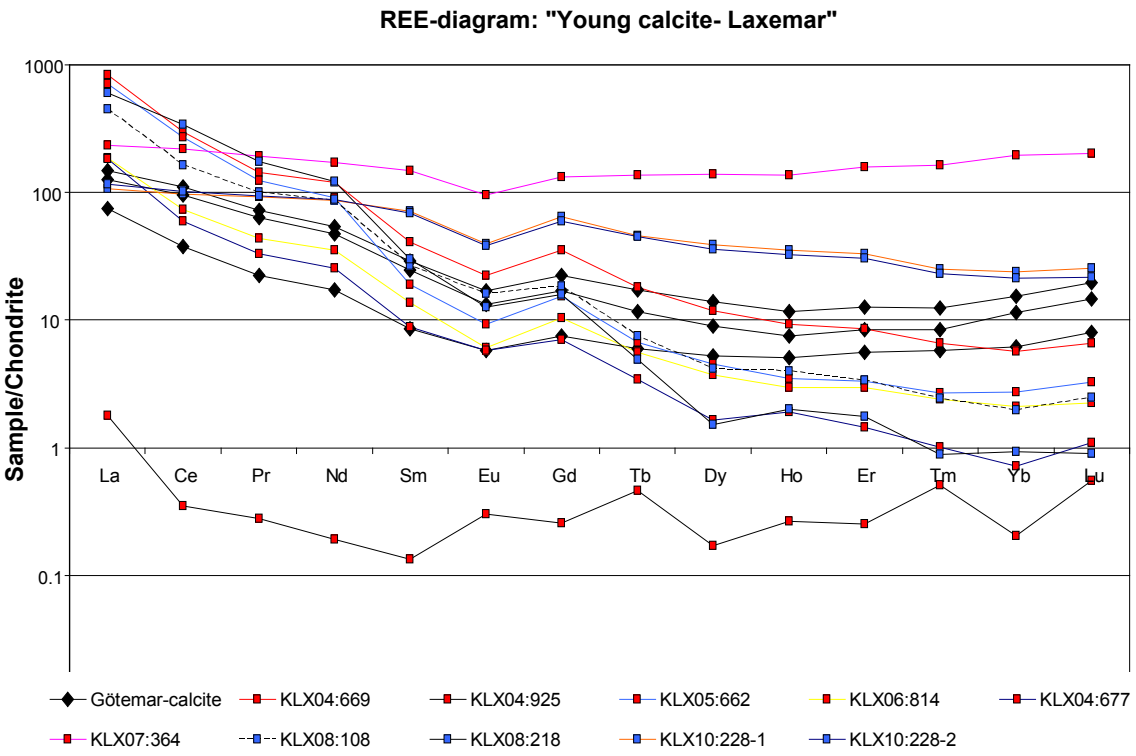

Figure 7-23. *Calcite of generation 6 and 7 from sealed and open fractures plotted together with calcite from calcite-fluorite filled fractures in the Götemar granite (black markers, data in Appendix 13). Needle shaped crystals have blue symbols. Chondrite values from /Evansen et al. 1978/.*

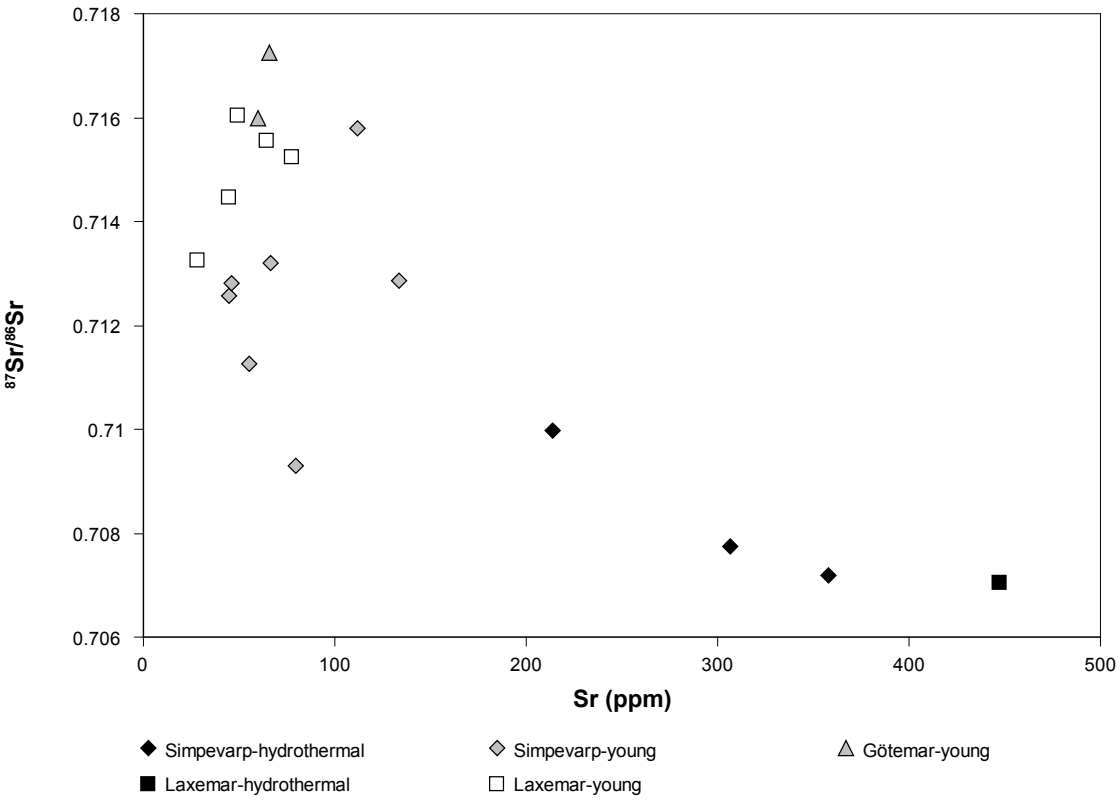

Figure 7-24. *Plot of Sr concentrations vs. $^{87}Sr/^{86}Sr$-ratios for calcite from Laxemar along with samples from Götemar and Simpevarp (from the additional data in Appendix 13 and /Drake and Tullborg 2004, 2006ab/).*

Mn concentrations are very high (> 3,000 ppm) in some calcite samples (especially in some of the samples of generation 6, and all of the needle shaped samples, Figure 7-25). Some of the hydrothermal calcites from generation 3–5 have Mn contents higher than 3,000 ppm. Mg concentrations are less than 150 ppm for all samples, except for two old hydrothermal calcite samples and samples with needle shaped crystals (these have concentrations between 300 and 700 ppm).

The gypsum samples have very low REE-concentrations. One sample (KLX10A: 696 m) is contaminated by biotite. Sr concentrations are between 131 and 221 ppm.

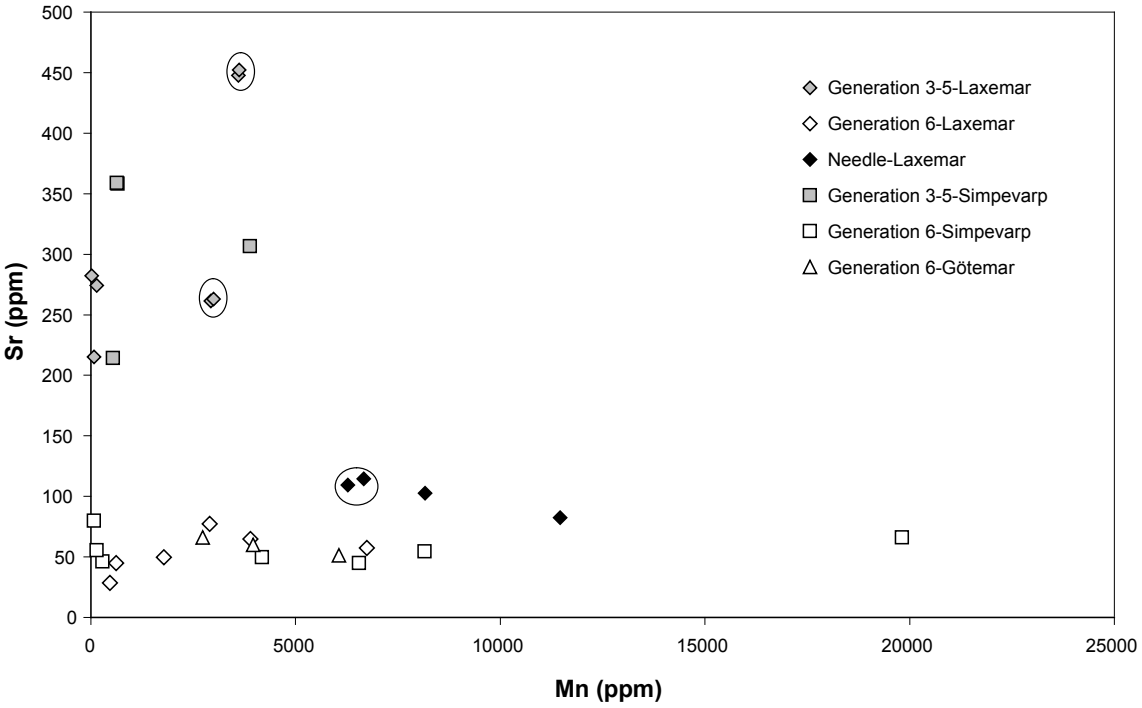

Figure 7-25. *Plot of Sr concentrations vs. Mn concentrations for calcite from Laxemar along with samples from Götemar and Simpevarp (from the additional data in Appendix 13 and /Drake and Tullborg 2004/). Re-analysed samples are within a circle.*

8 Red-stained wall rock

Red-stained wall rock is common adjacent to fractures filled by generation 1–4 and sometimes by generation 5 minerals. Red-stained wall rock is most common in association to deformation zones and prehnite filled fractures. Detailed studies of red-stained rock have been carried out on drill cores KSH01A+B and KSH03A+B, Simpevarp /Drake and Tullborg 2006a/ and KLX04, Laxemar /Drake and Tullborg 2006b/.

The orientation of the fractures with red-stained wall rock was studied for boreholes KLX03, KLX04, KLX06 and KLX07A+B. All fracture with red-stained wall rock was investigated using BIPS and the direction of each fracture was noted using Boremap data from /Ehrenborg and Dahlin 2005abcd/. Younger fractures that cut through red-stained rock were excluded. In KLX06, only the interval 100–305 m was investigated since the rest of the drill core features a major deformation zone (laumontite-altered) and greisen-like alteration. Stereographic plots of fractures (sealed and open) with red-stained wall rock are found in Figure 8-1.

The most common orientation of the fractures with red-stained wall rock is sub-horizontal. Sub-vertical fractures striking E-W and N-S are also quite common.

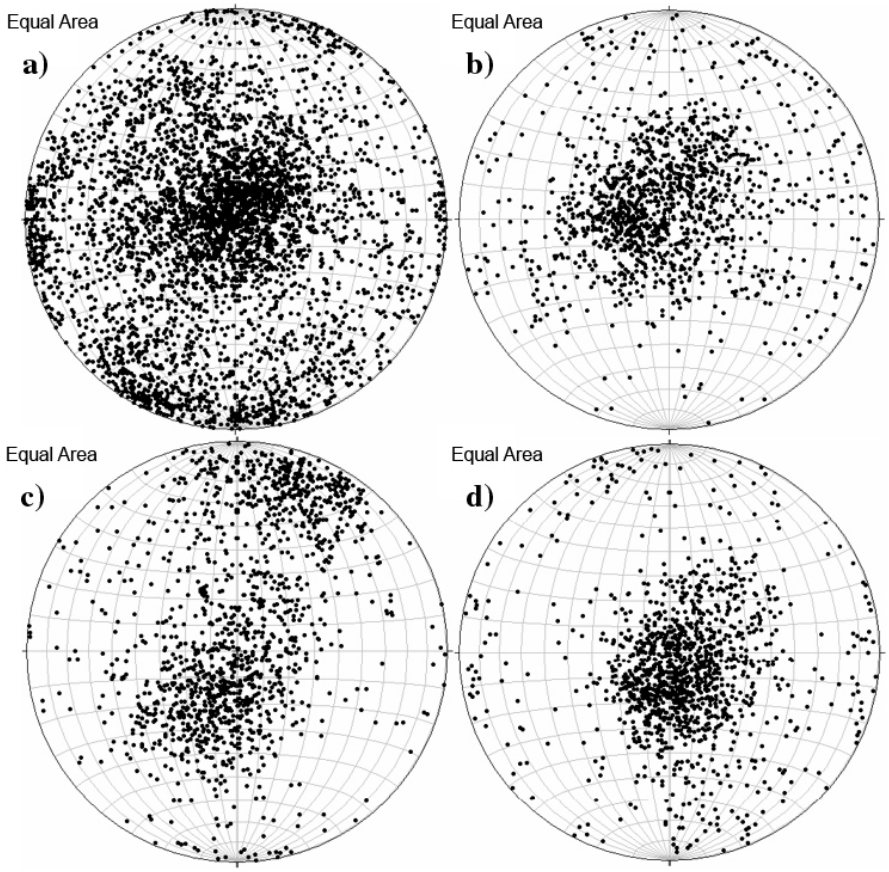

Figure 8-1(a-d). *Stereographic plot showing poles to planes of fractures with red-stained wall rock. a) KLX03, b) KLX04, c) KLX06 (100–305 m), and d) KLX07A+B.*

9 Summary

The characteristics of the fracture fillings are similar in the investigated drill cores from Laxemar to what has earlier been reported from the Simpevarp subarea /Drake and Tullborg 2004, 2006a/ and Äspö /Tullborg 1988, 1997, Drake and Tullborg 2005/. Fracture filling generation 6 from the Laxemar-Simpevarp area is also present in fractures in the Götemar granite /Drake and Tullborg 2006b/.

The fractures are commonly re-activated. Mylonites are often re-activated by cataclasite and later formed brittle fractures. The formation temperatures of the different generations of fracture fillings are successively lower with time, indicated by early formed epidote followed by lower temperature minerals like prehnite and even later zeolites (laumontite and subsequent harmotome). The earliest deformation in the area (mylonites, cataclasites and fractures filled with epidote, prehnite and early formed laumontite) are mainly Pre-Cambrian. It is suggested that fractures filled with e.g. calcite, fluorite, pyrite, gypsum, barite, apophyllite and harmotome is mainly Palaeozoic. Gypsum and apophyllite are more common in the Laxemar subarea than in the Simpevarp subarea where cataclasites are more common. The fracture frequency in the Simpevarp subarea is also higher than in the Laxemar subarea. In borehole KLX06 below the deformation zone ZSMEW002, greisen-like alteration and coarse-grained quartz, muscovite, fluorite and pyrite have been observed. Gypsum-filled fractures and greisen-related fractures have the most preferred directions (sub-vertical NNW-trending and sub-horizontal, respectively), while fractures occupied by minerals of other generations show more random orientations due to re-activation of older fractures, mylonites and cataclasites.

Stable isotopes, Sr-isotopes and trace element analyses confirm that calcite and pyrite have been formed at different events with gradually lower temperatures (and increasing biogenic influence), while all analysed gypsum and probably also barite have been formed during a single period (or less likely at several events under similar conditions).

10 Acknowledgements

We would like to thank the staff at the SKB site investigations at Oskarshamn for their support. Owe Gustafsson at Earth Sciences Centre, Göteborg University carried out the O and C isotope analyses on calcite and trace element analyses on calcite and gypsum. Göran Åberg at Institute for Energy Technology, Norway carried out Sr isotope analyses on calcite, fluorite, gypsum and whole rock samples. Tony Fallick at Scottish Universities Environmental Research Centre, Glasgow carried out sulphur isotope analyses on pyrite, barite and gypsum. Kjell Helge and Ali Firoozan have carried out thin section preparation. Sven Åke Larson, Göteborg University contributed with valuable comments to the manuscript. Björn Sandström, Göteborg University, is thanked for providing references. Fredrik Hartz, SKB, kindly helped us with the map for the area.

11 References

Alm E, Sundblad K, 2002. Fluorite-calcite-galena-bearing fractures in the counties of Kalmar and Blekinge, Sweden. SKB R-02-42. 116 pp. Svensk Kärnbränslehantering AB.

Bath A, Milodowski A, Ruotsalainen P, Tullborg E-L, Cortés Ruiz A, Aranyossy J-F, 2000. Evidences from mineralogy and geochemistry for the evolution of groundwater systems during the quaternary for use in radioactive waste repository safety assessment (EQUIP project). EUR report 19613.

Drake H, Tullborg E-L, 2004. Oskarshamn site investigation. Fracture mineralogy and wall rock alteration, results from drill core KSH01A+B. SKB P-04-250. 120 pp. Svensk Kärnbränslehantering AB.

Drake H, Tullborg E-L, 2005. Oskarshamn site investigation. Fracture mineralogy and wall rock alteration, results from drill cores KAS04, KA1755A and KLX02. SKB P-05-174. 69 pp. Svensk Kärnbränslehantering AB.

Drake H, Tullborg E-L, 2006a. Oskarshamn site investigation. Fracture mineralogy, Results from drill core KSH03A+B. SKB P-06-03. 65 pp. Svensk Kärnbränslehantering AB.

Drake H, Tullborg E-L, 2006b. Oskarshamn site investigation. Fracture mineralogy of the Götemar granite, Results from drill cores KKR01, KKR02 and KKR03. SKB P-06-04. 61 pp. Svensk Kärnbränslehantering AB.

Drake H, Tullborg E-L, 2006c. Oskarshamn site investigation. Mineralogical, chemical and redox features of red-staining adjacent to fractures, Results from drill cores KSH01A+B and KSH03A+B. SKB P-06-01. 115 pp. Svensk Kärnbränslehantering AB.

Drake H, Tullborg E-L, 2006d. Oskarshamn site investigation. Mineralogical, chemical and redox features of red-staining adjacent to fractures, Results from drill core KLX04. SKB P-06-02. 105 pp. Svensk Kärnbränslehantering AB.

Ehrenborg J, Dahlin P, 2005a. Oskarshamn site investigation. Boremap mapping of core drilled borehole KLX03. SKB P-05-24. Svensk Kärnbränslehantering AB.

Ehrenborg J, Dahlin P, 2005b. Oskarshamn site investigation. Boremap mapping of core drilled borehole KLX04. SKB P-05-23. 85 pp. Svensk Kärnbränslehantering AB.

Ehrenborg J, Dahlin P, 2005c. Oskarshamn site investigation. Boremap mapping of core drilled borehole KLX06. SKB P-05-185. Svensk Kärnbränslehantering AB.

Ehrenborg J, Dahlin P, 2005d. Oskarshamn site investigation. Boremap mapping of core drilled boreholes KLX07A and KLX07B. SKB P-05-263. Svensk Kärnbränslehantering AB.

Ehrenborg J, Dahlin P, 2006a. Oskarshamn site investigation. Boremap mapping of core drilled borehole KLX08. SKB P-06-42. Svensk Kärnbränslehantering AB.

Ehrenborg J, Dahlin P, 2006b. Oskarshamn site investigation. Boremap mapping of core drilled boreholes KLX10A, KLX10B and KLX10C. SKB P-report. Svensk Kärnbränslehantering AB (in prep).

Evansen N M, Hamilton P J, O'Nions R K, **1978.** Rare Earth Abundances in Chondritic Meteorites, Geochimica et Cosmochimica Acta, 42, p. 1199–1212.

Field C W, Fifarek R H, 1985. Light stable-isotopes systematics in the epithermal environment. In,1985, Geology and geochemistry of epithermal systems. 2. p. 99–128. Society of Economic Geologists, Socorro, NM, United States.

Gaal G, Gorbatschev R, 1987. An outline of the Precambrian evolution of the Baltic Shield. In,1987, Precambrian geology and evolution of the central Baltic Shield; 1st Symposium on the Baltic Shield. 35. p. 15–52. Elsevier, Amsterdam, International.

Jorgensen B B, Isaksen M F, Jannasch H W, **1992.** Bacterial sulfate reduction above 100 degrees C in deep-sea hydrothermal vent sediments, Science, 258, p. 1756–1757.

Kornfält K A, Wikman H, 1987. Description of the map of solid rocks around Simpevarp. SKB PR-25-87-02. 45 pp. Svensk Kärnbränslehantering AB.

Kornfält K A, Persson P O, Wikman H, **1997.** Granitoids from the Äspo area, southeastern Sweden; geochemical and geochronological data, GFF, 119, p. 109–114.

Kresten P, Chyssler J, 1976. The Götemar Massif in south-eastern Sweden; a reconnaissance survey, Geologiska Föreningen i Stockholm Förhandlingar, 98, Part 2, p. 155–161.

Larson S Å, Berglund J, 1992. A chronological subdivision of the Transscandinavian igneous belt three magmatic episodes? Geologiska Föreningen i Stockholm Förhandlingar, p. 459–461.

Machel H G, Krouse H R, Sassen R, **1995.** Products and distinguishing criteria of bacterial and thermochemical sulfate reduction, Applied Geochemistry, 10, p. 373–389.

Maddock R H, Hailwood E A, Rhodes E J, Muir Wood R, 1993. Direct fault dating trials at the Äspö Hard Rock Laboratory. SKB TR-93-24. 189 pp. Svensk Kärnbränslehantering AB.

McKibben M A, Eldridge C S, **1994.** Micron-scale isotopic zoning in minerals; a record of large-scale geologic processes, Mineralogical Magazine, 58A, p. 587–588.

Milodowski A E, Tullborg E-L, Buil B, Gomez P, Turrero M-J, Haszeldine S, England G, Gillespie M R, Torres T, Ortiz J E, Zacharias, Silar J, Chvatal M, Strnad L, Sebek O, Bouch J, Chenery S R, Chenery C, Sheperd T J, Mc Kervey J A, 2005. Application of Mineralogical, Petrological and Geochemical tools for Evaluating the Palaeohydrogeological Evolution of the PADAMOT Study Sites. PADAMOT Project Technical Report WP2.

Ohmoto H, Rye R O, 1979. Isotopes of sulfur and carbon.; 2. In,1979, Geochemistry of hydrothermal ore deposits. p. John Wiley & Sons, New York, NY, United States.

O'Neil J R, Clayton R N, Mayeda T K, 1969. Oxygen isotope fractionation in divalent metal carbonates, Journal of Chemistry and Physics, 51, p. 5547–5558.

Persson Nilsson K, Bergman T, Eliasson T, 2004. Oskarshamn site investigation. Bedrock mapping 2004 – Laxemar subarea and regional model area. Outcrop data and description of rock types. SKB P-04-221. Svensk Kärnbränslehantering AB.

Robinson B W, Kusakabe M, 1975. Quantitative preparation of sulphur dioxide for $^{34}S/^{32}S$ analyses from sulphides by combustion with cuprous oxide. Analytical Chemistry, 47, p. 1179–1181.

Shcherba G N, 1970. Greisens. International Geology Review, v. 12: 2, p. 114–150.

Sundblad K, Alm E, Huhma H, Vaasjoki M, Sollien D B, **2004.** Early Devonian tectonic and hydrothermal activity in the Fennoscandian Shield; evidence from calcite-fluorite-galena mineralization, In: Mertanen S (ed), Extended abstracts, 5th Nordic Paleomagnetic workshop. Supercontinents, remagnetizations and geomagnetic modelling. Geological Survey of Finland, p. 67–71.

Tullborg E-L, 1988. Fracture fillings in the drillcores from Äspö and Laxemar. In: Wikman.H, Kornfält K-A, Riad L, Munier R, Tullborg E-L, 1988: Detailed investigations of the drillcores KAS02, KAS03 and KAS04 on Äspö Island and KLX01 at Laxemar. SKB PR 25-88-11. 30 pp. Svensk Kärnbränslehantering AB.

Tullborg E-L, 1997. Recognition of low-temperature processes in the Fennoscandian Shield: Doctoral thesis, Earth Science Centre A17, Göteborg University, 35 pp.

Tullborg E-L, 2000. Ancient microbial activity in crystalline bedrock; results from stable isotope analyses of fracture calcites. In,2000, Hydrogeology of crystalline rocks. 34. p. 261–275. Kluwer Academic Publishers, Dordrecht, Netherlands.

Tullborg E-L, **2004.** Palaeohydrogeological evidences from fracture filling minerals_ Results from the Äspö/Laxemar area., Mat. Res.Soc. Symp., Vol 807, p. 873–878.

Wahlgren C-H, Ahl M, Sandahl K-A, Berglund J, Petersson J, Ekström M, Persson P-O, 2004. Oskarshamn site investigation. Bedrock mapping 2003 – Simpevarp subarea. Outcrop data, fracture data, modal and geochemical classification of rock types, bedrock map, radiometric dating. SKB P-04-102. 59 pp. Svensk Kärnbränlehantering AB.

Wahlgren C-H, Bergman T, Persson Nilsson K, Eliasson T, Ahl M, Ekström M, 2005. Oskarshamn site investigation. Bedrock map of the Laxemar subarea and surroundings. Description of rock types, modal and geochemical analyses, including the cored boreholes KLX03, KSH03 and KAV01, SKB P-05-180, Svensk Kärnbränslehantering AB.

Wahlgren C-H, Hermanson J, Forssberg O, Curtis P, Triumf C-A, Drake H, Tullborg E-L, 2006. Oskarshamn site investigation. Geological description of rock domains and deformation zones in the Simpevarp and Laxemar subareas. Preliminary site description Laxemar subarea – version 1.2. SKB R-05-69, Svensk Kärnbränslehantering AB.

Wallin B, Peterman Z, **1999.** Calcite fracture fillings as indicators of palaeohydrogeology at Laxemar at the Äspö Hard Rock Laboratory, southern Sweden. Applied Geochemistry, Vol. 14, p. 953–962.

Åberg G, Löfvendahl R, Levi B, 1984. The Götemar granite-isotopic and geochemical evidence for a complex history of an anorogenic granite, Geologiska Föreningen i Stockholm Förhandlingar, 106, p. 327–333.

Åhäll K-I, 2001. Åldersbestämning av svårdaterade bergarter i sydöstra Sverige. SKB R-01-60. 28 pp. Svensk Kärnbränslehantering AB.

Åhäll K-I, Larson S Å, **2000.** Growth-related 1.85–1.55 Ga magmatism in the Baltic Shield; a review addressing the tectonic characteristics of Svecofennian, TIB 1-related, and Gothian events, GFF, 122, p. 193–206.

Appendix 1

Sample descriptions KLX03

"n.d." = below the detection limit for SEM-EDS.

KLX03: 195.95–196.15 m

Sample type: Surface sample.

Rock type: Ävrö granite.

Fracture: Open, re-activated fracture (270°/88°). Older fracture filling is a 2 mm thick calcite-dominated filling. The open fracture is covered with a thin, dark green to brownish red cover, with scattered minute, glittering crystals, sometimes in aggregates.

Minerals: Harmotome, calcite, pyrite, chlorite/corrensite(?) and hematite.

Euhedral harmotome crystals, with a size of about 10–60 µm, are present in clusters scattered over the fracture surface. Each cluster consists of numerous harmotome crystals along with somewhat scalenohedral, euhedral calcite crystals of less than 50 µm length along the c-axis. Harmotome is much more abundant than calcite. Cubic pyrite crystals (< 10 µm) are present on the crystal surfaces of calcite and harmotome, and thus postdate the formation of these minerals. Aggregates of platy crystals, occasionally attached as spherical aggregates, are also present in the harmotome-rich clusters. These aggregates are made up of chlorite or corrensite, (no proper analysis could be made). Single harmotome crystals are also scattered across the surface of the open fracture.

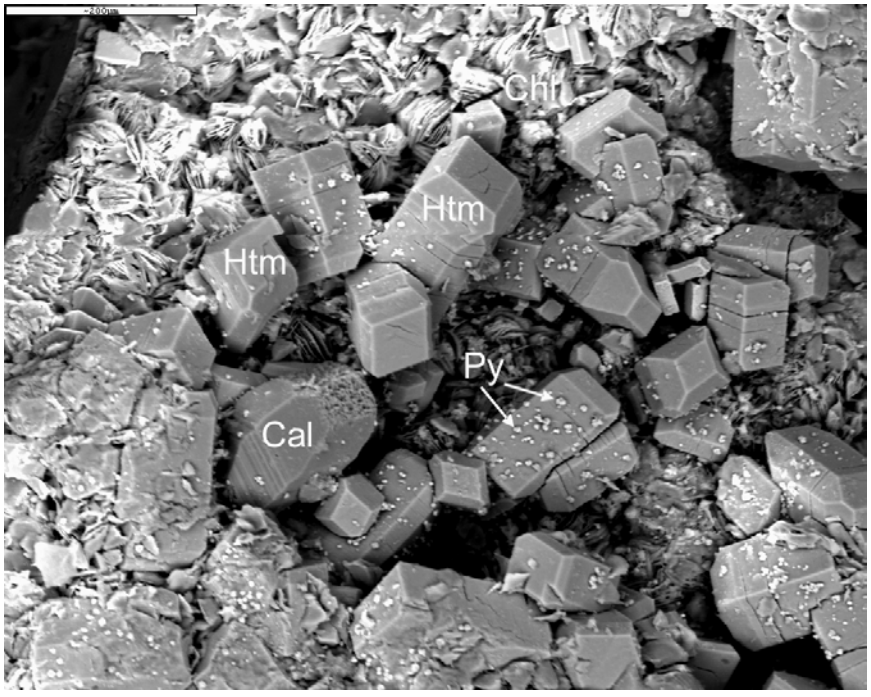

Euhedral harmotome (Htm), calcite (Cal) and aggregates of chlorite/corrensite (Chl). Euhedral pyrite crystals (Py) have grown on the surfaces of harmotome and calcite crystals. Scale bar is 200 µm. Back-scattered SEM-image. Sample KLX03: 195.95–196.15 m

KLX03: 266.62–266.71 m

Sample type: Surface sample.

Rock type: Ävrö granite.

Fracture: Open fracture (171°/38°, 1.0 mm wide) covered with a thin, dark greenish red cover, with scattered minute, glittering crystals, sometimes in aggregates, which are brighter in colour.

Minerals: Harmotome, barite, pyrite, (Cu-, Sn-rich mineral, chlorite, calcite and halite).

Euhedral harmotome crystals, with a size of less than 400 µm, are present in clusters scattered over the surface. Each cluster consists of numerous harmotome crystals along with anhedral to subhedral barite crystals in aggregates, and euhedral, cubic pyrite crystals of 10–80 µm in size. Harmotome is much more abundant than barite and pyrite.

Single (50–60 µm) barite crystals also exist on the fracture surface. Crystals of chlorite, calcite, a Cu-(Sn-) rich mineral and halite are found to a small extent.

KLX03: 416.46–416.58 m

Rock type: Ävrö granite.

Fracture: Sealed fracture (341°/29°) with red-stained wall rock.

Minerals: Quartz and calcite.

Photograph of the drill core KLX03: 416.46–416.58 m.

KLX03: 457.60–457.75 m

Sample type: Surface sample.

Rock type: Ävrö granite.

Fracture: Open fracture (308°/76°, 0.0 mm wide). The fracture surface is partially covered by a whitish grey, glittering cover.

Minerals: Calcite, barite, pyrite and quartz.

The whitish grey cover is made up of calcite and barite. Cubic pyrite is also present. Calcite crystals are scalenohedral and coeval with euhedral barite crystals which are less than 1 mm along the a-axis. All crystals show sign of dissolution.

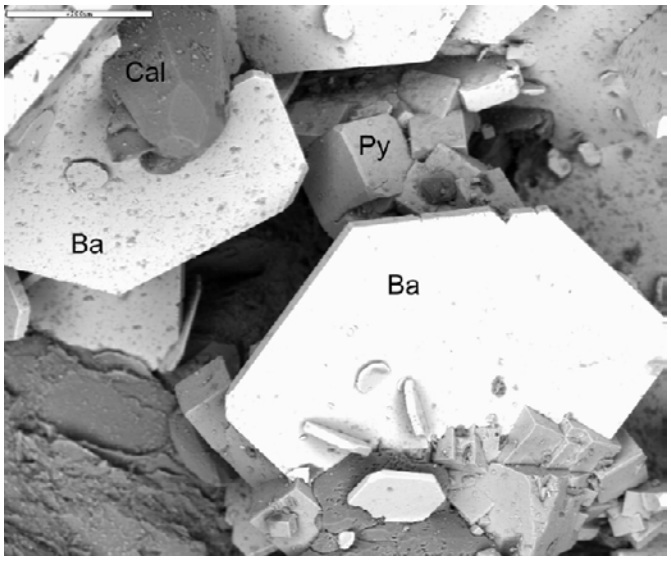

Intergrowth of coeval scalenoedral calcite (Cal), euhedral barite (Ba) and cubic pyrite (Py). Scale bar is 200 µm. Back-scattered SEM-image. Sample KLX03: 457.60–457.75 m.

KLX03: 533.10–533.25 m

Rock type: Ävrö granite.

Fracture: Open fracture with fresh wall rock.

Mineral: Gypsum.

KLX03: 535.58–535.70 m

Rock type: Ävrö granite.

Fracture: Open fracture with fresh wall rock.

Mineral: Gypsum.

Photograph of the drill core KLX03: 535.58–535.70 m showing the fracture surface partially covered with gypsum. Drill core diameter is 50 mm.

KLX03: 572.10–572.30 m

Rock type: Ävrö granite.

Fracture: Open fracture with fresh wall rock.

Minerals: Gypsum.

Photograph of the drill core KLX03: 572.10–572.30 m showing the fracture surface partially covered with gypsum. Drill core diameter is 50 mm.

KLX03: 590.79–590.96 m

Rock type: Ävrö Granite/Diorite-gabbro.

Fracture: Open fracture with fresh wall rock.

Minerals: Gypsum.

KLX03: 591.33–591.33 m

Rock type: Diorite-gabbro/Ävrö granite.

Fracture: Presently open (18°/23°), re-activated fracture originally sealed by quartz and pyrite. The wall rock is fresh.

Minerals: Quartz and pyrite.

Photograph of the drill core KLX03: 591.33–591.33 m showing a re-activated fracture originally sealed by quartz and pyrite. Drill core diameter is 50 mm.

KLX03: 627.26–627.31 m

Rock type: Quartz monzodiorite.

Fracture: Presently open (132°/8°), re-activated fracture originally sealed by quartz and pyrite. The wall rock is slightly red-stained.

Minerals: Quartz and pyrite (mixed layer clay and chlorite on the fracture surface).

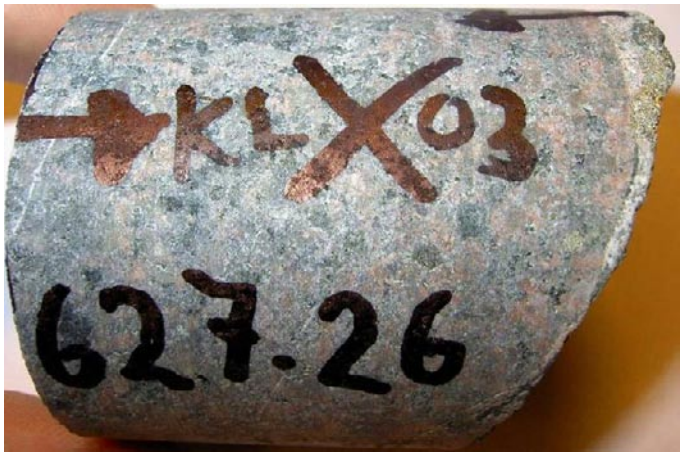

Photograph of the drill core KLX03: 627.26–627.31 m showing a re-activated fracture originally sealed by quartz and pyrite. Drill core diameter is 50 mm.

KLX03: 662.33–662.65 m

Sample type: Surface sample.

Rock type: Quartz monzodiorite.

Fracture: Open fracture. The fracture surface is partially covered by a whitish grey, glittering cover.

Minerals: Calcite, barite, pyrite, galena and quartz.

The cover is mostly made up of scalenohedral calcite but also barite, pyrite, galena and quartz. Some calcite crystals have overgrowths.

Photograph of the drill core KLX03: 662.33–662.65 m showing the surfaces of the open fracture. Drill core diameter is 50 mm.

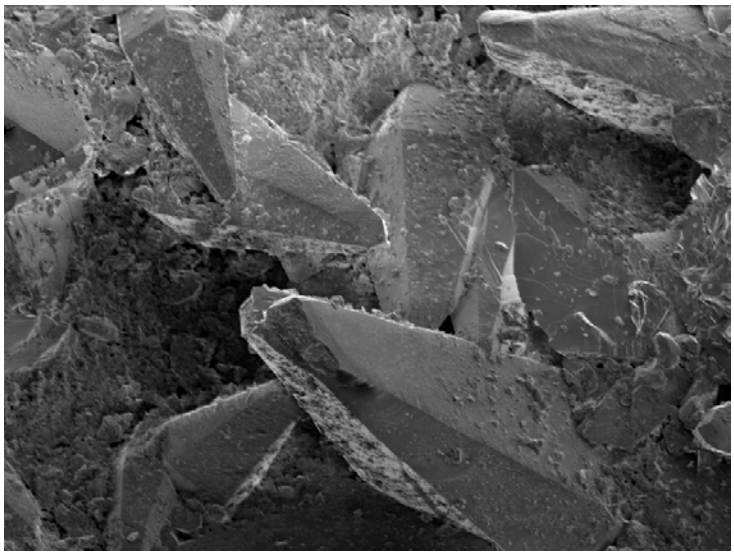

SEM-image of scalenohedral calcite (note the overgrowth on the crystal in the upper right corner). Sample KLX03: 662.33–662.65 m.

KLX03: 722.72–722.96 (I) m

Sample type: Thin section.

Rock type: Quartz monzodiorite.

Fracture: Open fracture (88°/7°, 8.0 mm wide) coated by an old fracture filling made up of several generations. The fracture filling is 10–15 mm thick and consists of dominantly quartz and calcite. The quartz and calcite filling is cut by a green filling made up of chlorite and a reddish filling made up of hematite-stained K-feldspar. Thin fractures filled with prehnite are present close to the open fracture.

Minerals: Quartz, calcite, chlorite, epidote, prehnite, K-feldspar (adularia), fluorite, hematite and pyrite.

Order:

1. Euhedral quartz, calcite (MnO_2=0–1.4%), spherulitic chlorite, epidote, porous K-feldspar (adularia) with Fe(III)-rich minerals (hematite) in voids.
2. A thin prehnite filled fracture is cutting through the minerals in generation 1. Chlorite, calcite and epidote are present as fragments in the prehnite filling and generations 1 and 2 seem to be more or less coeval.
3. Mg-rich chlorite and adularia is observed in voids in prehnite and in fractures through prehnite.
4. Pyrite is found in a thin fracture through prehnite.

Wall rock alteration:

The wall rock is bleached close to the filled fracture, and more reddish 1–2 centimetres away from the fracture. The colour in these sections depends on the features of the plagioclase alteration. The red part is made up of plagioclase pseudomorphs of albite, K-feldspar, muscovite (sericite) and prehnite and the primary albite-twinning is sometimes inherited. The red colour originates from minute hematite crystals in micro-pores in the secondary minerals in the plagioclase pseudomorphs. Whitish parts consist of plagioclase pseudomorphs occupied by well-ordered albite, prehnite and euhedral muscovite. Most biotite is replaced by chlorite.

KLX03: 722.72–722.96 (II) m

Sample type: Thin section.

Rock type: Quartz monzodiorite.

Fracture: Closed fracture (84°/26°) coated by quartz and calcite and filled with dark green chlorite. The fracture has later been re-activated and a 5 millimetre wide fracture filled with prehnite is cutting through the chlorite-quartz-calcite filling.

Minerals: Quartz, calcite, chlorite, epidote and prehnite.

Order:

1. Euhedral quartz, calcite, spherulitic chlorite and epidote.
2. Prehnite is filling a fracture cutting through generation 1 in the fracture filling. Chlorite, calcite and epidote are present as fragments in the prehnite filling and generations 1 and 2 are slightly coeval, probably.

Wall rock alteration:

The wall rock is whitish close to the filled fracture, and more reddish 1–2 centimetres away from the fracture depending on the features of the plagioclase alteration. The red part is made up of plagioclase pseudomorphs of albite, K-feldspar, muscovite (sericite) and prehnite and the primary albite-twinning is sometimes inherited. The red colour originates from minute hematite crystals in micro-pores in the secondary minerals in the plagioclase pseudomorphs. Whitish parts consist of plagioclase pseudomorphs occupied by well-ordered albite, prehnite and euhedral muscovite. Most biotite is replaced by chlorite. Epidote is also present in the wall rock.

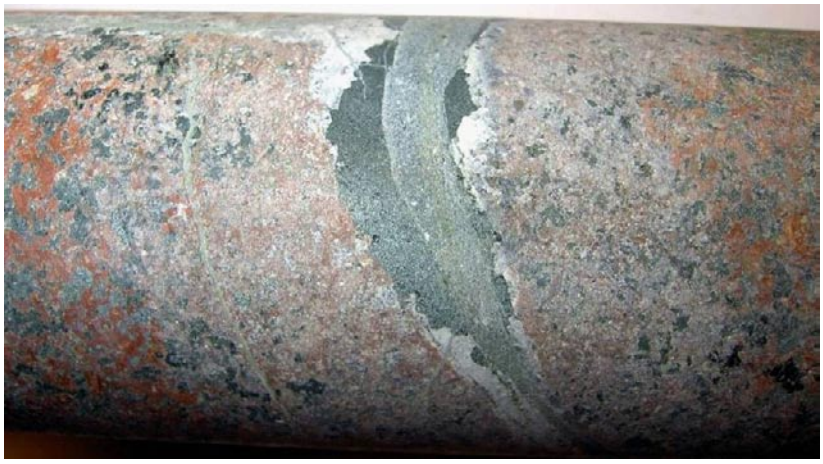

Photograph of the drill core KLX03: 722.72–722.96 m showing a fracture filled with chlorite, calcite and quartz that is cut by a fracture filled with predominantly prehnite. Note the shifting colouration of the wall rock towards the fracture.

KLX03: 733.49–733.53 m

Rock type: Fine-grained granite.

Fracture: Open fracture coated by a 2–3 cm thick old sealing with coarse-grained minerals. The wall rock is red-stained.

Minerals: Quartz, calcite, chlorite, epidote and pyrite.

KLX03: 742.23–742.36 m

Rock type: Fine-grained diorite-gabbro.

Fracture: Sealed fracture.

Minerals: Quartz, pyrite, calcite and chlorite.

Photograph of the drill core sample KLX03: 742.23–742.36 m showing a fracture filled with quartz, pyrite, calcite and chlorite.

KLX03: 897.76–897.89 m

Rock type: Quartz monzodiorite.

Fracture: Sealed fracture (209°/80°) filled with quartz, titanite and later formed epidote.

KLX03: 970.04–970.07 m

Sample type: Surface sample.

Rock type: Quartz monzodiorite.

Fracture: Open fracture (192°/2°, 5.0 mm wide) that borders to a parallel 2 centimetre wide epidote-dominated mylonite/cataclasite. The fracture surface is covered by a less than 3 millimetre thick greyish white cover. Platy euhedral crystals are visible macroscopically on the surface.

Minerals: Apophyllite, (calcite and barite).

Platy, euhedral apophyllite crystals of sizes up to 1 millimetre covers most of the surface. Small amounts of calcite and barite are also present.

Appendix 2

Sample descriptions KLX04

KLX04: 114.12–114.33 m

Rock type: Ävrö granite.

Fracture: Open fracture (332°/53°), coated by several generations of earlier formed fracture fillings.

Minerals: Calcite, quartz, chlorite, prehnite, K-feldspar and hematite.

KLX04: 188.19–188.39 m

Rock type: Ävrö granite.

Fracture: Partially open fracture (318°/26°), re-activating an old sealed fracture containing epidote and fluorite. The wall rock is faintly red-stained.

Minerals: Epidote and fluorite.

Photograph of the drill core KLX04: 188.19–188.39 m showing a fracture filled with epidote (green) and fluorite (purple).

KLX04: 274.65–274.92 m

Rock type: Fine-grained dioritoid.

Fracture: Sealed network of prehnite filled fractures and a dark brown filling (adularia, chlorite and hematite; main fracture has orientation: 61°/43°). Prehnite is cut by a thin fracture filled with quartz.

Minerals: Prehnite, adularia, chlorite, hematite and quartz.

Photograph of the drill core KLX04: 274.65–274.92 m.

KLX04: 322.04–322.25 m

Sample type: Thin section.

Rock type: Ävrö granite.

Fracture: Strongly deformed sample consisting of homogenous cataclasite/breccia sealed by prehnite and subsequently by e.g. calcite, illite and laumontite. The largest calcite-filled fractures have an orientation of (350°/35°).

Minerals: Prehnite, illite, adularia, laumontite, calcite, hematite, quartz and barite.

Order:

1. The earliest formed part of the sample (except for wall rock fragments) is dominated by prehnite, which is formed in several pulses (both fine-grained and coarse-grained). Subsequent dissolution of euhedral prehnite crystals is common.
2. Illite, adularia (euhedral with additional euhedral quartz) and fine-grained hematite fill voids that are coated by euhedral and partly dissolved prehnite. Mn-rich calcite (without twin-lamellae) often fills the centre of the void. Laumontite that is coeval with illite and adularia cuts through prehnite in fractures coated by hematite and fill voids together with illite. The calcite might be considerably younger than the other minerals.
3. Mn-poor calcite (<0.4% MnO_2) in a thin fracture that is cutting through illite. This calcite is found together with barite and hematite.

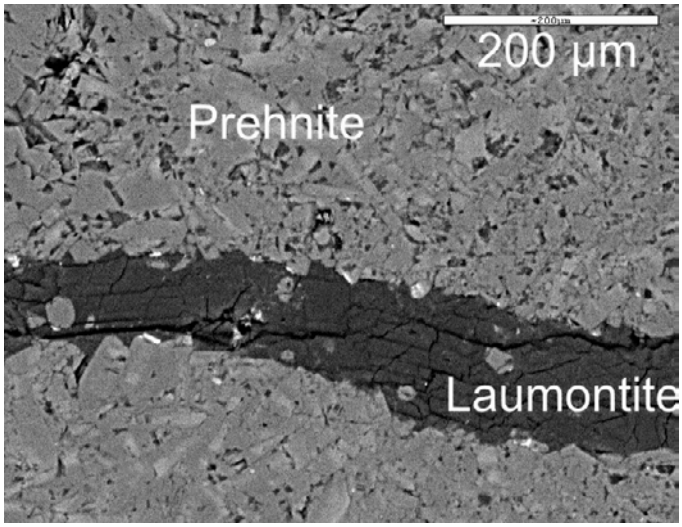

Back-scattered SEM-image of a laumontite-filled fracture cutting through earlier formed prehnite. Sample KLX04: 322.04–322.25 m.

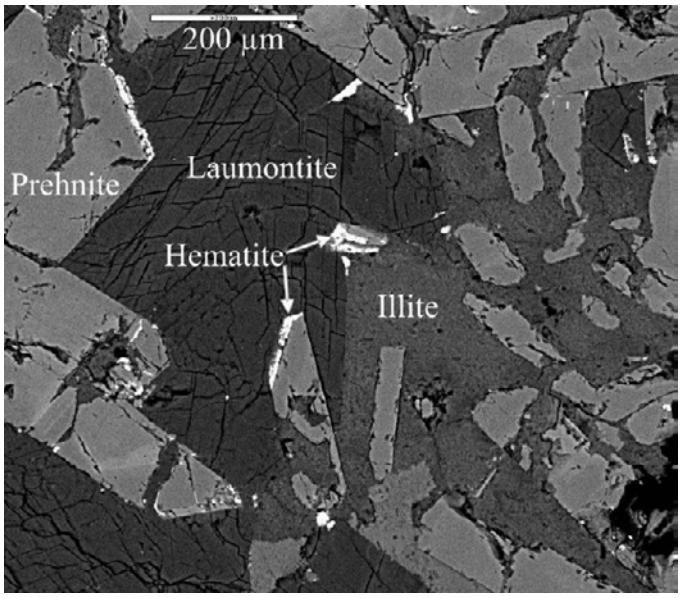

Back-scattered SEM-image showing parts of a fracture coated by partly dissolved prehnite crystals. The fracture is subsequently filled with illite, laumontite and hematite. Sample KLX04: 322.04–322.25 m.

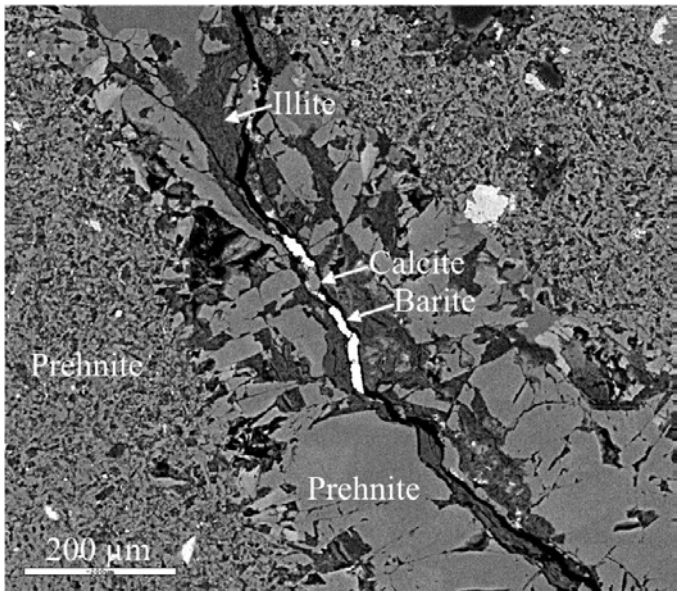

Back-scattered SEM-image of prehnite (both as fine-grained and more coarse-grained varieties) that is cut by a fracture filled with illite and subsequently barite, calcite and hematite (not visible in this image). Sample KLX04: 322.04–322.25 m.

KLX04: 346.46–346.58 m

Rock type: Ävrö granite.

Fracture: Several generations of cataclasite cut by two calcite filled fractures of different orientation (one is 318°/43°).

KLX04: 349.66–349.79 m

Sample type: Thin section.

Rock type: Ävrö granite.

Fracture: Several generations of cataclasites and some calcite filled fractures.

Minerals: K-feldspar, titanite, albite, quartz, chlorite, adularia, calcite, epidote, illite, hematite, corrensite, U-silicate and pyrite.

Order:

1. Red-stained fine-grained filling consisting mainly of crushed wall rock with more coarse-grained fragments from the wall rock (quartz, K-feldspar, titanite etc.). The fine-grained part of the filling is stained with hematite.
2. Thin fractures filled with adularia, calcite and illite (+some Mg-rich chlorite). Fe-rich chlorite, corrensite and small amounts of hematite are found in these fractures as well. Pyrite is found in some thin fractures along with calcite. Additional crystals of U-silicate are also present along with calcite.

KLX04: 669.31–669.55 m

Sample type: Surface sample.

Rock type: Ävrö Granite.

Fracture: Open fracture (310°/63°) re-activating an older 1–2 cm wide calcite-filled fracture.

Minerals on the fracture surface: Calcite (scalenohedral), barite, pyrite and quartz.

Photograph of the drill core KLX04: 669.31–669.55 m showing the surface of the open fracture. Drill core diameter is 50 mm.

KLX04: 673.78–674.05 m

Sample type: Surface sample.

Rock type: Fine-grained diorite-gabbro.

Fracture: Open fracture (102°/89°) re-activating an older 1–2 cm wide calcite-filled fracture.

Minerals: Calcite (scalenohedral), hematite and pyrite.

The fracture surface is covered with hematite. Calcite and pyrite (cubic) is found on top of hematite.

Photograph of the drill core KLX04: 673.78–674.05 m showing hematite (red) and pyrite (small crystals) on the surface of the open fracture.

KLX04: 677.39–677.70 m

Rock type: Fine-grained diorite-gabbro.

Fracture: Open fracture (296°/87°). The fracture has re-activated a 5 millimetre wide undulating fracture. Sulphides and other minerals have grown on calcite crystals from the old fracture filling. Parts of the surface are red-stained.

Minerals: Calcite (scalenohedral/equant), chalcopyrite, adularia, hematite, pyrite, barite, fluorite and a Cu-(Sn-, Ni-) rich mineral.

The fracture coating is dominated by calcite. On top of the calcite crystals are big subhedral crystals of chalcopyrite. Small pyrite crystals are present in very small amounts.

The red-stained parts consist of subhedral to euhedral calcite and adularia, which are less then 10 in μm size, with fine-grained hematite coatings on the crystal surfaces.

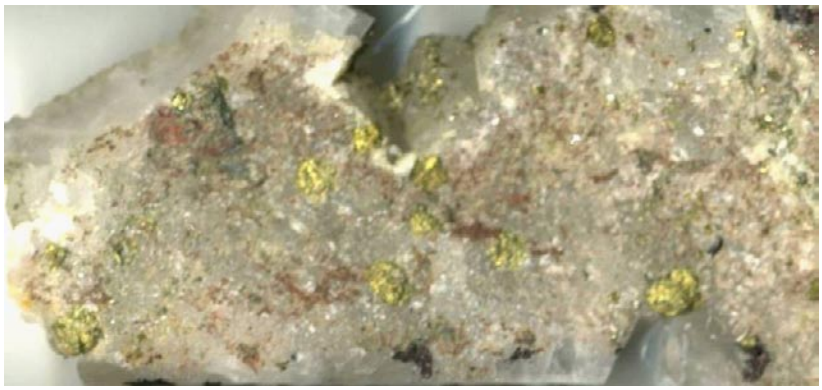

Photograph of the fracture surface sample that was investigated with SEM-EDS. Three features that are visible macroscopically are abundant calcite, chalcopyrite and hematite-stained sections. Width of the photograph is 32 mm. Sample KLX04: 677.39–677.70 m.

KLX04: 878.18–878.24 m

Rock type: Fine-grained diorite-gabbro.

Fracture: Sealed fracture (61°/40°). The fracture is filled with prehnite. The prehnite-filled fracture is re-activated and sealed by hematite and calcite.

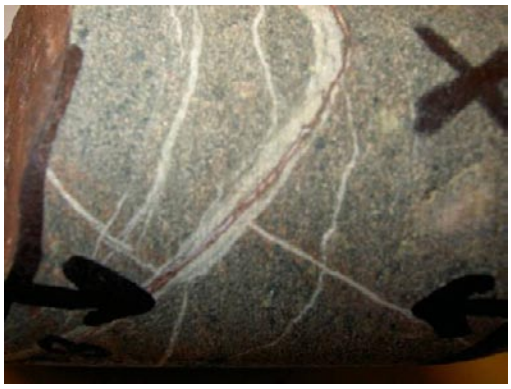

Photograph of the drill core KLX04: 878.18–878.24 m.

KLX04: 925.60–925.68 m

Sample type: Surface sample.

Rock type: Granite.

Fracture: Open fracture (129°/72°).

Minerals: Fluorite, calcite (equant), pyrite, barite, Cu-(Sn-, Ni-) rich mineral, quartz, (adularia and, hematite).

The fracture surface is mainly coated with purple, cubic fluorite crystals and equant calcite crystals. The other minerals are only found in small amounts.

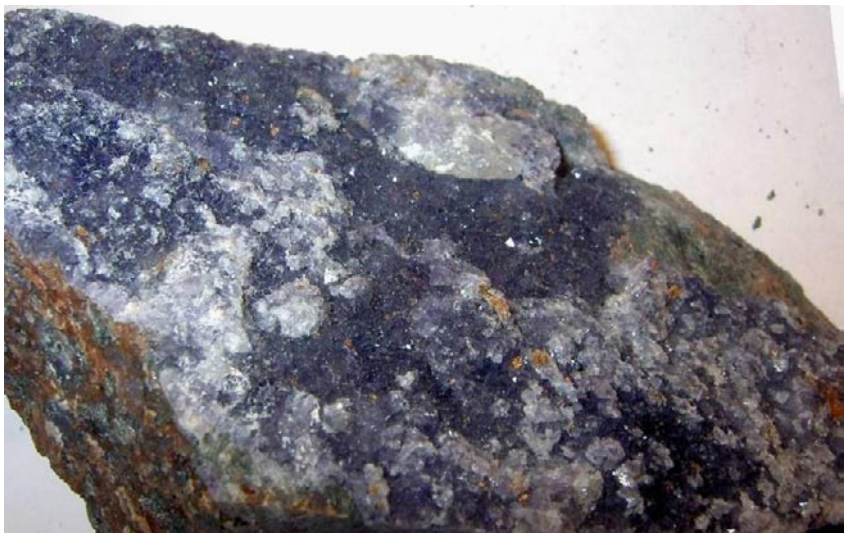

Photograph of the drill core KLX04: 925.60–925.68 m showing fluorite (purple) and calcite (white) on the surface of the open fracture.

KLX04: 970.48–970.52 m

Rock type: Ävrö granite.

Fracture: Cataclasites and sealed fractures.

At least two varieties of cataclasites are cut by two fractures. The first formed fracture is filled with laumontite and the second is filled with calcite.

Photograph of the drill core KLX04: 970.48–970.52 m showing cataclasites (one brown and one green variety) cut by a laumontite-filled fracture (L) which is cut by a calcite-filled fracture (C).

Appendix 3

Sample descriptions KLX06

KLX06: 321.01–321.16 m

Sample type: Thin section.

Rock type: Granite.

Fracture: 15–20 mm wide sealed fracture, containing mostly prehnite and fluorite. Orientation of upper rim is 325°/48° and orientation of lower rim is 325°/46°. Numerous thin fractures filled with dark reddish material are cutting through the prehnite filling. Red-stained wall rock.

Minerals: Prehnite, fluorite, hematite, Mn-rich epidote and pyrite.

Order:

1. The major part of the fracture filling consists of prehnite and subordinately of coeval fluorite. The filling contains wall rock fragments (quartz, K-feldspar and red-stained plagioclase pseudomorphs).
2. Hematite (euhedral) occupies fractures cutting through prehnite. Prehnite and Mn-rich epidote is also present in these fractures. Most of the reddish filling cutting through prehnite is however a later pulse of prehnite with hematite-staining (about 1 µm big hematite crystals)
3. Mg-rich chlorite and adularia are present in voids in the prehnite filling and fractures in fractures cutting through prehnite.
4. Pyrite is present in a thin fracture through prehnite.

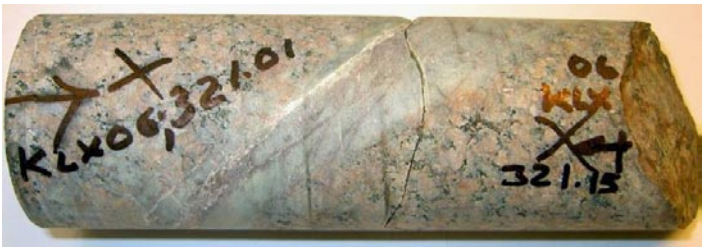

Photograph of the drill core KLX06: 321.01–321.16 m.

KLX06: 333.53–333.67 m

Rock type: Ävrö granite.

Fracture: 20 mm wide sealed fracture, containing mostly prehnite and subordinately fluorite. Orientation of upper rim is 313°/30° and orientation of lower rim is 310°/26°. The wall rock is red-stained.

Minerals: Prehnite and fluorite.

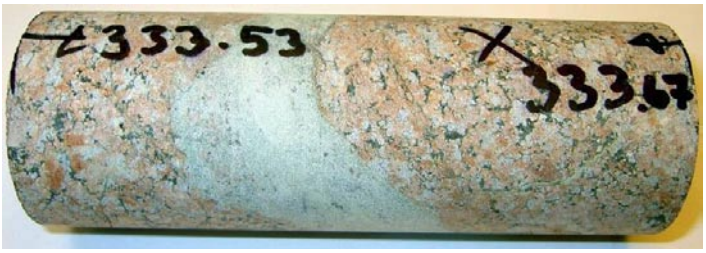

Photograph of the drill core KLX06: 333.53–333.67 m.

KLX06: 381.42–381.58 m

Rock type: Mylonite.

Fracture: Mylonite cut by hematite-cataclasite (adularia, chlorite and hematite etc).

Photograph of the drill core KLX06: 381.42–381.58 m.

KLX06: 384.23–384.28 m

Sample type: Thin section.

Rock type: Cataclasite with extremely fine-grained parts, consisting of hematite-stained wall rock material. Laumontite seals subsequently formed fractures.

Fracture: Laumontite fills fractures of different orientations but orientation 100°/52° is most common.

Minerals: Laumontite, hematite, adularia, epidote, chlorite, corrensite and illite.

Order:

1. Very fine-grained filling consisting Fe/Mg-chlorite, epidote and muscovite along with small amounts of wall rock fragments. The filling is stained with very fine-grained hematite crystals. Bigger aggregates of epidote crystals also occur within this filling. Later laumontite of (generation 2 in this sample) is also present in this filling.
2. Euhedral laumontite is present in fractures cutting through the fine-grained filling and epidote aggregates of generation 1, respectively. Small hematite crystals and small amounts of illite and adularia are found together with laumontite.
3. Hematite, corrensite and illite occupy very thin fractures (c. 1–5 µm wide) that cut through the laumontite fillings. Illite seems to be oldest of these three minerals.

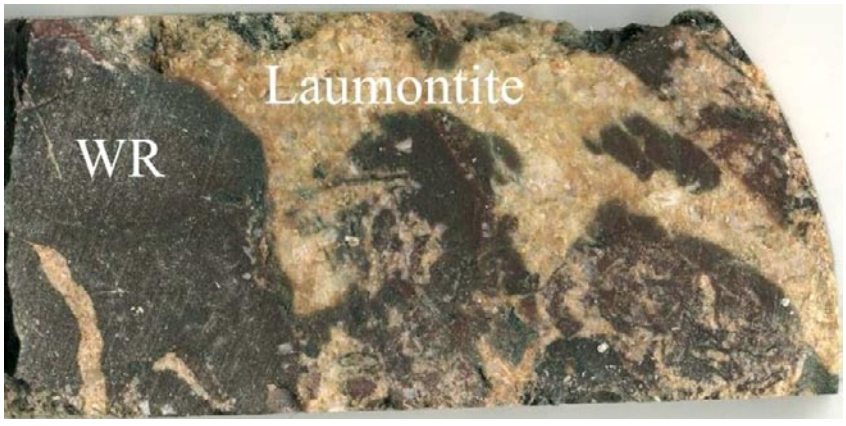

Photograph of the rock chip used for thin section preparation, showing red-stained fine-grained wall rock material (WR) and subsequently formed bright coloured laumontite. Sample KLX06: 384.23–384.28 m.

KLX06: 387.95–388.07 m

Sample type: Thin section.

Rock type: Ävrö granite.

Fracture: Sealed, 10 millimetre wide, fracture with orientation 75°/72°. The fracture is primary filled with green to yellow epidote. The fracture has been re-activated and subsequently filled with a more reddish material.

Minerals: Epidote, quartz, hematite, chlorite, adularia, titanite.

Order:

1. Fairly homogenous filling of fine-grained epidote along with smaller crystals of titanite and some K-feldspar is the earliest formed filling in this sample.
2. Fine-grained brown-to reddish brown filling consisting of Fe-Mg-chlorite, hematite, quartz, epidote and titanite is formed subsequently to the epidote-rich filling in generation 1 in this sample.
3. Thin fractures filled with quartz are cutting through earlier formed fillings. Quartz is occasionally accompanied by partly spherulitic hematite, some Fe-Mg-chlorite and adularia.

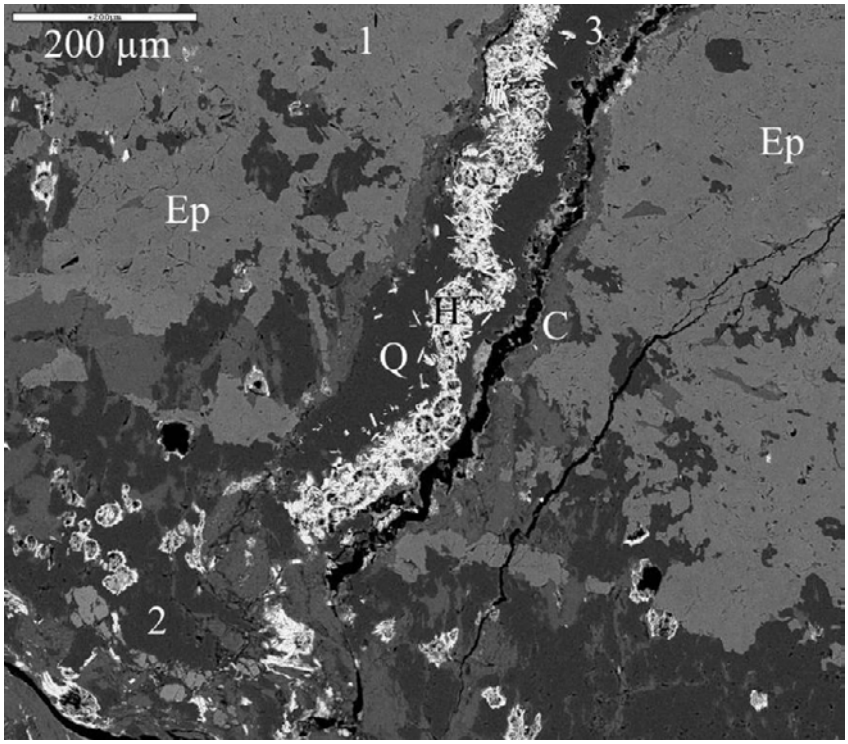

Back-scattered SEM-image of three generations of fracture fillings. Generation 1 consists of e.g. epidote (Ep), K-feldspar and titanite. Generation 2 consists of Fe-Mg-chlorite, hematite, quartz, epidote and titanite. Generation 3 consists of Fe/Mg-chlorite (C), quartz (Q), hematite (H) and adularia. Sample KLX06: 387.95–388.07 m

KLX06: 392.23–392.57 m

Rock type: Ävrö granite.

Fracture: Laumontite-altered rock with small amounts of calcite.

KLX06: 394.83–394.96 m

Rock type: Ävrö granite.

Fracture: Laumontite-altered rock with small amounts of calcite.

KLX06: 446.67–446.80 m

Rock type: Ävrö granite.

Fracture: Open fracture with old millimetre-wide coating.

Minerals: Quartz and muscovite.

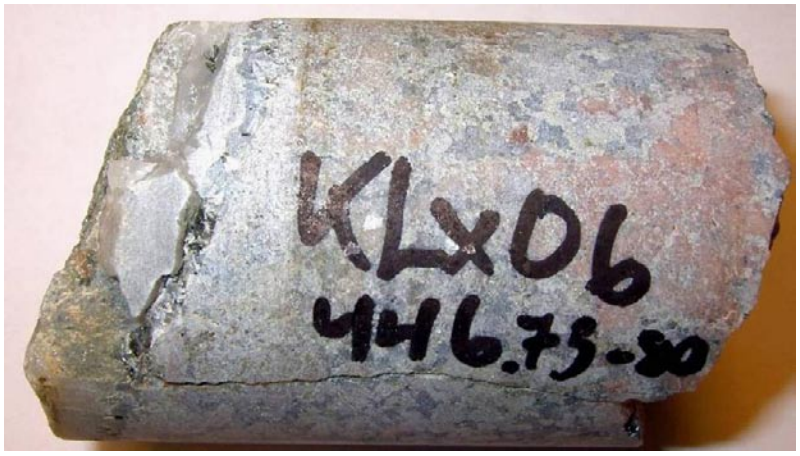

Photograph of the drill core KLX06: 446.67–446.80 m.

KLX06: 472.84–472.92 m

Rock type: Ävrö granite.

Fracture: Open fracture with old centimetre-wide coating.

Minerals: Muscovite, quartz and fluorite.

KLX06: 499.03–499.13 m

Rock type: Fine-grained diorite-gabbro.

Minerals: Quartz and titanite.

KLX06: 535.10–535.26 m

Sample type: Surface sample.

Rock type: Fine-grained diorite-gabbro.

Fracture: 2–3 cm wide, sealed fracture coated by coarse-grained muscovite and filled with coarse-grained pyrite and small amounts of calcite.

Minerals: Muscovite, pyrite, calcite and quartz.

KLX06: 535.40–535.50 m

Rock type: Fine-grained diorite-gabbro.

Fracture: 4–5 cm wide, sealed fracture filled with coarse-grained quartz, muscovite, pyrite and fluorite (yellowish green). Diffuse contact to the wall rock, which is heavily sericitized.

Minerals: Quartz, muscovite, pyrite and fluorite.

Photograph of the drill core KLX06: 535.40–535.50 m.

KLX06: 557.81–557.91 m

Rock type: Granite.

Fracture: Open fracture with old millimetre-wide coating. The wall rock is heavily sericitized.

Minerals: Muscovite and fluorite.

KLX06: 565.22–565.38 m

Rock type: Granite.

Fracture: About 10 cm wide, filled with coarse-grained quartz, muscovite and fluorite. Diffuse contact to the wall rock, which is heavily sericitized.

Minerals: Quartz, muscovite and fluorite.

KLX06: 566.25–566.35 m

Rock type: Granite.

Fracture: Open fractures coated by old muscovite, quartz and pyrite. Diffuse contact to the wall rock, which is heavily sericitized.

Minerals: Muscovite, pyrite and quartz..

KLX06: 572.40–572.46 m

Rock type: Fine-grained diorite-gabbro.

Fracture: 4 cm wide, sealed fracture filled with coarse-grained quartz, muscovite and fluorite (red). Diffuse contact to the wall rock, which is heavily sericitized.

Minerals: Quartz, muscovite and fluorite.

Photograph of the drill core KLX06: 572.40–572.46 m.

KLX06: 576.09–576.21 m

Sample type: Surface sample.

Rock type: Fine-grained diorite-gabbro.

Fracture: Open fracture (303°/77°, 0 mm wide) with brown (titanite) and black (hornblende) minerals on the fracture surface.

Minerals: Titanite and hornblende.

KLX06: 590.66–590.72 m

Rock type: Ävrö granite.

Fracture: Open fractures coated by a 5 mm thick, old filling which consist of muscovite, quartz, pyrite and fluorite. Diffuse contact to the wall rock, which is heavily sericitized.

Minerals: Muscovite, pyrite, quartz and fluorite.

Photograph of the drill core KLX06: 590.66–590.72 m. The coating is made up of muscovite, pyrite, quartz and fluorite.

KLX06: 593.40–593.55 m

Rock type: Ävrö granite.

Fracture: About 10 cm wide, filled with coarse-grained quartz, muscovite, K-feldspar, fluorite and calcite. Diffuse contact to the wall rock on one side of the fracture. The wall rock is heavily sericitized.

Minerals: Quartz, muscovite, K-feldspar, fluorite and calcite.

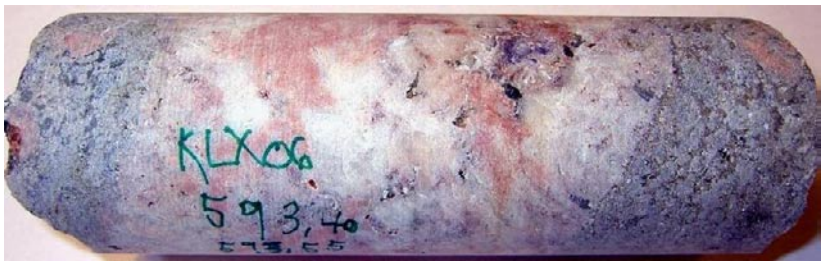

Photograph of the drill core KLX06: 593.40–593.55 m. The coating is made up of muscovite (shiny), quartz (whitish grey), K-feldspar (pink), fluorite (purple) and calcite (white, next to fluorite).

KLX06: 595.08–595.18 m (1)

Sample type: Thin section.

Rock type: Ävrö granite.

Fracture: About 2–3 cm wide, sealed fracture bordering to a presently open fracture. The wall rock is heavily sericitized.

Minerals: Quartz, muscovite, fluorite, Fe-Mg-chlorite, Ti-oxide (Nb- and Ta-rich), chalcopyrite, sphalerite, sylvite, topaz and albite.

Quartz, muscovite and fluorite are coarse-grained and most abundant in this sample. Muscovite is coating the fracture and quartz is found in the centre of the fracture. The other minerals are found in small amounts.

KLX06: 595.08–595.18 m (2)

Sample type: Thin section.

Rock type: Ävrö granite.

Fracture: About 2–3 cm wide, sealed fracture bordering to a presently open fracture. The wall rock is heavily sericitized.

Minerals: Quartz, muscovite, fluorite, Ti-oxide (Nb- and Ta-rich), chalcopyrite, halite, native gold, barite, Fe-oxide, MnFe-oxide, zircon and an unidentified sulphide rich in Cu, As, Sn, Sb and Fe.

Quartz and muscovite are coarse-grained and most abundant in this sample. Muscovite is coating the fracture and quartz is found in the centre of the fracture. The other minerals are found in small amounts.

Photograph of the drill core KLX06: 595.08–595.18 m. Visible is muscovite and quartz.

KLX06: 607.06–607.14 m

Rock type: Ävrö granite.

Fracture: Open fracture with old millimetre-wide coating. The wall rock is sericitized.

Minerals: Quartz and muscovite.

Photograph of the drill core KLX06: 607.06–607.14 m.

KLX06: 622.57–622.73 m

Sample type: Thin section.

Rock type: Ävrö granite.

Fracture: Fine-grained quartz- and muscovite rich filling with some coarse-grained, cubic, pyrite crystals. Other minerals are only found in small amounts. The contact to the wall rock is very diffuse and the wall rock is heavily sericitized.

Minerals: Quartz, fluorite, muscovite, pyrite, hematite, barite, Nb-rich mineral, monazite, (and epidote).

KLX06: 789.41–789.48 m

Sample type: Surface sample.

Rock type: Border zone of Ävrö granite and fine-grained granite.

Fracture: Open fracture (107°/69°, 0 mm wide) partially covered with a thin coating of gypsum, fluorite and calcite. Parts of the coating are reddish coloured from minute hematite crystals.

Minerals: Gypsum, fluorite, calcite, galena, barite, Fe-chlorite, hematite and Cu-rich mineral.

Gypsum and fluorite are the most abundant minerals in the coating. Gypsum crystals are mostly platy and sheet-like while fluorite crystals are subhedral to euhedral (cubic). Hematite appears as spherical aggregates made up of platy crystals. Sometimes the spherical aggregates are more or less massive.

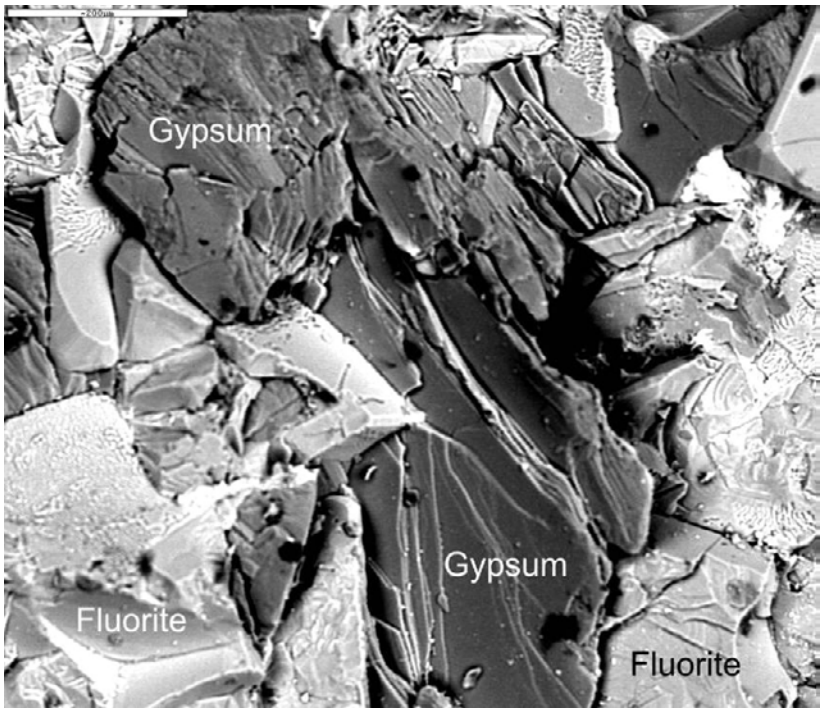

Back-scattered SEM-image of gypsum and fluorite. Scale bar is 200 µm. Sample KLX06: 789.41–789.48 m.

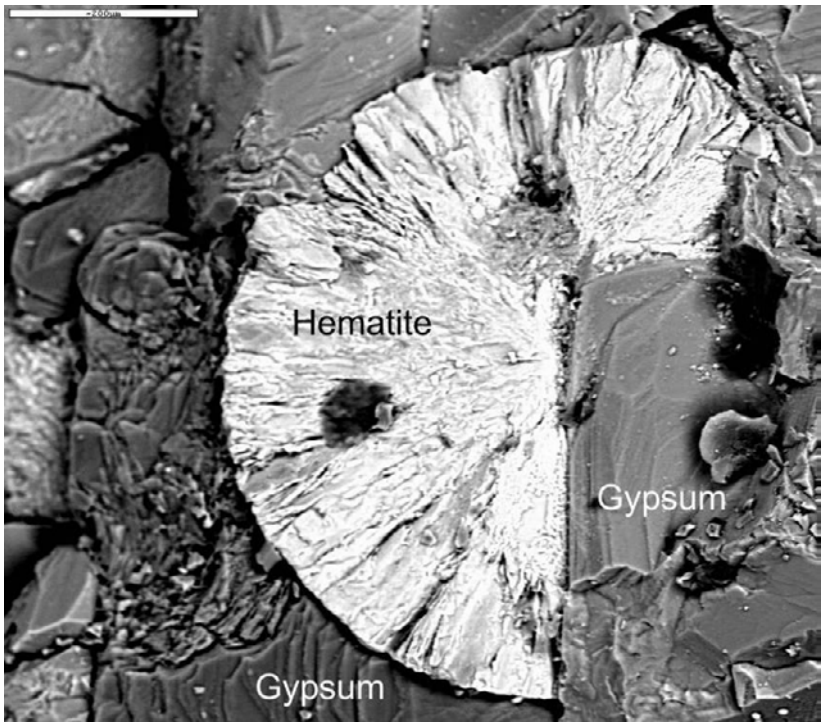

Back-scattered SEM-image of gypsum and a spherical aggregate of hematite. Scale marker bar is 200 µm. Sample KLX06: 789.41–789.48 m.

KLX06: 814.86–814.95 m

Sample type: Surface sample.

Rock type: Ävrö granite.

Fracture: Open fracture (290°/79°, 6 mm wide), coated by a 5 millimetre thick coating of euhedral fluorite (yellow) and calcite (white).

Minerals: Fluorite, calcite, barite, (apophyllite, galena, quartz and hematite).

Euhedral fluorite (cubic) and calcite are the dominant minerals in the coating. Barite crystals are present in a cluster. These crystals are 30–50 µm big. Small amounts of galena, hematite, quartz and apophyllite are also present.

Photographs of the drill core sample showing the fracture coating that is dominated by fluorite (yellow) and whitish calcite. Drill core diameter is 50 mm. Right photograph is a close-up of the fluorite rich part. Sample KLX06: 814.86–814.95 m.

KLX06: 831.32–831.38 m

Sample type: Surface sample.

Rock type: Ävrö granite.

Fracture: Open fracture (299°/86°, 4 mm wide) with crystals of fluorite and aggregates of calcite. The fluorite crystals are partially covered by reddish and dark greenish material, sometimes as platy and metallic crystals and sometimes as spherical aggregates.

Minerals: Fluorite, hematite, corrensite, (adularia), (sphalerite), (barite), Cu (Sn-) rich mineral, quartz.

The fracture coating is dominated by euhedral, cubic, transparent, colourless fluorite crystals, which grow from the fracture wall. Spherical aggregates of platy green coloured corrensite and red coloured hematite grow upon the fluorite crystals. Hematite is also commonly occurring as single platy crystals that lie flat on the fluorite crystal surfaces. These platy crystals are 50–150 µm big give these parts of the coating a metallic lustre. The spherical corrensite aggregates are 50–200 µm in diameter.

Small amounts of euhedral adularia are also present in this sample. Calcite that is in paragenesis with fluorite is visible macroscopically on the fracture surface, but no calcite crystals were included in the section that was investigated with SEM-EDS.

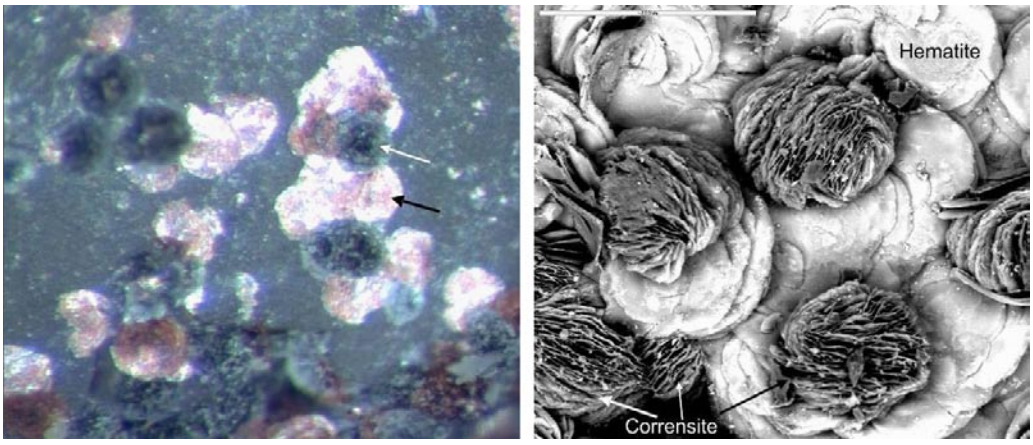

Stereo microscope photograph (left) and back-scattered SEM-image(right) of red platy hematite crystals (black arrow-left image, bright – right image) and green spherical corrensite aggregates (white arrow –left image, dark – right image). Widths of aggregates and crystals are 50–150 µm (left). Scale marker is 200 µm (right). Sample KLX06: 831.32–831.38 m.

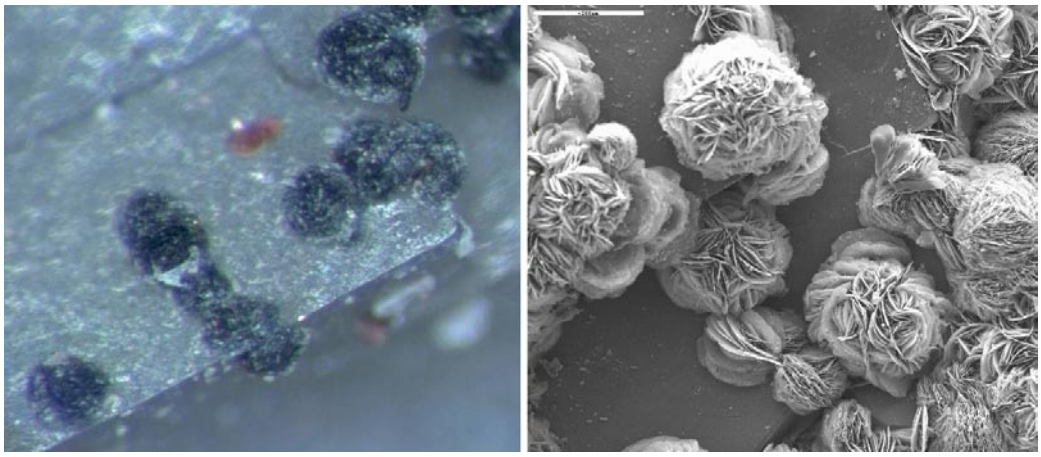

Stereo microscope photograph (left) and scanning electron SEM-image(right) of green spherical corrensite aggregates. Widths of aggregates are 100–200 µm (left). Scale marker is 200 µm (right). Sample KLX06: 831.32–831.38 m.

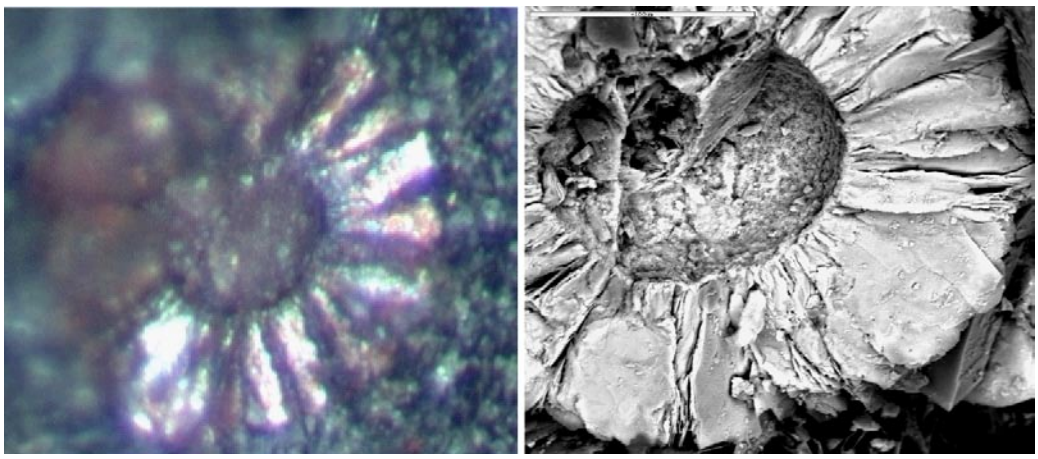

Stereo microscope photograph (left) and back-scattered SEM-image(right) of a cross-section of a red spherical aggregate of platy hematite crystals. Widths of aggregate are about 200 µm (left). Scale marker is 100 µm (right). Sample KLX06: 831.32–831.38 m.

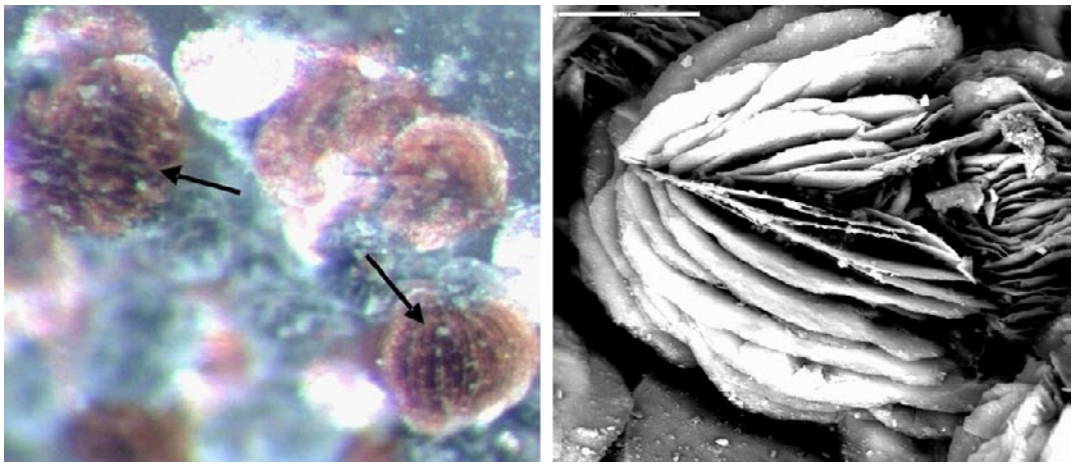

Stereo microscope photograph (left) and back-scattered SEM-image (right) of red platy hematite crystals (black arrows-left image, bright – right image) and green spherical corrensite aggregates (left image). Widths of aggregates are 100–200 µm (left). Scale marker is 100 µm (right). Sample KLX06: 831.32–831.38 m.

Appendix 4

Sample descriptions KLX07A

KLX07A: 106.25–106.41 m

Sample type: Thin section.

Rock type: Ävrö granite.

Fracture: Open fracture coated by a 3–4 cm thick, old fracture filling (224°/27°) made up of several generations of fracture minerals. The filling is dominated by quartz, laumontite and calcite. The wall rock is red-stained.

Minerals: Quartz, calcite, laumontite, chlorite, K-feldspar, epidote, fluorite, (pyrite, barite, hematite and U-silicate).

Order:

1. Coarse-grained quartz with undulose extinction and sub-grain formation.
2. Fine-grained epidote, chlorite and K-feldspar.
3. Euhedral laumontite and calcite. Laumontite has partially replaced epidote in places.
4. Calcite, illite, Fe-rich chlorite and small amounts of pyrite, barite, hematite and U-rich silicate are found in fractures cutting through laumontite.

Fluorite is found together with calcite in fractures cutting through quartz.

KLX07A: 184.83–184.92 m

Sample type: Surface sample.

Rock type: Ävrö granite.

Fracture: Open fracture, cutting through a sealed network of fractures filled with dominantly prehnite.

Minerals: Calcite, fluorite, REE-carbonate, Cu-(Ni, Zn, Fe-) rich mineral, topaz (?), pyrite, hematite, apophyllite, Zn-oxide (?) and barite (small crystals).

The fracture surface is dominated by calcite crystals. Other minerals are found in quite small amounts.

Photograph of the fracture surface KLX07A: 184.83–184.92 m.

KLX07A: 193.63–193.87 m

Sample type: Surface sample.

Rock type: Ävrö granite.

Fracture: Open fracture (168°/82°).

Minerals: Pyrite, calcite (scalenohedral), harmotome, barite and REE-carbonate.

The fracture surface is partially covered with euhedral pyrite, calcite (scalenohedral), harmotome, barite and REE-carbonate. The minerals seem to be coeval.

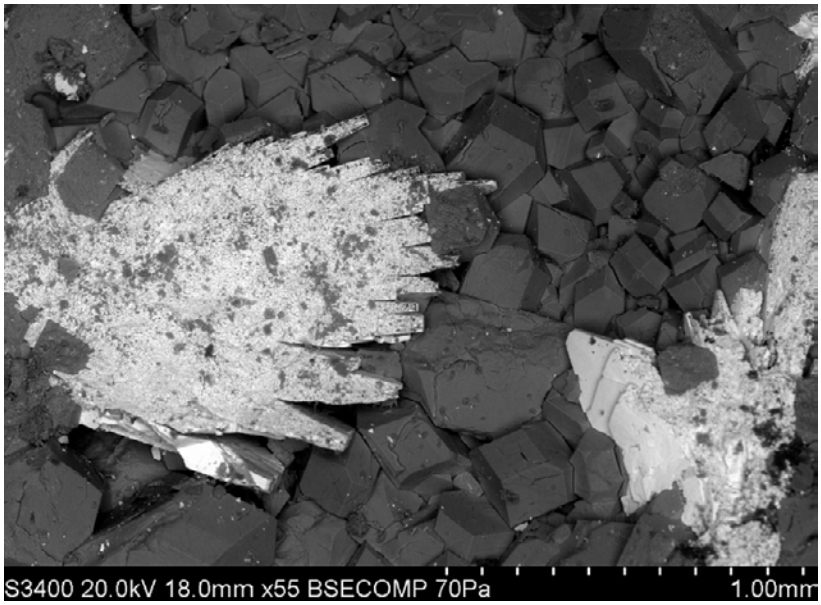

Back-scattered SEM-image of euhedral harmotome (dark grey) and barite (bright). Sample KLX07A: 193.63–193.87 m.

KLX07A:227.24–227.38 m

Rock type: Ävrö granite.

Fracture: Sealed fractures (main directions 263°/12°, 285°/19°). Red-stained wall rock.

Minerals: Prehnite and coeval or just later formed calcite and chlorite.

Photograph of sealed fractures filled with prehnite (bluish grey), calcite (white) and chlorite (dark). Sample KLX07A:227.24–227.38 m.

KLX07A: 320.32–320.49 m

Sample type: Surface sample.

Rock type: Ävrö granite.

Fracture: Open fracture (24°/75°).

Minerals: Calcite (scalenohedral), REE-carbonate, barite, clay minerals, quartz, Fe-chlorite, pyrite, W-rich mineral (probably wolframite) and galena.

The fracture surface is dominated by scalenohedral calcite. The other minerals are found in smaller amounts.

Photograph of the fracture surfaces. The closest surface is dominated by calcite. Sample KLX07A: 320.32–320.49 m.

KLX07A: 321.47–321.58 m

Sample type: Surface sample.

Rock type: Ävrö granite.

Fracture: Open fracture dominated by calcite, pyrite and harmotome. The other minerals are found in small amounts.

Minerals: Calcite (scalenohedral), pyrite, harmotome, barite, W-rich mineral (probably wolframite), apophyllite, argentite, sylvite, harmotome, clay minerals (corrensite), quartz and hematite.

Barite, harmotome and pyrite are related.

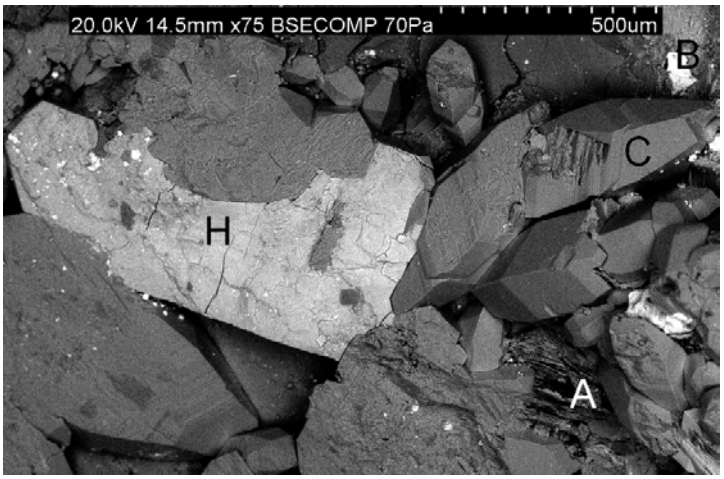

Back-scattered SEM-image of calcite (C), harmotome (H), barite (B) and apophyllite (A). Sample KLX07A: 321.47–321.58 m

KLX07A: 346.73–346.82 m

Sample type: Surface sample.

Rock type: Ävrö granite.

Fracture: Open fracture (337°/85°). The fracture surface is dominated by calcite. Pyrite is e.g. found as small crystals on the surface of calcite crystals.

Minerals: Calcite (scalenohedral), pyrite, barite (small crystals) and Fe-chlorite.

Photograph of the fracture surface KLX07A: 346.73–346.82 m.

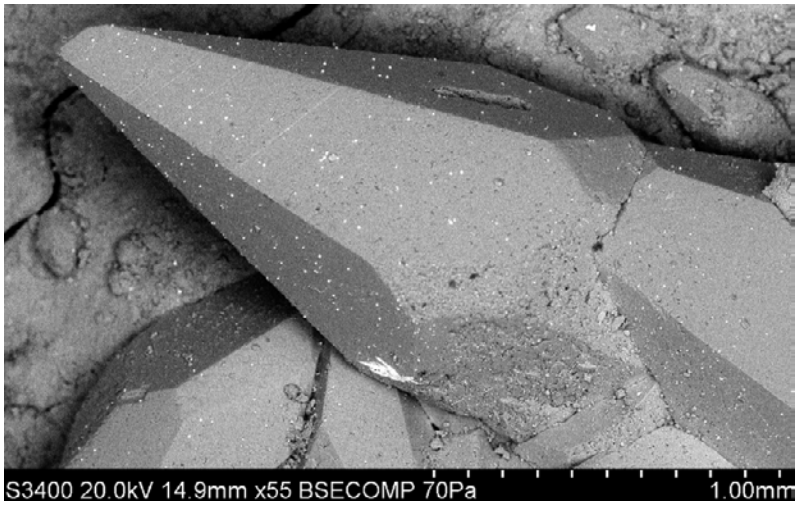

Back-scattered SEM-image of scalenohedral calcite with pyrite (small bright spots) and barite (small aggregate of bright crystals, lower part of the image) on the surface. Sample KLX07A: 346.73–346.82 m.

KLX07A: 356.93–356.96 m

Sample type: Surface sample.

Rock type: Ävrö granite.

Fracture: Open fracture, partially covered with calcite, fluorite and pyrite and smaller amounts of barite and REE-carbonate.

Minerals: Calcite (equant), pyrite, barite, fluorite and REE-carbonate.

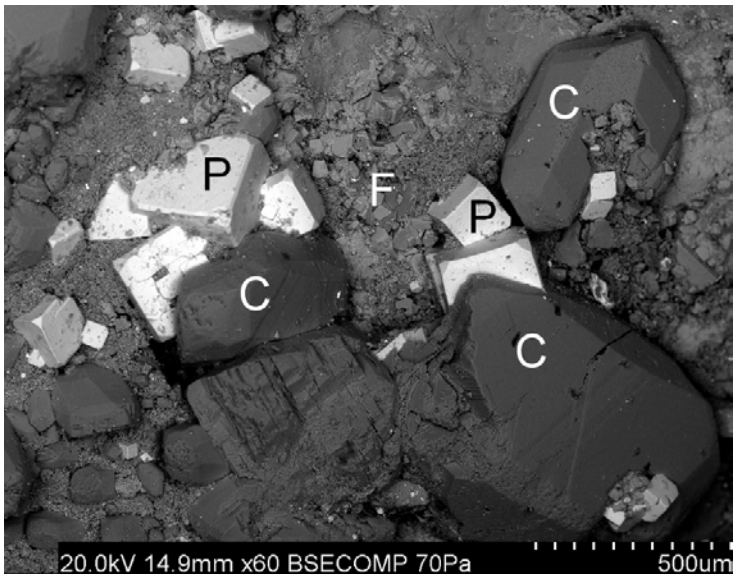

Back-scattered SEM-image of calcite (C, equant), fluorite (F, cubic) and pyrite (P, cubic). Sample KLX07A: 356.93–356.96 m.

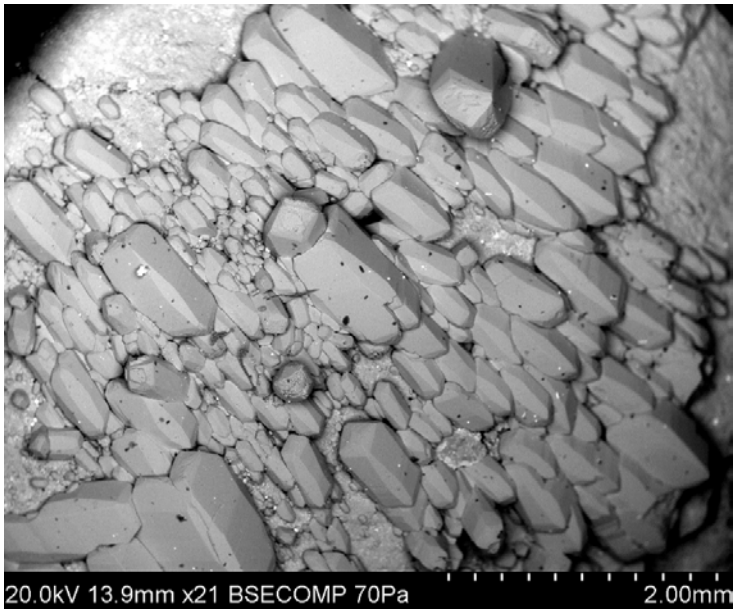

Back-scattered SEM-image of calcite crystals. Sample KLX07A: 356.93–356.96 m.

KLX07A: 364.17–364.41 m

Sample type: Surface sample.

Rock type: Ävrö granite.

Fracture: Closely space open and sealed fractures. Calcite, fluorite, pyrite and galena are found in both sealed and open fractures.

Minerals: Calcite, fluorite, pyrite and galena.

Photograph of the drill core KLX07A: 364.17–364.41 m.

KLX07A: 373.70–373.97 m

Sample type: Surface sample.

Rock type: Ävrö granite.

Fracture: Two parallel open fractures, (145°/78° and 149°/77°).

Minerals: Calcite (scalenohedral with overgrowths), pyrite, chalcopyrite, galena and a W-rich mineral (probably wolframite).

Calcite and pyrite dominate the fracture surfaces. The calcite crystals are scalenohedral and have overgrowths, which are richer in Mn than the primary crystal. Galena is related to pyrite.

Photograph of the fracture surfaces. Sample KLX07A: 373.70–373.97 m.

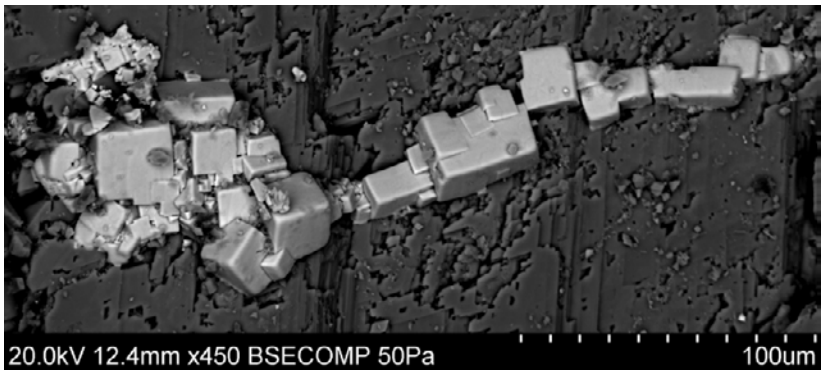

Back-scattered SEM-image of pyrite on top of calcite. Sample KLX07A: 373.70–373.97 m

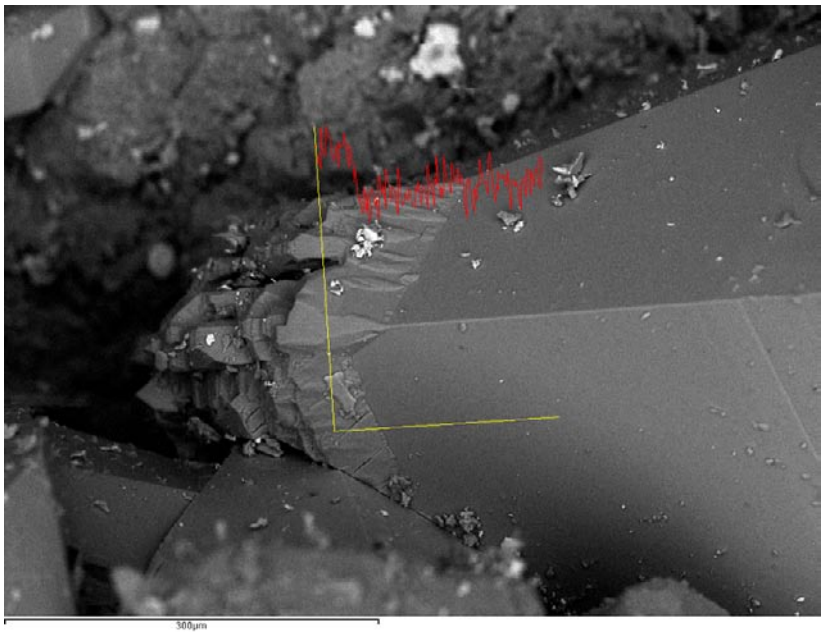

Back-scattered SEM-image of a calcite crystal with an overgrowth of younger calcite. The graph shows that the overgrowth has a higher Mn-content than the primary crystal. Sample KLX07A: 373.70–373.97 m.

KLX07A: 423.21–423.39 m

Rock type: Ävrö granite.

Fracture: 2–3 cm wide, sealed fracture (244°/13°).

Minerals: Quartz, pyrite, calcite and chlorite.

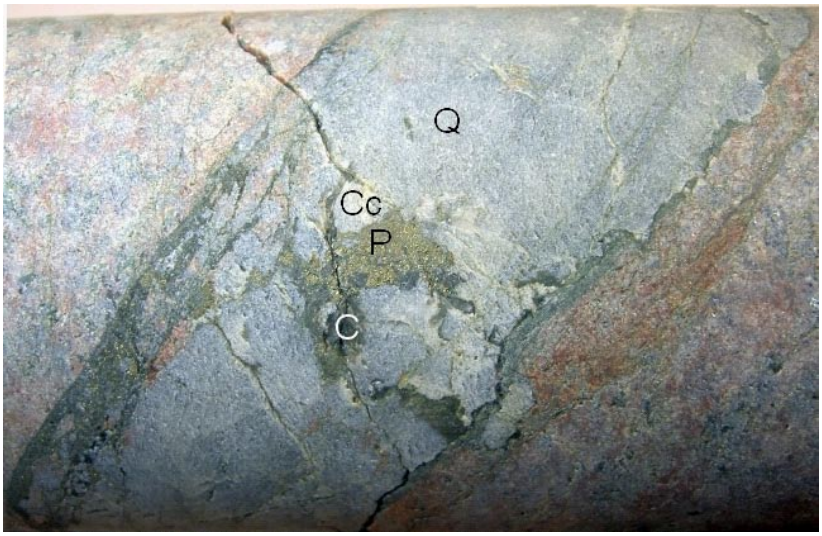

Photograph of the sealed fracture KLX07A: 423.21–423.39 m (Q = quartz, Cc = calcite, P = pyrite, C = chlorite).

KLX07A: 557.83–557.94 m

Sample type: Surface sample.
Rock type: Ävrö granite.
Fracture: Open fracture (151°/78°).
Minerals: Calcite (bladed) and a Cu (Fe-) rich mineral.

Photograph of the fracture surface KLX07A: 557.83–557.94 m. Bladed calcite is visible.

KLX07A: 668.98–669.22 m

Sample type: Surface sample.
Rock type: Ävrö granite.
Fracture: Open fracture (103°/84°).
Minerals: Calcite (equant), pyrite, barite and a Ni-Cu rich mineral.

Photograph of the fracture surface KLX07A: 668.98–669.22 m. Calcite and pyrite is visible.

KLX07A: 696.68–696.83 m

Sample type: Surface sample.
Rock type: Ävrö granite.
Fracture: Open fracture (148°/45°).
Minerals: Calcite (equant) and pyrite (on the surface of calcite).

Calcite has grown on a corrensite/chlorite coating (striated).

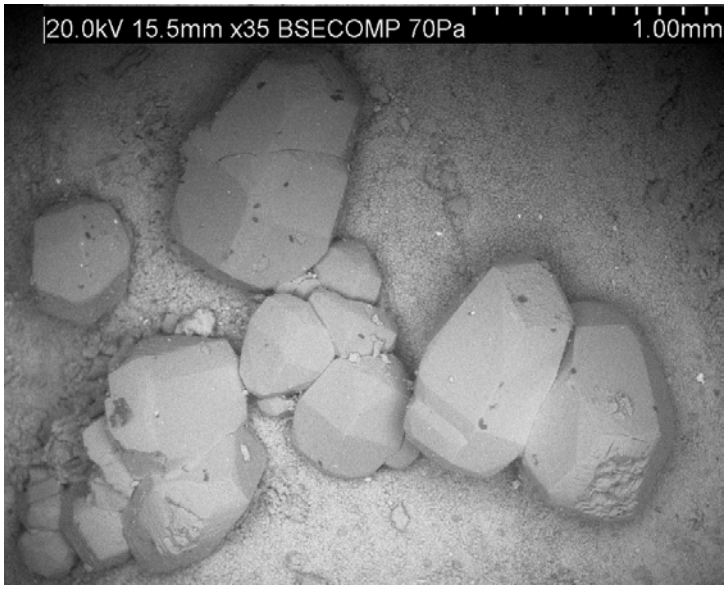

Back-scattered SEM-image of equant calcite crystals (KLX07A: 696.68–696.83 m).

Appendix 5

Sample descriptions KLX08

KLX08: 108.24–108.33 m

Sample type: Surface sample.

Rock type: Ävrö granite.

Fracture: Open fracture (266°/49°), partly covered by chlorite and clay minerals with needle shaped calcite on top. Pyrite and chalcopyrite are found on the crystal surfaces of the calcite.

Minerals: Calcite (needle shaped), chlorite (mixed-layer clay), pyrite, hematite and chalcopyrite.

Photograph of the fracture surface KLX08: 108.24–108.33 m. Dark green parts are dominated by chlorite and clay minerals while the bright parts are dominated by needle shaped calcite.

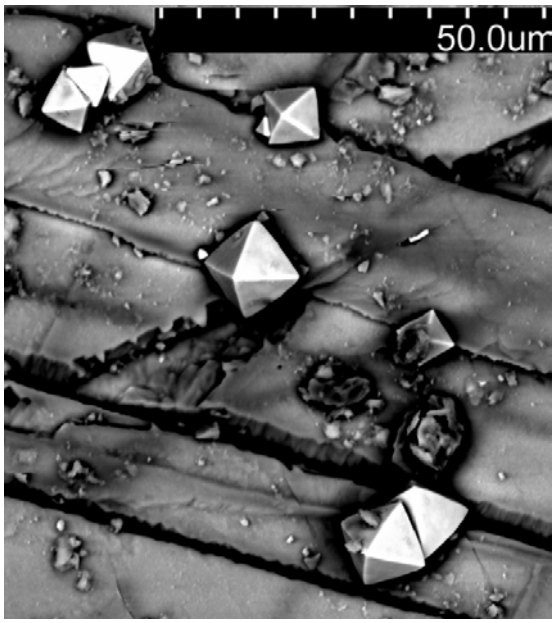

Back-scattered SEM-image of pyrite crystals on top of calcite. Sample KLX08: 108.24–108.33 m.

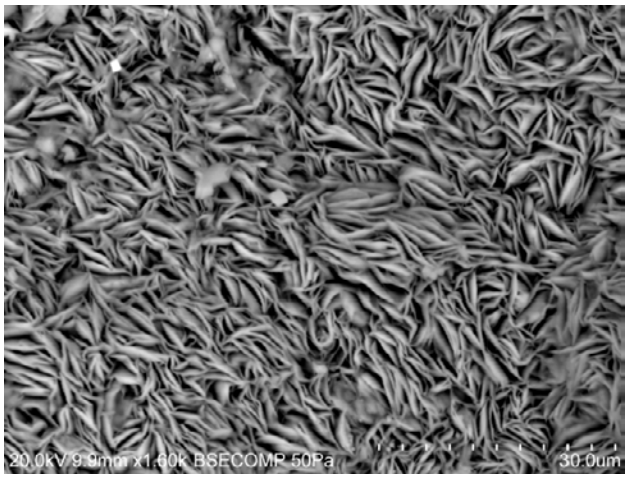

Back-scattered SEM-image chlorite and mixed-layer clay (probably corrensite). Sample KLX08: 108.24–108.33 m.

KLX08: 218.29–218.39 m

Sample type: Surface sample.

Rock type: Ävrö granite

Fracture: Open fracture covered with needle shaped calcite, with related REE-carbonate and adularia.

Minerals: Calcite (needles), REE-carbonate and adularia.

Back-scattered SEM-image of needle shaped calcite. Sample KLX08: 218.29–218.39 m.

Back-scattered SEM-image of needle shaped calcite. Sample KLX08: 218.29–218.39 m.

KLX08: 366.43–366.58 m

Rock type: Ävrö granite

Fracture: Sealed c. 5mm wide fracture (286°/55°) with red-stained wall rock.

Minerals: Prehnite and calcite.

Photograph of the sealed fracture KLX08: 366.43–366.58 m. Prehnite in bluish grey and calcite in white.

KLX08: 478.87–479.13 m

Sample type: Thin section.

Rock type: Ävrö granite

Fracture: About 3 cm wide, sealed fracture (233°/33°).

Minerals: Calcite, K-feldspar, hematite, chlorite, epidote, adularia, quartz, fluorite, pyrite (galena, apatite, albite, W-rich mineral and chalcopyrite).

Order:

1. Cataclasite: K-feldspar, hematite, Mg-chlorite, epidote and quartz.
2. Calcite (MnO = undetectable, no zonation) dominated filling. Also present are adularia, fluorite, quartz, epidote, (chlorite, pyrite, hematite, galena, apatite, albite and W-rich mineral). The calcite is made up of several (>15) crystals, elongated parallel or sub-parallel to the fracture wall.
3. Thin calcite filled fracture. Also present is adularia, pyrite (and chalcopyrite).

Photograph of the sealed, calcite-filled, fracture, which cuts through cataclasite (dark red-brown). Sample KLX08: 478.87–479.13 m.

KLX08: 676.92–677.13 m

Sample type: Thin section.

Rock type: Diorite/gabbro

Fracture: Sealed fracture (145°/64.5°)

Minerals: Pyrite, chalcopyrite, epidote (cuts pyrite in places), quartz, calcite, titanite, chlorite, magnetite, sphalerite, (albite, chloritized remnants of biotite and possibly pumpellyite).

The minerals in this filling are interpreted to be fairly coeval.

Photograph of the sealed fracture KLX08: 676.92–677.13 m.

KLX08: 679.83–680.01 m

Sample type: Surface sample.

Rock type: Diorite/gabbro

Fracture: Open fracture (56°/61.9°).

Minerals: Calcite, Ag-, Cu- (Sn), W-, rich minerals, pyrite, chlorite, corrensite and hematite.

Calcite is the most common mineral and the other minerals (except for chlorite and corrensite which are more abundant), are found on the surface of calcite crystals. The calcite crystals are mostly equant.

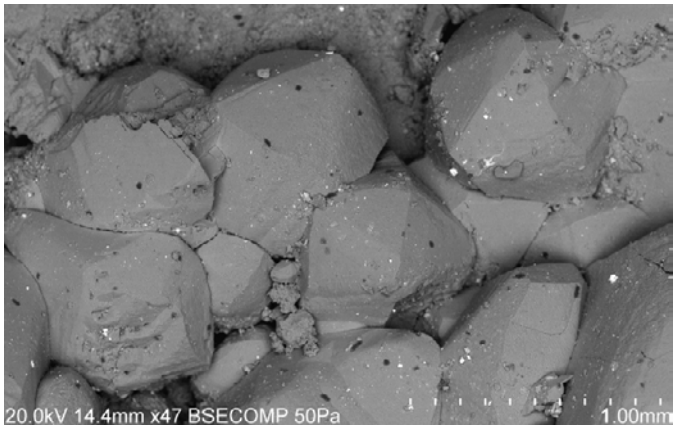

Back-scattered SEM-image of equant calcite crystals. Sample KLX08: 679.83–680.01 m.

KLX08: 772.49–772.69 m

Sample type: Thin section.

Rock type: Diorite/gabbro

Fracture: Cataclasite coated by calcite. Orientation of calcite rim = 31°/57°

The calcite coating is made up of scalenohedral crystals and also consists of minor amounts of hematite, barite, Cu/Zn-rich mineral, pyrite, REE-carbonate, quartz, Fe-chlorite, Ag-rich mineral, sphalerite, W-rich mineral, and is cut by a thin calcite vein. The scalenohedral calcite crystals are zoned. The Mn-content varies between the outer most part (0.2–0.6% MnO) and the core (2.2–3.6% MnO).

Cataclasite is made up of angular fragments of K-feldspar, albite, epidote, chlorite corrensite, quartz, calcite, barite, pyrite, (and titanite). Chlorite, corrensite, quartz and calcite are the most common minerals in the cataclasite. The cataclasite is made up of several parts with different grain sizes.

Photo of the sample KLX08: 772.49–772.69 m. Calcite in white and cataclasite in brown.

KLX08: 792.43–792.72 m

Rock type: Ävrö granite

Fracture: Open fracture (255°/83.1°). Fresh wall rock.

Minerals: Gypsum (covers most of the fracture surface as a thin cover).

Photograph of the fracture surfaces. Sample KLX08: 792.43–792.72 m.

KLX08: 795.15–795.36 m

Sample type: Surface sample

Rock type: Ävrö granite

Fracture: Open fracture (97°/70.2°). Fresh wall rock.

Minerals: Gypsum, fluorite, apophyllite, pyrite, sphalerite, hematite, corrensite and illite.

Gypsum and apophyllite is the most common minerals on the fracture surface.

Photograph of the fracture surfaces. Sample KLX08: 795.15–795.36 m.

KLX08: 820.93–821.16 m

Sample type: Surface sample

Rock type: Ävrö granite

Fracture: Open fracture (84°/75.6°). Fresh wall rock.

Minerals: Gypsum, apophyllite, corrensite, hematite and apatite.

Gypsum and apophyllite are found on top of corrensite. These three minerals are the most common minerals on the fracture surface. Other minerals are hematite and apatite.

Photograph of the fracture surfaces. Sample KLX08: 820.93–821.16 m.

KLX08: 821.70–821.92 m

Rock type: Ävrö granite

Fracture: Open fracture (81°/71.5°), fresh wall rock.

Minerals: Gypsum

Photograph of the fracture surfaces. Sample KLX08: 821.70–821.92 m.

KLX08: 822.41–822.61 m

Sample type: Thin section and surface sample

Rock type: Ävrö granite

Fracture: Open fracture (83°/69.2°), fresh wall rock.

Minerals: Gypsum, hematite and Mg-rich chlorite

The fracture surface is partially covered by gypsum together with some hematite and Mg-chlorite.

Wall rock:

Plagioclase is partially altered <50%. Biotite is fresh close to the fracture. Chlorite is only present just by the fracture rim.

Photograph of the fracture surfaces. Sample KLX08: 822.41–822.61 m.

KLX08: 868.65–868.83 m

Sample type: Thin section

Rock type: Ävrö granite

Fracture: Open fracture (93°/71.2°). Fresh wall rock.

Minerals: Gypsum, adularia, calcite, chlorite, corrensite, prehnite, apatite, albite (and sylvite).

Order:

1. Calcite, adularia, Mg-rich chlorite, albite (and Fe-rich chlorite) are present as a coating next to the wall rock. These minerals are also found in thin fractures which penetrate the wall rock. One of these fractures is coated by prehnite.
2. Homogeneous gypsum coating outside "1". One sylvite crystal is present within this coating.

Wall rock is fresh (biotite is unaltered at the fracture rim) plagioclase is fairly unaltered.

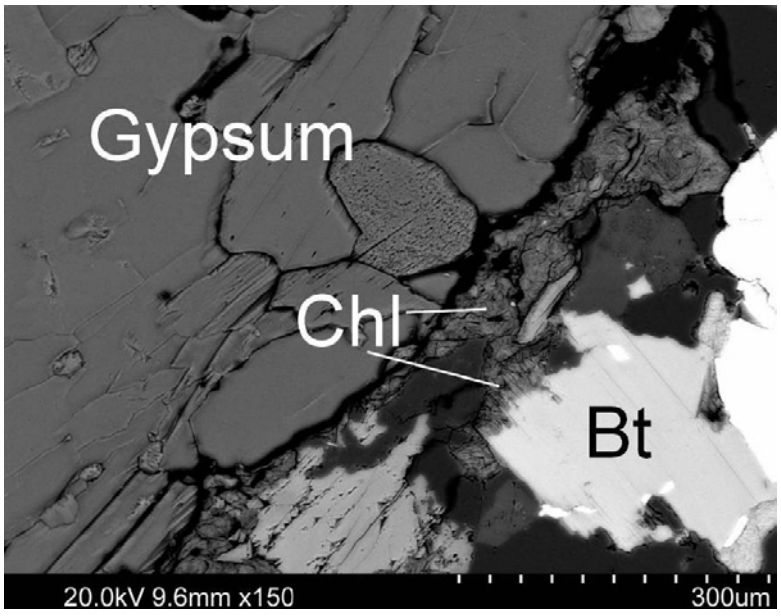

Back-scattered SEM-image showing the fracture-wall rock contact. Biotite (Bt) is fresh very close to the fracture. Chloritization (Chl = chlorite) is only found within the first 0.1 mm in the wall rock from the fracture rim. Sample KLX08: 868.65–868.83 m.

KLX08: 916.16–916.36 m

Sample type: Thin section and surface sample

Rock type: Ävrö granite

Fracture: Open fracture (82°/73.6°). The fracture surface is almost entirely covered with gypsum. The fracture surface beneath gypsum is dominated by chlorite and clay minerals (illite and corrensite). The wall rock is quite fresh.

Minerals: Gypsum, barite, hematite, illite, Mg-chlorite, corrensite, sphalerite, chalcopyrite and calcite.

Chlorite/corrensite, chalcopyrite and calcite are present in thin fractures cutting through the wall rock. Barite, hematite and sphalerite are found in small amount in association with gypsum.

Wall rock:

Biotite is partially chloritized next to fracture (50%). Plagioclase is altered c. 50%. The alteration of these two minerals only increases very close to the fracture rim.

Photograph of the fracture surfaces. Sample KLX08: 916.16–916.36 m.

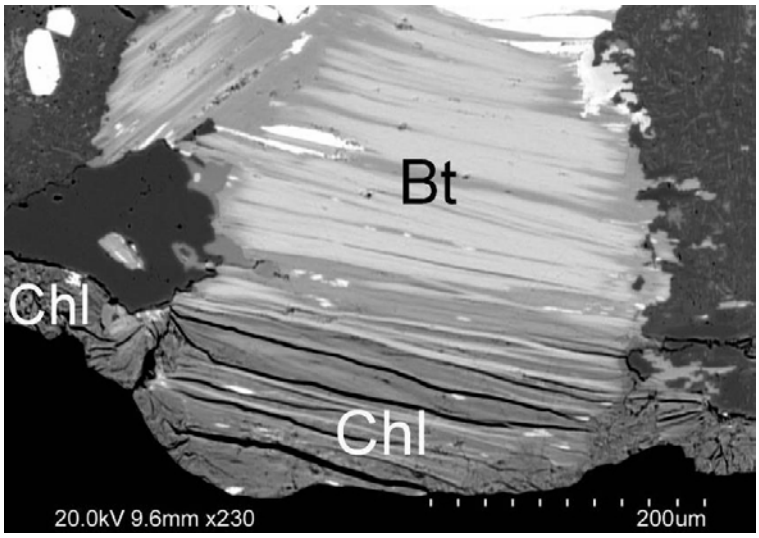

Back-scattered SEM-image, showing the fracture-wall rock contact. Biotite (Bt) is fresh very close to the fracture. Chloritization (Chl = chlorite) is only found within the first 0.1–0.2 mm in the wall rock from the fracture rim. Chlorite is also coating the fracture in the image. Sample KLX08: 916.16–916.36 m.

KLX08: 919.75–919.90 m

Rock type: Ävrö granite

Fracture: Open fracture (63°/76.8°). Gypsum covers the surface. The wall rock is rather fresh.

Photograph of the fracture surface KLX08: 919.75–919.90 m.

KLX08: 933.15–933.30 m

Sample type: Thin section

Rock type: Quartz monzodiorite

Fracture: Sealed, 1–3 mm wide (7°/29.7°). Red-stained wall rock.

Minerals: Hornblende, calcite, titanite (occasionally euhedral), K-feldspar, Fe-Mg chlorite, (magnetite, pyrite, albite and epidote).

Hornblende is the most abundant mineral in the fracture filling.

Photograph of the sample KLX08: 933.15–933.30 m.

Back-scattered SEM-image showing the sealed fracture. The titanite crystals may originate from the wall rock. Sample KLX08: 933.15–933.30 m.

Appendix 6

Sample descriptions KLX10A

KLX10A: 108.27–108.38 m

Sample type: Surface sample
Rock type: Fine-grained granite
Fracture: Open fracture 311°/89°
Minerals: Calcite and hematite

The calcite crystals are scalenohedral.

Photograph of the fracture surfaces KLX10A: 108.27–108.38 m.

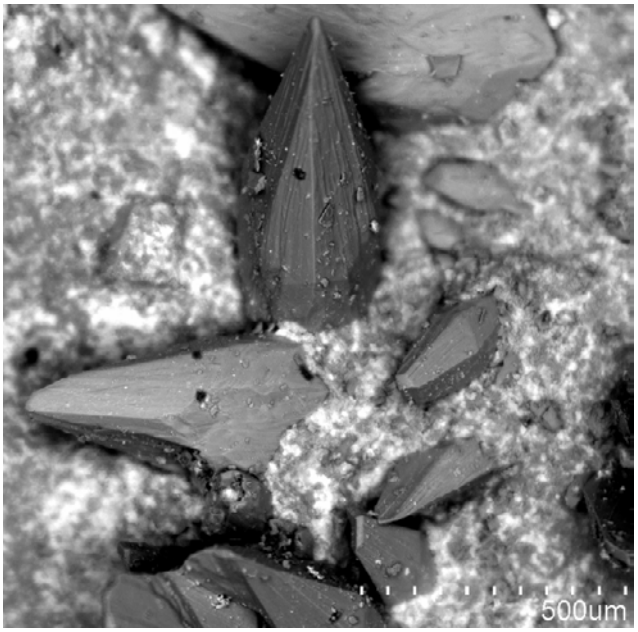

Back-scattered SEM-image showing scalenohedral calcite and hematite (bright). Sample KLX10A: 108.27–108.38 m.

KLX10A: 112.66–112.72 m

Rock type: Fine-grained granite
Fracture: Open fracture coated by an old filling (56.9°/6.9°)
Minerals: Epidote, calcite, fluorite, quartz and chlorite

Photograph of the fracture KLX10A: 112.66–112.72 m.

KLX10A: 200.72–201.02 m

Sample type: Surface sample
Rock type: Ävrö granite
Fracture: Open fracture (88.3°/81.9°)
Minerals: Calcite, hematite, quartz, pyrite, chalcopyrite and chlorite

Calcite (scalenohedral – without overgrowths) dominates. Chlorite is Fe-rich.

Photograph of the fracture surface KLX10A: 200.72–201.02 m.

Back-scattered SEM-image showing scalenohedral calcite. Sample KLX10A: 200.72–201.02 m.

KLX10A: 228.14–228.80 m

Sample type: Surface sample

Rock type: Ävrö granite

Fracture: Open fracture with thick coating cut and re-activate older epidote cataclasite/ mylonite.

Minerals: Calcite, quartz, chalcopyrite, pyrite, hematite, barite, chlorite (ML-clay), W-rich mineral, sphalerite, galena and Zn-rich mineral.

Calcite crystals are needle shaped and are very pure. More than 99% of the coating consists of calcite.

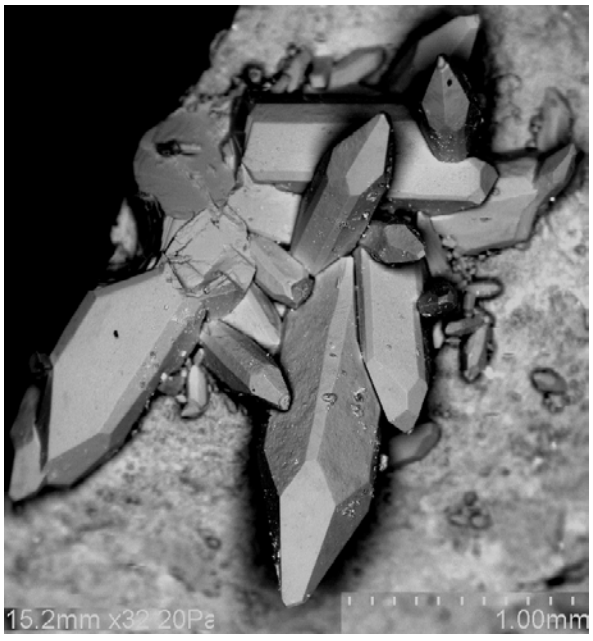

Back-scattered SEM-image showing needle shaped calcite. Sample KLX10A: 228.14–228.80 m.

KLX10A: 406.29–406.49 m

Sample type: Polished rock chip investigated with SEM.

Rock type: Fine-grained dioritoid

Fracture: Sealed fracture (335.7°/84°)

Minerals: Calcite, biotite, quartz, titanite, epidote, magnetite (and fluorite)

Calcite and biotite dominates, quartz, titanite, and epidote are subordinate whilst magnetite and fluorite are only found in trace amounts.

Photograph of the sample KLX10A: 406.29–406.49 m.

KLX10A: 519.40–519.62 m

Rock type: Ävrö granite

Fracture: Sealed (310.6°/74.7°)

Minerals: Calcite, quartz and epidote

Photograph of the sample KLX10A: 519.40–519.62 m.

KLX10A: 610.85–611.19 m

Sample type: Surface sample (2)

Rock type: Ävrö granite

Fracture: Open fracture (316.5°/85.1°)

Minerals: Corrensite, apophyllite, pyrite, barite and quartz.

The minerals on the fracture surface are probably coeval. Apophyllite crystals are euhedral. Pyrite crystals are cubic, barite crystals are subhedral.

Photograph of the fracture surface KLX10A: 610.85–611.19 m. The glittering crystals are apophyllite. The green colour comes from corrensite.

KLX10A: 789.80–790.10 m

Sample type: Surface sample

Rock type: Fine-grained diorite to gabbro

Fracture: Open fracture, re-activating some old calcite- and quartz-filled fractures (the stable analysis of this sample is from the old calcite).

Minerals: Calcite, barite, Zn-rich mineral, hematite, quartz, fluorite and pyrite.

Calcite is the most common mineral on the fracture surface. The calcite crystals are equant (possibly with some secondary overgrowths).

KLX10A 790.50–790.63 m

Rock type: Fine-grained diorite to gabbro

Sealed and open fractures: (187.6°/13.1°)

Minerals: old hydrothermal calcite and quartz.

Photograph of the sample KLX10A 790.50–790.63 m.

KLX10A: 895.00–895.20 m

Sample type: Polished rock chip investigated with SEM.

Rock type: Ävrö granite

Fracture: Open fracture (with red-stained wall rock 1–2 cm away from the fracture) (342°/2.9°). Two parallel fractures with similar features nearby have orientations 335°/9.1° and 231°/5.2° respectively.

Minerals: Biotite, calcite, quartz, K-feldspar, (gypsum?, muscovite?)

Photograph of the sample KLX10A: 895.00–895.20 m.

KLX10A: 919.44–919.62 m

Rock type: Ävrö granite

Fracture: Sealed (179°/73.6°) with red-stained wall rock

Minerals: Very homogeneous calcite, prehnite and minor amount of chlorite and quartz. Calcite is the most common mineral.

Photograph of the sample KLX10A: 919.44–919.62 m.

KLX10A: 969.13–969.28 m

Sample type: Surface sample

Rock type: Ävrö granite

Fracture: Open fracture (297°/72.3°).

Minerals: Gypsum, apophyllite, hematite, Fe-chlorite

The coating is dominated by gypsum and apophyllite.

Photograph of the fracture surfaces KLX10A: 969.13–969.28 m.

KLX10A: 970.50–970.65 m

Sample type: Surface sample

Rock type: Ävrö granite

Fracture: Open fracture. The wall rock is fresh.

Minerals: Gypsum, galena, barite, corrensite, hematite, (and quartz)

Gypsum and corrensite dominate.

Photograph of the fracture surfaces KLX10A: 970.50–970.65 m.

KLX10A: 971.70–972.00 m

Sample type: Surface sample

Rock type: Ävrö granite

Fracture: Two parallel open fractures; 348/77, 350/75

Minerals: Gypsum, apophyllite, corrensite, sphalerite, pyrite, Cu-(Fe-, Sn-, Ni-, Co-)-rich mineral and hematite.

Gypsum, apophyllite and corrensite dominate.

Photograph of one of the fracture surfaces KLX10A: 971.70–972.00 m.

Appendix 7

SEM-EDS-analyses

The SEM-EDS analyses give values of the total Fe-oxide content, distinctions of Fe^{2+} and Fe^{3+} are not made. "n.d." = below the detection limit. EDS analyses of surface samples do not give accurate values due to the morphology of the surface.

Adularia	Na_2O	Al_2O_3	SiO_2	K_2O	CaO	FeO	BaO	Total
KLX04-322-1	n.d.	19.04	65.13	16.81	n.d.	n.d.	0.3	101.28
KLX04-322-2	n.d.	19.26	65.63	16.86	n.d.	n.d.	n.d.	101.75
KLX04-322-3	n.d.	18.80	64.64	16.91	n.d.	n.d.	n.d.	100.35
KLX04-349-1	n.d.	18.66	64.69	16.36	n.d.	0.18	n.d.	99.89
KLX04-349-2	n.d.	18.45	64.17	16.38	0.11	n.d.	0.15	99.25
KLX04-349-3	n.d.	18.67	64.39	16.48	0.18	0.14	n.d.	99.86
KLX08-933-1	0.43	18.26	62.70	15.93	n.d.	n.d.	0.84	98.16
KLX08-933-2	0.43	18.33	62.80	15.92	n.d.	n.d.	0.88	98.36

Barite	Na_2O	Al_2O_3	SiO_2	SO_3	K_2O	FeO	BaO	Total
KLX03-266	0.66	0.86	2.70	26.35	0.23	0.27	61.5	92.56

Calcite	Al_2O_3	K_2O	CaO	MnO	FeO	Total	Comments
KLX03-722-1-1	0.16	n.d.	53.31	0.18	n.d.	53.65	
KLX03-722-1-2	0.18	n.d.	51.41	0.83	n.d.	52.42	
KLX03-722-1-3	0.20	n.d.	54.20	0.11	n.d.	54.51	
KLX03-722-1-4	0.18	n.d.	53.17	n.d.	n.d.	53.35	
KLX03-722-2-1	0.37	n.d.	52.90	0.18	n.d.	53.44	
KLX03-722-2-2	0.33	n.d.	52.07	0.33	n.d.	52.90	
KLX03-722-2-3	n.d.	n.d.	54.23	n.d.	n.d.	54.23	

Calcite	Al_2O_3	K_2O	CaO	MnO	FeO	Total	Comments
KLX03-722-2-4	n.d.	n.d.	51.52	1.37	n.d.	52.89	
KLX03-722-2-5	n.d.	n.d.	50.91	0.85	1.40	53.16	
KLX04-322-1	0.60	n.d.	48.79	3.89	n.d.	53.28	Euhedral
KLX04-322-2	0.49	n.d.	47.08	4.12	n.d.	51.69	Euhedral
KLX04-349-1	0.16	0.17	51.85	n.d.	n.d.	52.17	
KLX04-349-2	n.d.	0.15	51.89	n.d.	0.12	52.16	
KLX04-349-3	n.d.	0.10	49.83	0.87	n.d.	50.97	SiO_2=0.16
KLX07-106-1	n.d.	n.d.	53.55	n.d.	n.d.	53.55	
KLX07-106-2	n.d.	n.d.	54.05	n.d.	n.d.	54.05	
KLX07-106-3	n.d.	n.d.	53.86	n.d.	n.d.	53.86	
KLX08-676-1	n.d.	n.d.	52.98	0.38	n.d.	53.59	MgO=0.16
KLX08-676-2	n.d.	n.d.	54.24	n.d.	0.19	54.43	
KLX08-676-3	n.d.	n.d.	52.18	0.67	0.21	53.06	
KLX08-772-1	n.d.	n.d.	49.82	2.24	n.d.	52.06	Core
KLX08-772-2	n.d.	n.d.	48.11	3.63	0.23	51.97	Core
KLX08-772-3	n.d.	n.d.	51.93	0.38	n.d.	52.31	Low Mn-top of xx
KLX08-772-4	n.d.	n.d.	51.82	0.63	n.d.	52.43	Low Mn-top of xx
KLX08-868	n.d.	n.d.	53.52	n.d.	n.d.	53.52	
KLX08-933-1	n.d.	n.d.	51.52	0.62	0.62	53.01	MgO=0.25
KLX08-933-2	n.d.	n.d.	52.66	0.29	n.d.	52.95	
KLX08-933-3	n.d.	n.d.	53.38	n.d.	n.d.	53.38	

Fe-Mg-chlorite	Na_2O	MgO	Al_2O_3	SiO_2	K_2O	CaO	MnO	FeO	Total	Comments
KLX03-722-1-1	n.d.	15.81	21.15	25.72	n.d.	n.d.	0.53	24.59	87.81	
KLX03-722-2-1	n.d.	15.85	21.56	25.88	n.d.	n.d.	0.42	24.29	87.99	
KLX03-722-2-2	n.d.	15.53	21.55	25.76	n.d.	n.d.	0.55	25.34	88.73	
KLX06-384-1	n.d.	17.21	20.08	28.14	0.23	0.16	0.50	19.82	86.15	
KLX06-384-2	n.d.	18.43	18.10	27.47	n.d.	n.d.	0.68	20.44	85.12	

Fe-Mg-chlorite	Na_2O	MgO	Al_2O_3	SiO_2	K_2O	CaO	MnO	FeO	Total	Comments
KLX06-387-1	n.d.	18.78	18.95	27.78	n.d.	n.d.	0.64	20.21	86.36	
KLX06-387-2	n.d.	19.00	19.13	28.22	n.d.	n.d.	0.53	20.00	86.89	
KLX06-387-3	n.d.	18.94	17.27	29.73	n.d.	0.50	0.53	19.30	86.29	
KLX07-106	n.d.	14.37	19.45	27.77	0.26	0.19	0.41	25.18	87.94	CoO=0.32
KLX08-676-1	n.d.	17.74	18.52	26.23	n.d.	n.d.	0.63	21.93	86.09	CoO=0.36, SrO=0.67
KLX08-676-2	n.d.	18.02	18.58	26.57	n.d.	n.d.	0.53	21.98	86.32	CoO=0.33
KLX08-676-3	n.d.	18.70	15.48	27.82	n.d.	n.d.	0.44	21.67	84.48	CoO=0.37
KLX08-676-4	0.34	18.05	19.09	26.36	n.d.	n.d.	0.63	21.99	87.35	CoO=0.35, MoO_3=0.54
KLX08-933-1	n.d.	17.08	17.16	26.96	n.d.	n.d.	0.55	23.99	85.73	
KLX08-933-2	0.36	16.42	18.02	26.81	n.d.	n.d.	0.71	25.59	87.91	
KLX08-933-3	n.d.	16.14	18.00	26.73	n.d.	0.13	0.74	26.05	87.80	
KLX08-933-4	0.39	18.38	16.65	28.04	n.d.	n.d.	0.52	23.79	87.77	

Mg-chlorite	Na_2O	MgO	Al_2O_3	SiO_2	K_2O	CaO	MnO	FeO	Total	Comments
KLX03-722-1-1	n.d.	22.76	12.11	37.68	n.d.	1.68	0.47	12.16	86.87	Unpure
KLX03-722-1-2	n.d.	19.45	13.83	37.76	1.28	2.36	0.34	11.53	86.55	Unpure

Fe-chlorite	Na_2O	MgO	Al_2O_3	SiO_2	K_2O	CaO	MnO	FeO	Total	Comments
KLX04-349-1	0.32	7.94	13.79	30.34	0.14	0.60	0.43	35.24	88.81	
KLX04-349-2	n.d.	7.45	13.93	30.16	0.39	0.60	0.39	34.91	87.87	
KLX04-349-3	0.34	7.38	13.12	28.73	0.15	0.58	0.43	34.90	85.63	
KLX07-106	0.30	5.64	14.88	27.32	n.d.	0.29	0.19	39.77	89.03	CoO=0.64

Corrensite	Na_2O	MgO	Al_2O_3	SiO_2	K_2O	CaO	TiO_2	MnO	FeO	Total	Comments
KLX04-322-1	n.d.	2.73	11.65	29.83	2.20	3.25	0.12	0.21	39.25	89.25	
KLX04-322-2	n.d.	1.78	9.49	22.68	0.77	6.77	0.12	0.21	49.97	91.79	
KLX04-322-3	n.d.	4.98	11.27	27.86	2.85	1.50	n.d.	0.12	46.57	95.17	
KLX04-322-4	n.d.	3.19	6.51	17.76	1.70	2.18	0.12	0.18	53.02	84.65	
KLX04-349	n.d.	7.43	14.74	33.16	1.80	0.75	n.d.	0.30	32.89	91.07	
KLX06-384-1	0.31	7.15	20.17	39.95	3.26	2.23	0.38	0.28	19.32	93.05	
KLX06-384-2	0.30	5.92	20.11	40.90	4.16	1.76	0.16	0.23	15.39	88.93	
KLX06-831-1	0.72	9.00	13.04	36.59	0.36	3.10	n.d.	n.d.	30.68	93.49	Surface sample
KLX06-831-2	0.54	12.11	15.52	43.60	0.22	1.65	n.d.	n.d.	34.02	107.66	Surface sample

Epidote	MgO	Al_2O_3	SiO_2	CaO	TiO_2	MnO	FeO	Total	Comments
KLX03-722-1-1	n.d.	20.88	37.63	22.36	n.d.	n.d.	15.26	96.15	
KLX03-722-2-1	n.d.	20.16	37.88	22.91	0.13	n.d.	16.39	97.48	
KLX06-321-1	2.10	17.02	34.71	21.74	n.d.	14.07	0.35	90.00	Very Mn-rich
KLX06-321-2	n.d.	17.52	39.81	18.05	n.d.	6.88	8.19	94.12	SrO=1.95, La_2O_3=0.81,Ce_2O_3=0.92
KLX06-321-3	n.d.	18.69	36.82	20.54	n.d.	6.20	8.33	92.72	La_2O_3=1.06,Ce_2O_3=1.07
KLX06-384-1	n.d.	22.54	35.95	21.18	n.d.	0.71	11.28	92.22	Fine-grained, SrO=0.56
KLX06-384-2	0.16	22.98	35.99	21.51	0.22	0.36	11.28	93.76	Fine-grained, SrO=1.27
KLX06-384-3	0.19	21.56	36.27	20.56	n.d.	0.73	11.72	92.39	Fine-grained, SrO=1.38
KLX06-387-1	n.d.	22.97	37.62	22.90	n.d.	0.30	12.94	96.73	Fine-grained
KLX06-387-2	n.d.	23.18	37.97	22.53	0.15	0.22	12.39	96.43	Fine-grained
KLX07-106	0.37	23.27	37.80	22.55	n.d.	0.37	13.27	97.64	
KLX08-676-1	n.d.	22.67	36.79	23.24	n.d.	0.19	12.92	95.80	
KLX08-676-2	n.d.	19.09	36.12	22.85	n.d.	n.d.	17.34	95.59	
KLX08-676-3	n.d.	19.07	36.45	23.10	0.20	n.d.	17.23	96.05	
KLX08-676-4	n.d.	22.22	36.84	23.45	n.d.	0.23	13.26	96.01	

Harmotome	Na_2O	Al_2O_3	SiO_2	K_2O	FeO	BaO	Total
KLX03-266	2.57	19.24	55.36	1.09	0.24	18.49	96.98

Hornblende	Na_2O	MgO	Al_2O_3	SiO_2	K_2O	CaO	TiO_2	MnO	FeO	Total
KLX06-576-1	1.39	14.83	8.08	50.44	0.61	9.92	0.98	0.16	12.15	98.55
KLX06-576-2	1.08	14.66	8.01	50.32	0.57	9.90	0.89	0.26	11.98	97.67
KLX08-933-1	0.69	13.17	4.65	49.85	0.33	12.14	n.d.	0.50	15.60	96.93
KLX08-933-2	0.70	13.32	4.65	49.65	0.38	12.21	0.21	0.54	15.80	97.46
KLX08-933-3	0.54	13.77	3.52	51.16	0.22	12.46	n.d.	0.45	15.07	97.19
KLX08-933-4	0.72	12.76	4.92	49.79	0.39	12.33	n.d.	0.56	16.48	97.95

Illite	MgO	Al_2O_3	SiO_2	K_2O	CaO	MnO	FeO	Total	Comments
KLX04-322-1	4.64	22.62	55.30	8.03	0.55	n.d.	4.61	95.75	
KLX04-322-2	4.45	21.82	54.07	8.01	0.58	n.d.	4.58	93.52	
KLX04-322-3	4.65	23.40	56.59	7.54	0.76	n.d.	2.96	95.90	
KLX04-322-4	4.52	22.38	54.95	7.47	0.60	n.d.	3.98	93.90	
KLX04-349-1	7.29	21.48	48.85	6.18	0.62	0.29	3.28	87.99	Fine-grained
KLX04-349-2	3.83	20.52	53.15	9.14	0.43	0.27	2.33	89.66	
KLX06-384-1	4.00	24.95	55.68	6.00	1.01	0.14	0.84	92.61	
KLX06-384-2	4.08	24.62	54.93	6.23	0.71	0.10	0.80	91.45	

Laumontite	Na_2O	Al_2O_3	SiO_2	K_2O	CaO	Total	Comments
KLX04-322-1	n.d.	21.65	52.75	0.66	10.63	85.87	FeO=0.18
KLX04-322-2	n.d.	22.03	52.68	n.d.	11.94	86.65	
KLX06-384-1	0.57	21.66	51.18	0.24	10.52	84.18	
KLX06-384-2	0.28	21.03	50.18	0.14	11.03	82.66	
KLX07-106-1	0.34	21.35	52.24	0.97	11.19	86.09	
KLX07-106-2	0.31	21.15	52.32	1.06	10.97	85.81	
KLX07-106-3	0.81	20.94	51.23	1.19	10.71	84.87	

Muscovite	Na^2O	MgO	Al^2O^3	SiO^2	K^2O	FeO	BaO	Total	Comments
KLX03-722-2-1	0.36	1.54	32.67	46.61	11.22	3.38	0.40	96.17	In plagioclase
KLX06-384-1	0.31	1.21	31.66	44.00	10.54	3.39	0.72	92.30	TiO^2=0.46

Prehnite	Al_2O_3	SiO_2	CaO	FeO	Total	Comments
KLX03-722-1-1	18.60	42.48	26.18	8.16	95.41	
KLX03-722-1-2	24.16	44.35	26.78	1.31	96.60	
KLX03-722-2-1	18.38	42.65	26.36	8.33	95.73	
KLX03-722-2-2	23.58	44.16	27.07	2.14	96.95	
KLX03-722-2-3	21.45	43.73	26.64	4.86	96.69	
KLX04-322-1	25.18	43.87	26.78	0.55	96.37	
KLX04-322-2	21.05	43.03	26.49	5.25	95.82	
KLX04-322-3	22.29	43.62	25.91	3.41	95.23	Fine-grained
KLX06-321-1	23.00	43.40	26.26	3.64	96.30	
KLX06-321-2	22.34	43.50	26.96	3.07	95.87	

Titanite	Al_2O_3	SiO_2	CaO	TiO_2	V_2O_5	Cr_2O_3	FeO	Total	Comments
KLX06-387-1	4.42	31.33	28.19	32.43	n.d.	n.d.	1.79	98.16	
KLX06-387-2	3.47	31.21	28.16	34.46	n.d.	n.d.	1.65	99.07	MnO=0.11
KLX08-676-1	1.36	30.16	29.25	38.91	0.54	0.25	0.55	102.22	SrO=0.61,HfO_2=0.58
KLX08-676-2	1.95	30.39	28.90	37.87	0.58	n.d.	0.71	100.41	
KLX08-933-1	2.65	30.40	28.30	36.50	n.d.	n.d.	1.38	99.23	
KLX08-933-2	2.78	30.56	29.08	35.58	n.d.	0.25	1.97	100.22	

Appendix 8

Fracture minerals

The Table shows the relative chronological order of the fracture minerals in each sample. Minerals in brackets are found in small amounts. Mineral abbreviations: ab = albite, adu = adularia (K-feldspar), amp = amphibole, apa = apatite, apo = apophyllite, arg = argentite, Au = native gold, ba = barite, bt = biotite, cc = calcite, chl = chlorite (Fe-, Mg- or Fe-Mg-rich), clay min = clay mineral, corr = corrensite, cpy = chalcopyrite, ep = epidote, fl = fluorite, ga = galena, gy = gypsum, ha = halite, har = harmotome, hbl = hornblende, hem = hematite, ill = illite, kfs = K-feldspar, lau = laumontite, mlc = Mixed layer clay, mt = magnetite, mus = muscovite, mz = monazite, pre = prehnite, pump = pumpellyite, py = pyrite, qz = quartz, REEc = REE-carbonate, sph = sphalerite, syl = sylvite, tit = titanite, tz = topaz, zir = zircon.

"Cu-" stands for an unidentified mineral rich in Cu, commonly with a significant amount of one or more of the elements Zn, Ni, Sn and Fe. "W-" stands for an unidentified W-rich mineral (probably wolframite). "Zn-" and "Nb-" stands for unidentified Zn- and Nb-rich minerals, respectively. "U-sil" stands for an unidentified U-rich silicate. Myl = mylonite and cata = cataclasite.

Sample (m)	Generation 1	Generation 2	Generation 3	Generation 4
KLX03				
195.95–196.15	har, cc, py, hem, (Fe-chl), corr			
266.62–266.71	cc, har, py, ba, hem, Cu-, ha			
416.46–416.58	qz, cc			
457.60–457.75	cc, py, ba, qz			
533.10–533.25	Gy			
535.58–535.70	Gy			
572.10–572.30	Gy			
590.79–590.96	Gy			
591.33–591.33	py, qz			
627.26–627.31	py, mlc, qz			
662.33–662.65	Cc	cc, py, ba, ga, qz		
722.72–722.96	qz, cc, chl, ep, kfs, (hem)	Pre	Mg-chl, adu	py
733.49–733.53	qz, cc, chl, ep, py			
742.23–742.36	py, cc, qz			
897.76–897.89	qz, tit	ep		
970.04–970.07	Ep	apo, cc, ba		

Sample (m)	Generation 1	Generation 2	Generation 3	Generation 4
KLX04				
114.12–114.33	Pre	cc, adu, chl		
188.19–188.39	ep, fl			
274.65–274.92	pre, adu, chl, hem	qz		
322.04–322.25	Pre	ill, adu, hem, cc, lau	cc, ba, hem	
346.46–346.58	cata:kfs, chl, hem	pre	lau	cc
349.66–349.79	qz, kfs, tit, hem, chl	cc, py, U-sil, Fe-chl, hem, adu, ill, corr, ab, Mg-chl		
669.31–669.55	Cc	cc, py, ba, qz		
673.78–674.05	Cc	cc, hem, py		
677.39–677.70	Cc	cc, py, ba, cpy, hem, fl, Fe-chl, Cu-		
878.18–878.24	Pre	cc, hem		
925.60–925.68	fl, cc, py, ba, Cu-, (adu, hem), qz			
970.48–970.52	cata:kfs, chl, hem	lau	cc	
KLX06				
321.01–321.16	pre, fl, Mn-ep, hem	Mg-chl, adu	py	
333.53–333.67	pre, fl			
381.42–381.58	Myl	cata:adu, chl, hem		
384.23–384.28	cata:Fe-Mg-chl, ep, musc, hem	lau, (adu, Mg-chl, hem)	hem, corr, ill,	
387.95–388.07	ep, tit, kfs	Fe-Mg-chl, ep, hem, qz, tit	qz, Fe-Mg-chl, hem, adu	
392.23–392.57	cc, lau			
394.83–394.96	cc, lau			
446.67–446.80	qz, mus			
472.84–472.92	mus, qz, fl			
499.03–499.13	tit, qz			
535.10–535.26	mus, py, qz, cc			
535.40–535.50	mus, qz, py, fl			
557.81–557.91	mus, fl			
565.22–565.38	mus, qz, fl			

Sample (m)	Generation 1	Generation 2	Generation 3	Generation 4
566.25–566.35	mus, qz, py			
572.40–572.46	qz, mus, fl			
576.09–576.21	tit, hbl			
590.66–590.72	mus, qz, py			
593.40–593.55	qz, mus, fl, cc, kfs			
595.08–595.18	qz, mus, fl, Ti-ox, cpy, ha, Au, ba, Fe-Mg-chl, tz, sph, syl, ab, Fe-ox, 3Mn/Fe-ox, zir, Cu/As/Sn/Sb/Fe-sulphide(?)			
607.06–607.14	qz, mus			
622.57–622.73	qz, fl, mus, py, hem, ba, Nb-, mz, (ep)			
789.41–789.48	cc, ba, ga, gy, Fe-chl, hem, Cu-			
814.86–814.95	cc, fl, ba, ga, apo, hem, qz			
831.32–831.38	fl, corr, hem, cc, ba, sph, Cu-, qz			
KLX07A				
106.25–106.41	Qz	ep, chl, kfs	cc, lau	Fe-chl, ill, cc, (py, ba, hem, U-sil)
184.83–184.92	cc, py, ba, REEc, fl, apo, hem, Cu-, Zn-			
193.63–193.87	cc, har, py, ba, REEc			
227.24–227.38	pre, cc, chl, (fl)			
320.32–320.49	cc, py, ba, ga, REEc, Fe-chl, qz, W-			
321.47–321.58	cc, py, ba, W-, arg, syl, har, clay min(corr), qz, hem, apo			
346.73–346.82	cc, py, ba, Fe-chl			
356.93–356.96	cc, py, ba, fl, REEc			
364.17–364.41	cc, fl, py, ga			
373.70–373.97	cc, py, ba, ga, cpy, W-			
423.21–423.39	qz, cc, py, chl			
557.83–557.94	cc, Cu-			
668.98–669.22	cc, py, ba, Ni-Cu-			
696.68–696.83	cc, py, chl			

Sample (m)	Generation 1	Generation 2	Generation 3	Generation 4
KLX08				
108.24–108.33	cc, chl(mlc), py, hem, cpy			
218.29–218.39	cc, REEc, adu			
366.43–366.58	pre, cc			
478.87–479.13	cata:kfs, hem, Mg-chl, ep, qz	cc, kfs, hem, Mg-chl, ep, qz, adu, fl, py, (ga, apa, ab, W-)	cc, adu, py, (cpy)	
676.92–677.13	py, cpy, ep, qz, cc, tit, chl, mt, sph, (ab), pump?			
679.83–680.01	cc, Ag-, Cu-(Sn), W-, py, chl, corr, hem			
772.49–772.69	cc, hem, ba, Cu/Zn-, py, REEc, qz, Fe-chl, Ag-, sph, W, kfs, ab, ep, chl(corr), (tit)	cata:kfs, ab, ep, chl, (corr), qz, cc, ba, py, (tit)		
795.15–795.36	gy, fl, apo, py, sph, hem, corr, ill			
820.93–821.16	gy, apo, corr, hem, apa			
821.70–821.92	Gy			
822.41–822.61	gy, hem, Mg-chl			
868.65–868.83	adu, cc, chl, corr, pre, apa, ab	gy, (syl)		
916.16–916.36	gy, ba, hem, ill, Mg-chl, corr, sph, cpy, cc			
919.75–919.90	Gy			
933.15–933.30	hbl, cc, tit, kfs, chl(Fe-Mg), (mt, py, ab, ep)			
KLX10				
108.27–108.38	cc, hem			
112.66–112.72	ep, cc, fl, qz, chl			
200.72–201.02	cc, hem, qz, py, cpy, Fe-chl			
228.14–228.80	cc, qz, Zn-, cpy, py, hem, ba, chl(mlc), W-, sph, ga			
406.29–406.49	cc, bt, qz, tit, ep, mt, (fl)			
519.40–519.62	cc, qz, ep			
610.85–611.19	corr, apo, py, ba, qz			
789.80–790.10	cc, ba, Zn-, hem, qz, fl, py			
790.50–790.63	cc, qz			
895.00–895.20	bt, cc, qz, kfs, (gy?, mus?)			
919.44–919.62	cc, pre, chl, qz			
969.13–969.28	gy, apo, hem, Fe-chl			
970.50–970.65	gy, ga, ba, corr, hem, (qz)			
971.70–972.00	gy, apo, corr, sph, py, Cu-, hem			

Appendix 9

Stable isotopes and $^{87}Sr/^{86}Sr$

Results from calcite (cc), fluorite (fl), gypsum (gy), pyrite (py) and barite (ba) samples.

Sample	$\delta^{13}C_{cc}$	$\delta^{18}O_{cc}$	$^{87}Sr/^{86}Sr_{cc}$	±	$^{87}Sr/^{86}Sr_{fl}$	±	$^{87}Sr/^{86}Sr_{gy}$	±	$\delta^{34}S_{py}$	$\delta^{34}S_{gy}$	$\delta^{34}S_{ba}$
KLX03											
195.95–196.15	–9.458	–8.845									
416.46–416.58	–4.061	–19.61									
457.60–457.75A	–66.714	–4.892							5.1		20.8
457.60–457.75B	–68.308	–5.099									
533.10–533.25							0.713106	0.000011		6.3	
535.58–535.70										5.9	
572.10–572.30										6.6	
590.79–590.96							0.714425	0.000018		6.8	
591.33–591.33									–2.9		
627.26–627.31									–0.1		
662.33–662.65A	–57.67	–6.258	0.715561	0.000024					18.6		12.8
662.33–662.65B	–55.439	–7.389									
722.72–722.96	–5.081	–20.773									
733.49–733.53	–4.854	–19.365	0.707053	0.000016					0.5		
742.23–742.36	–6.537	–20.854	0.707926	0.000024					0.1		
KLX04											
114.12–114.33	–5.178	–8.326									
188.19–188.39					0.707967	0.000011					
322.04–322.25	–8.378	–9.945									
346.46–346.58	–5.731	–13.21									
669.31–669.55A	–62.233	–6.709	0.715237	0.000023					16.9		17.3

Sample	$\delta^{13}C_{cc}$	$\delta^{18}O_{cc}$	$^{87}Sr/^{86}Sr_{cc}$	±	$^{87}Sr/^{86}Sr_{fl}$	±	$^{87}Sr/^{86}Sr_{gy}$	±	$\delta^{34}S_{py}$	$\delta^{34}S_{gy}$	$\delta^{34}S_{ba}$
669.31–669.55B	–13.672	–15.44									
673.78–674.05A	–15.615	–10.908	0.715280	0.000055					6.9		
673.78–674.05B	–13.955	–14.877									
677.39–677.70	–19.452	–12.154	0.714449	0.000027					5.8		
878.18–878.24	–3.225	–15.172									
925.60–925.68	–8.751	–8.833	0.716041	0.000012	0.720744	0.000014					
970.48–970.52	–10.059	–9.132									
KLX06											
321.01–321.16	–3.403	–17.996									
392.23–392.57	–11.89	–7.821									
394.83–394.96	–9.777	–9.702	0.714438	0.000013							
535.10–535.26									2.8		
565.22–565.38					0.746809	0.000014					
566.25–566.35									2.6		
590.66–590.72									1.9		
593.40–593.55	–2.9	–19.805	0.709583	0.000013	0.706760	0.000016					
595.08–595.18					0.705930	0.000013					
814.86–814.95	–11.428	–15.45	0.713247	0.000015	0.711632	0.000017					
KLX07A											
106.25–106.41	–2.578	–23.533									
193.63–193.87											21
227.24–227.38	–4.812	–11.364									
346.73–346.82	n.a.	–7.422									
356.93–356.96	–20.721	–9.063	0.716300	0.000013					54/54.8		
364.17–364.41	–10.129	–11.786							15.9		
373.70–373.97	–15.543	–8.056							11.8		
423.21–423.39	–2.578	–20.729							–1.7		
668.98–669.22	–13.6	–7.592	0.716366	0.000012							
696.68–696.83	–14.655	–7.226	0.716276	0.000010							

Sample	$\delta^{13}C_{cc}$	$\delta^{18}O_{cc}$	$^{87}Sr/^{86}Sr_{cc}$	±	$^{87}Sr/^{86}Sr_{fl}$	±	$^{87}Sr/^{86}Sr_{gy}$	±	$\delta^{34}S_{py}$	$\delta^{34}S_{gy}$	$\delta^{34}S_{ba}$
KLX08											
108.24–108.33	–8.93	–6.476	0.715602	0.000013							
218.29–218.39	–9.648	–8.209									
366.43–366.58	–3.252	–20.827	0.707697	0.000014							
478.87–479.13	–2.932	–20.799									
772.49–772.69	–8.119	–8.692	0.716153	0.000017							
795.15–795.36							0.714802	0.000016		9.4	
820.93–821.16										7.4	
822.41–822.61									–42/–42.5	8	
868.65–868.83							0.712345	0.000013		3.7	
919.75–919.90							0.712924	0.000015		12.1	
KLX10A											
108.27–108.38	–0.522	–7.146									
112.66–112.72	–4.496	–18.631									
200.72–201.02	–6.123	–7.35									
228.14–228.80A	–3.393	–8.531	0.715959	0.000014							
228.14–228.80B	–8.639	–8.776									
228.14–228.80G	–7.894	–11.492	0.716475	0.000016							
406.29–406.49	–5.495	–21.032									
789.80–790.10	–4.298	–17.971									
895.00–895.20	–4.296	–21.183									
919.44–919.62	–3.313	–23.377	0.707042	0.000015							
969.13–969.28							0.714240	0.000015			
970.50–970.65							0.713820	0.000023			

Appendix 10

ICP-MS analyses – calcite

"B" = Re-analysed sample.

Borehole Sample (ppm)	KLX03 662.33–662.65	KLX03 722.72–722.96	KLX03 722.72–722.96B	KLX03 733.49–733.53	KLX03 733.49–733.53B
Na	47.63	112.40	106.70	119.30	139.80
Mg	122.30	339.40	331.50	491.90	501.90
Al	14.69	78.84	78.52	18.52	18.32
K	74.98	79.48	74.42	82.09	85.33
Sc	0.67	4.65	5.07	8.05	9.01
Ca	341,400	357,100	357,300	382,700	381,000
Mn	3,899	2,930	3,000	3,598	3,618
Fe	1,165	2,508	2,586	3,296	3,384
Rb	0.27	0.23	0.17	0.12	0.20
Sr	64.78	261.40	263.10	447.60	452.10
Y	8.86	9.44	9.87	7.19	7.41
Ba	734.40	1.63	–0.22	3.47	4.00
La	173.10	0.47	0.53	1.02	1.36
Ce	171.90	0.77	0.85	1.69	2.08
Pr	11.89	0.17	0.11	0.23	0.24
Nd	42.80	0.48	0.46	1.01	1.17
Sm	2.94	0.13	0.14	0.28	0.33
Eu	0.54	0.04	0.05	0.15	0.15
Gd	3.16	0.25	0.21	0.51	0.49
Tb	0.25	0.08	0.07	0.11	0.11
Dy	1.14	0.81	0.81	0.69	0.78
Ho	0.20	0.33	0.32	0.21	0.23
Er	0.55	2.15	2.24	1.15	1.26
Tm	0.07	0.50	0.51	0.24	0.25
Yb	0.45	5.99	6.25	2.74	2.87
Lu	0.08	1.74	1.79	0.80	0.90
Th	0.07	0.06	0.08	0.03	0.02
U	0.11	0.07	0.05	0.51	0.53

Borehole Sample (ppm)	KLX04 669.31–669.55	KLX04 677.39–677.70	KLX04 925.60–925.68	KLX06 814.86–814.95
Na	26.41	21.83	22.16	25.00
Mg	98.90	48.45	22.22	64.72
Al	9.62	74.14	0.99	5.22
K	53.05	46.61	41.65	67.52
Sc	1.67	0.37	0.09	0.14
Ca	357,400	370,600	381,000	240,600
Mn	2,901	616	1,784	467
Fe	1,182	1,192	1,154	767
Rb	0.04	0.03	0.02	0.35
Sr	77.32	44.80	49.66	28.60
Y	24.14	4.66	0.60	8.82
Ba	554.60	635.70	–1.93	6.94
La	205.60	44.92	0.44	45.75
Ce	190.80	38.23	0.22	47.22
Pr	13.93	3.17	0.03	4.19
Nd	56.86	12.07	0.09	16.62
Sm	6.25	1.35	0.02	2.10
Eu	1.30	0.34	0.02	0.35
Gd	7.19	1.43	0.05	2.14
Tb	0.68	0.13	0.02	0.21
Dy	3.00	0.42	0.04	0.95
Ho	0.53	0.11	0.02	0.17
Er	1.42	0.24	0.04	0.49
Tm	0.17	0.03	0.01	0.06
Yb	0.94	0.12	0.03	0.35
Lu	0.17	0.03	0.01	0.06
Th	0.01	0.01	0.01	0.01
U	0.04	0.02	0.04	0.10

Borehole Sample (ppm)	KLX07A 106.25–106.41	KLX07A 364.17–364.41	KLX08 108.24–108.33	KLX08 218.29–218.39	KLX08 478.87–479.13
Na	45.23	35.34	22.12	20.20	22.56
Mg	26.10	88.38	663.80	419.90	43.49
Al	253.10	21.30	20.75	28.92	23.89
K	70.86	52.76	54.37	64.49	52.92
Sc	0.16	4.85	0.34	0.26	0.13
Ca	387,000	383,800	380,700	383,700	391,400
Mn	145	6,745	11,460	8,165	23
Fe	1,208	1,394	3,604	2,976	1,236
Rb	0.20	0.06	0.03	0.09	0.04
Sr	274.10	57.43	82.36	102.70	282.10
Y	0.36	197.90	9.43	3.91	0.02
Ba	23.99	2.33	6.42	8.45	0.74
La	1.01	57.32	109.60	148.60	3.02
Ce	1.00	140.60	105.00	215.90	0.83
Pr	0.08	18.67	9.63	16.92	0.13
Nd	0.26	81.84	41.12	57.64	0.37
Sm	0.03	22.93	4.10	4.65	0.01
Eu	0.02	5.57	0.94	0.73	0.00
Gd	0.07	26.86	3.77	3.24	0.02
Tb	0.01	5.15	0.28	0.18	0.00
Dy	–0.14	35.24	1.06	0.39	–0.18
Ho	0.02	7.80	0.23	0.11	0.00
Er	0.02	26.28	0.56	0.29	0.01
Tm	0.01	4.16	0.06	0.02	0.00
Yb	0.03	32.39	0.33	0.15	0.00
Lu	0.01	5.11	0.06	0.02	0.00
Th	0.02	0.09	0.08	0.97	0.01
U	0.02	0.02	0.39	0.32	0.02

Borehole Sample (ppm)	KLX10A 228.14–228.80	KLX10A 228.14–228.80B	KLX10A 919.44–919.62
Na	4.97	7.32	17.15
Mg	427.10	364.50	9.68
Al	5.08	20.07	23.00
K	56.64	67.35	55.19
Sc	1.17	1.04	0.07
Ca	376,600	397,800	131,000
Mn	6,666	6,272	76.74
Fe	2,825	2,546	457
Rb	0.04	0.21	0.02
Sr	114.40	109.30	215.10
Y	63.79	58.56	0.17
Ba	7.77	8.39	0.25
La	26.17	28.38	0.48
Ce	61.79	65.44	0.47
Pr	8.87	9.13	0.06
Nd	41.33	41.41	0.21
Sm	11.03	10.59	0.03
Eu	2.29	2.21	0.01
Gd	13.13	12.24	0.05
Tb	1.73	1.69	0.01
Dy	9.97	9.17	–0.16
Ho	2.00	1.85	0.01
Er	5.51	5.07	0.02
Tm	0.64	0.59	0.00
Yb	3.95	3.50	0.01
Lu	0.64	0.55	0.00
Th	0.14	0.20	0.00
U	0.06	0.05	0.01

Appendix 11

ICP-MS analyses – gypsum

Values in red are very much higher than the highest standard measurement.

Borehole Sample ppm	KLX08 795.15–795.36	KLX08 868.65–868.83	KLX08 919.75–919.90
Na	34.80	12.14	27.17
Mg	261.50	33.56	157.10
Al	252.80	34.26	132.00
K	16.99	14.12	24.46
Ca	231,900	236,100	235,400
Sc	0.09	0.04	0.08
Mn	14.79	1.62	8.82
Fe	1,741	886	1,335
Rb	0.09	0.04	0.12
Sr	131.90	155.00	221.60
Y	0.04	0.01	0.02
Ba	3.86	6.22	16.09
La	0.24	0.08	0.46
Ce	0.18	0.08	0.58
Pr	0.02	0.01	0.05
Nd	0.04	0.03	0.14
Sm	0.01	0.01	0.02
Eu	0.01	0.00	0.01
Gd	0.01	0.01	0.01
Tb	0.00	0.01	0.00
Dy	0.01	0.00	0.01
Ho	0.00	0.00	0.00
Er	0.00	0.00	0.00
Tm	0.00	0.00	0.00
Yb	0.00	0.01	0.01
Lu	0.00	0.00	0.01
Th	0.01	0.01	0.02
U	0.02	0.00	0.02

Borehole Sample ppm	KLX10A 969.13–969.28	KLX10A 970.50–970.65	KLX10A 970.50–970.65B
Na	144.30	12.24	24.34
Mg	966.70	91.36	129.60
Al	687.40	71.02	94.96
K	6,272	4.27	16.80
Ca	222,800	227,300	238,100
Sc	0.41	0.04	0.06
Mn	24.36	2.33	3.43
Fe	2,225	1,008	1,165
Rb	47.45	0.01	0.02
Sr	161.50	183.50	184.60
Y	0.12	0.01	0.04
Ba	6.28	4.69	10.87
La	11.85	0.03	0.06
Ce	8.27	0.04	0.08
Pr	0.58	0.01	0.02
Nd	1.79	0.02	0.05
Sm	0.11	0.00	0.01
Eu	0.03	0.01	0.01
Gd	0.10	0.00	0.02
Tb	0.01	0.01	0.01
Dy	0.02	0.01	0.02
Ho	0.01	0.01	0.01
Er	0.01	0.00	0.01
Tm	0.00	0.00	0.01
Yb	0.02	0.00	0.02
Lu	0.00	0.01	0.01
Th	0.05	0.01	0.01
U	0.02	0.00	0.01

Appendix 12

$^{87}Sr/^{86}Sr$ for rock types in the area

Sample	Area	Rock type	87Sr/86Sr	±
KKR03: 643.82–643.90	Götemar	Götemar granite	0.976111	0.000173
KKR03: 643.82–643.90B	Götemar	Götemar granite	0.978129	0.000045
KSH01:536-2G	Simpevarp	Fine-grained dioritoid	0.715110	0.000019
KLX04:108G	Laxemar	Ävrö granite	0.716009	0.000037
PSM004484A	Laxemar	Quartz monzodiorite	0.713540	0.000023

B = ion-exchanged twice.

Appendix 13

Additional data from other fracture mineralogy studies

Some samples from earlier reports e.g. /Drake and Tullborg, 2004, 2005, 2006ab/ have been analysed with different methods ($^{87}Sr/^{86}Sr$, $\delta^{13}C$, $\delta^{18}O$ and ICP-MS analyses of calcite and $\delta^{34}S$ analyses of pyrite and gypsum) after the reports were published. The results from these analyses are presented here. $\delta^{13}C$, $\delta^{18}O$ and $^{87}Sr/^{86}Sr$ results for a calcite filled fracture related to a sandstone filled fracture in a road cutting close to Oskarshamn Nuclear Power Plant (O3) is also published here, as well as $\delta^{13}C$, $\delta^{18}O$ and $^{87}Sr/^{86}Sr$ for calcite from a laumontite-rich deformation zone in borehole KAS17, Äspö. All of the analyses are executed using the same method description as the analyses in the present study.

Calcite ($\delta^{13}C$, $\delta^{18}O$, $^{87}Sr/^{86}Sr$)

KSH01A (m)	$\delta^{13}C$	$\delta^{18}O$	$^{87}Sr/^{86}Sr$	Sample description
239	–10.817	–6.469		Scalenohedral with barite and pyrite (open fracture)
376.44-376.56	–2.055	–16.163		See /Drake and Tullborg 2004/
925	–6.858	–11.377		Scalenohedral
KLX02 (m)				
218.40-219.10	–3.139	–14.641		See /Drake and Tullborg 2005/
260.08-260.25	–6.424	–9.318		See /Drake and Tullborg 2005/
525.06-525.66	–6.679	–10.533		See /Drake and Tullborg 2005/
KA1755A (m)				
200.84-200.99	–5.75	–22.37		See /Drake and Tullborg 2005/
204.90-205.10	–3.749	–23.326		See /Drake and Tullborg 2005/
211.70-211.75	–4.285	–14.174		See /Drake and Tullborg 2005/
KAS17 (m)				
155	–2.339	–15.803		In laumonote-rich zone
156	–20.417	–11.372	0.716633	In laumonote-rich zone
Road cutting (O3)				
O3	–9.865	–8.276	0.710814	Sealed fracture next to sandstone

Pyrite ($\delta^{34}S$)

KSH01A (m)	$\delta^{34}S$	Sample description
24.00-24.10	–1.1	See /Drake and Tullborg 2004/
239	32.2 and 26.7	Cubic crystals with barite and calcite (open fracture), re-analysed
873.55-873.60	–6.858	See /Drake and Tullborg 2004/
KSH03A (m)		
863.66-863.84	8.8	See /Drake and Tullborg 2006a/

Gypsum ($\delta^{34}S$)

KSH03A (m)	$\delta^{34}S$	Sample description
495.42	15.5	See /Drake and Tullborg 2006a/
684.46	15.1	See /Drake and Tullborg 2006a/

ICP-MS analyses of calcite

See /Drake and Tullborg 2006ab/ for sample descriptions. “B” = Re-analysed sample.

Borehole Sample (m) (ppm)	KSH03A 177.74–177.81	KSH03A 177.74–177.81B	KSH03A 186.52–186.62	KSH03A 220.15–220.31	KKR02 48.95–49.00	KKR03 52.25–52.37	KKR03 54.83–54.86
Na	65.83	53.39	41.32	68.65	40.26	29.60	31.14
Mg	108.90	110.90	49.84	145.70	33.85	54.08	48.55
Al	58.63	59.39	6.77	141.00	49.20	16.07	10.55
K	193.90	146.80	63.69	660.20	61.89	51.83	60.33
Sc	0.20	0.18	1.57	0.77	0.30	1.59	3.12
Ca	384,600	369,500	390,900	359,200	386,200	379,900	380,000
Mn	655	634	8,155	4,181	2,727	3,963	6,055
Fe	1,166	1,206	1,244	2,037	2,597	2,157	1,896
Rb	0.49	0.51	0.23	5.33	0.32	0.07	0.07
Sr	358.20	358.80	54.62	49.68	65.97	59.93	51.23
Y	1.00	1.00	73.40	24.49	17.33	32.99	20.27
Ba	2.96	3.12	-0.17	19.74	422.60	9.69	4.32
La	2.93	2.78	33.98	33.06	18.31	36.03	31.08
Ce	3.15	3.06	88.71	51.09	24.14	70.81	61.22
Pr	0.29	0.29	11.57	6.32	2.15	7.03	6.16
Nd	1.28	1.17	57.26	26.78	8.16	25.71	22.48
Sm	0.12	0.14	13.13	4.34	1.32	4.47	3.82
Eu	0.04	0.02	2.49	0.81	0.34	0.99	0.77
Gd	0.15	0.14	12.43	4.36	1.53	4.61	3.46
Tb	0.02	0.02	1.82	0.60	0.22	0.64	0.44
Dy	0.09	0.09	10.46	3.17	1.33	3.53	2.30
Ho	0.03	0.02	2.00	0.61	0.29	0.67	0.43
Er	0.06	0.06	6.55	1.93	0.92	2.09	1.39
Tm	0.01	0.01	0.93	0.26	0.15	0.32	0.22
Yb	0.06	0.05	7.27	2.01	1.01	2.54	1.90
Lu	0.02	0.02	1.24	0.32	0.20	0.50	0.37
Th	0.02	0.01	0.01	0.06	0.49	0.04	0.18
U	0.97	1.16	0.02	0.31	1.46	3.79	1.97